UC Davis

UC Davis Electronic Theses and Dissertations

Title

Targeting STAT3-Driven Mitochondrial Metabolism in Pancreatic Ductal Adenocarcinoma: Preclinical Development of YXL-182 and Nanoplatform-Based Therapeutic Perspectives

Permalink

https://escholarship.org/uc/item/2300r15x

ISBN

9798193262725

Author

Villa, Rodolfo

Publication Date

2026-09-08

Peer reviewed|Thesis/dissertation

eScholarship.org Powered by the California Digital Library
University of California

Targeting STAT3-Driven Mitochondrial Metabolism in Pancreatic Ductal Adenocarcinoma: Preclinical Development of YXL-182 and Nanoplatform-Based Therapeutic Perspectives

By

RODOLFO VILLA

DISSERTATION

Submitted in partial satisfaction of the requirements for the degree of

DOCTOR OF PHILOSOPHY

in

Biochemistry, Molecular, Cellular, and Developmental Biology

in the

OFFICE OF GRADUATE STUDIES

of the

UNIVERSITY OF CALIFORNIA

DAVIS

Approved:

Yuanpei Li, Chair

Kermit Carraway

Jeremy Chien

Committee in Charge - 2026

Table of Contents

Chapter 1 – Clinical and Biological Foundations of PDAC and STAT3 Targeting
1.1 Clinical challenge of PDAC and therapy resistance
1.2 Tumor microenvironment, immune suppression, and metabolic adaptation in PDAC
1.3 STAT3 as a central regulator of tumor survival and resistance
1.4 Therapeutic innovation through delivery platforms and mechanistic targeting
1.5 Thesis objectives and chapter overview
    1.5.1 Central hypothesis
    1.5.2 Overall objective of the dissertation
    1.5.3 Specific aims and guiding questions
    1.5.4 Significance and translational relevance

Chapter 2 – Nanoplatforms in Cancer Therapy
2.1 Introduction
    2.1.1 Overview of cancer Nanoplatforms
    2.1.2 Challenges in Current Drug Delivery
        2.1.2.1 PDAC-Specific Barriers to Drug Delivery and Immunotherapy
    2.1.3 Nanotechnology-Based Solutions to Delivery and Immunotherapy Limitations
2.2 Types of nanoplatforms
    2.2.1 Lipid nanoparticles
    2.2.2 Metal nanoparticles
    2.2.3 Polymer nanoparticles
    2.2.4 Organic nanoparticles
2.3 Advantages of nanoplatforms
    2.3.1 Nanoplatform modifications
    2.3.2 Stimuli-responsive designs
2.4 Mechanisms of immunomodulation
    2.4.1 Tumor-associated macrophages and regulatory T cells
    2.4.2 Direct immune cell activation
    2.4.3 Antigen-presentation enhancement
    2.4.4 Immunological memory
2.5 Combination approaches with nanoplatforms
    2.5.1 Combination with chemotherapy
    2.5.2 Combination with phototherapy
    2.5.3 Combination with radiotherapy
2.6 Clinical studies
2.7 Conclusion
2.8 Future perspectives

Chapter 3 – Development and Preclinical Evaluation of YXL-182, a Dual-Targeting Inhibitor of Canonical and Mitochondrial STAT3 in PDAC
3.1 Introduction
3.2 Methods
3.3 Results and Discussion
3.3.1 YXL-182 Directly Binds STAT3 and Disrupts Canonical Signaling
3.3.2 YXL-182 Is a Potent, Broadly Active STAT3 Inhibitor in PDAC Cells
3.3.3 YXL-182 Accumulates in Mitochondria and Disrupts Mitochondrial STAT3 and OXPHOS Function
3.3.4 YXL-182 Induces Mitochondria-Intrinsic Apoptosis
3.3.5 YXL-182 Is Tolerated In Vivo and Enhances Gemcitabine Activity
3.3.6 YXL-182 Enhances Gemcitabine Efficacy in Orthotopic KPC Models
3.4 Conclusion

Chapter 4 – Integrating Mechanistic STAT3 Targeting with Immunomodulatory Nanoplatforms
4.1 Overview of integrated therapeutic strategy in PDAC
4.2 Rationale for nano-encapsulation of YXL-182
4.3 Overall conclusions

Abstract

Pancreatic ductal adenocarcinoma (PDAC) is a deadly cancer that spreads early, has a dense stroma, adapts its metabolism, and resists treatment. Although gemcitabine-based therapies remain important for PDAC, the tumor's survival signals and shifts in mitochondrial metabolism limit their effectiveness. STAT3 is a key regulator of these processes, supporting tumor growth, survival, chemotherapy resistance, immune evasion, and metabolic changes through both its nuclear and mitochondrial roles. This dissertation explores whether targeting STAT3-driven mitochondrial oxidative phosphorylation (OXPHOS) could be a vulnerability in PDAC, and tests YXL-182, a small molecule that accumulates in the mitochondria and inhibits STAT3 activation, as a targeted treatment approach.

YXL-182 directly bound and inhibited STAT3, suppressing PDAC cell growth with IC_{50} values below 3 μM across tested cell lines. It reduced canonical and mitochondrial STAT3 signaling, impaired OXPHOS and mitochondrial respiration, increased mitochondrial reactive oxygen species, and induced apoptosis. In animal models, oral YXL-182 was well tolerated, slowed tumor growth, and prolonged survival. Combined treatment with gemcitabine further improved tumor control and survival in an orthotopic KPC mouse model, with reduced proliferation and STAT3 signaling and increased apoptosis in tumor tissue.in tumor tissue, and fewer blood-related side effects than gemcitabine alone.

Overall, these results show that YXL-182 works in two ways: it blocks normal STAT3 signaling and disrupts STAT3-controlled mitochondrial OXPHOS. The findings suggest that targeting both cancer signaling and metabolic adaptation simultaneously could help overcome chemotherapy resistance in PDAC. This dissertation also supports future work to package YXL-182 in nanoparticles to improve its solubility, stability, tumor penetration, and compatibility with other treatments in the dense PDAC tumor microenvironment.

List of Figures

Figure 1. Statistics of PDAC with treatment strategy.

Figure 2. Structural and cellular remodeling of the pancreatic tissue microenvironment during progression to PDAC.

Figure 3. Cytokine signaling through the JAK-STAT pathway.

Figure 4. Nanoparticle types and multifunctionality.

Figure 5. Key pathways of tumor-mediated immune suppression and representative nanoplatform strategies that counteract these mechanisms.

Figure 6. Combinatorial approaches integrating nanoplatforms with chemotherapy, radiotherapy, and phototherapy.

Figure 7. YXL-182 directly binds STAT3 and inhibits canonical STAT3 signaling in PDAC cells.

Figure 8. YXL-182 exhibits broad antiproliferative activity in PDAC cells.

Figure 9. YXL-182 localizes to mitochondria and disrupts mitochondrial STAT3-associated OXPHOS signaling.

Figure 10. YXL-182 induces mitochondrial dysfunction and intrinsic apoptosis in PDAC cells.

Figure 11. YXL-182 is tolerated in vivo, produces antitumor activity, and enhances gemcitabine response in PDAC models.

Figure 12. YXL-182 enhances gemcitabine activity in an orthotopic KPC PDAC model.

Acknowledgements

First, I want to express my gratitude to my advisor, Dr. Yuanpei Li, for his guidance, support, and encouragement. He has supported me throughout my doctoral training. Since I joined his lab in 2022, I have benefited greatly from his mentorship and his steady encouragement to grow as both a scientist and a person.

I am grateful to Dr. Yangxiong Li for his collaboration and for completing the chemistry work that contributed to this dissertation. I also want to thank my current and former lab members for their collaboration, advice, and support throughout this project, including Dr. Cindy Lin, Dr. Menghuan Tang, Dr. Sohaib Mahri, Kelsey Racacho, Dr. Yaping Shiau, Dr. Yanyu Huang, Dr. Qiufang Zong, and everyone else in the Li lab. I appreciate all the discussions, feedback, and teamwork that helped shape this work.

I would also want to thank the UC Davis core facilities and staff who provided research support. Dr. Gabriella Grigorean in the Proteomics Core, Dr. Jane Chen in the Pathology Core, Jonathan Van Dyke in the Flow Cytometry Core, and Dr. Jinhwan Kim for letting me use the VEVO ultrasound imaging system. Their expertise and help were important for completing this research.

I'm grateful for my dissertation committee members, Dr. Jeremy Chien and Dr. Kermit Carraway, for their guidance, thoughtful feedback, and support throughout my graduate training. I greatly appreciate the opportunity to discuss my work from different scientific perspectives, which strengthened both my research and development as a scientist. I also thank my 2021 BMCDB cohort for being such a supportive community, as well as my friends and family for their constant encouragement throughout this journey.

Finally, I want to thank my partner, Lucia Hau, and my daughter, Nia. I could not have finished this program without their love, patience, and constant support. Nia was just one month old when I started my doctoral program, and now she is a beautiful, smart, and funny five-year-old. My family has been my biggest source of motivation and strength. All the late nights, early mornings, and long hours of work were meaningful because of you.

This study was financially supported from NIH/NCI (R01CA294557), NIH/NCI (R01CA232845), NIH/NIDCR (R01DE029237), NIH/NIBIB (R01EB033677), NIH/NIBIB (R01EB035416), and NIH/NCI (P30CA093373).

Conflict of Interest

The authors declare no conflict of interest.

Chapter 1:

Clinical and Biological Foundations of PDAC and STAT3 Targeting

Introduction

1.1 Clinical challenge of PDAC and therapy resistance

Pancreatic ductal adenocarcinoma (PDAC) is one of the deadliest solid tumor cancers that accounts for over 90% of pancreatic cancer cases, with nearly as many deaths as new cases worldwide. As of 2020, pancreatic cancer caused an estimated 495,773 new cases and 466,003 deaths globally, highlighting its high mortality rate. (1) PDAC continues to have a poor prognosis, with a reported 5-year survival rate of approximately 10%, due in large part to its aggressive biology and the frequent absence of early symptoms, which often lead to diagnosis at an advanced stage, as summarized in **Figure 1**. (2) Because early-stage PDAC often causes no clear symptoms and the pancreas is located deep in the body, diagnosis is often delayed until the tumor has advanced or become metastatic, leaving only a minority of patients eligible for surgery with the potential for long-term disease control. Due to limited effective screening strategies, surgery that offers the best chance for long-term survival is possible in only about 10–20% of patients at diagnosis, and drug treatment options provide only limited survival benefit in advanced disease. (2) Together, these challenges continue to make PDAC difficult to treat and highlight the need for better strategies for early detection and therapy.

The treatment of PDAC depends on the stage of the disease and the patient's overall health. Surgery is the only option that can potentially control the disease long-term. However, since only some patients are eligible for surgery when they are diagnosed, preoperative therapy is now more commonly used in borderline resectable and some resectable cases to improve results. (3) For patients with unresectable or metastatic disease, chemotherapy is the main treatment. Gemcitabine has been the standard first-line drug for many years, but more intensive regimens like gemcitabine with nab-paclitaxel and FOLFIRINOX have shown better results and improved survival compared to gemcitabine alone. (4) FOLFIRINOX is usually chosen for healthier patients who can handle stronger treatment, as it often works better, while gemcitabine-based combinations are used when there are concerns about side effects. Treating PDAC is a balance, since using multiple drugs

can help patients live longer but also increases the risk of side effects like blood, stomach, and nerve problems.

Despite the development of multidrug regimens, gemcitabine remains clinically and experimentally important in PDAC because it continues to serve as a backbone of treatment in multiple regimens and remains widely used in mechanistic and preclinical studies of chemoresistance. Its activity, tolerability, and extensive use have made it a standard benchmark for evaluating new therapeutic strategies and combination treatments. (5) Several cellular and molecular factors contribute to gemcitabine resistance. These factors include reduced drug uptake from lower levels or changes in nucleoside transporters like hENT1 and hCNT1, less activation by deoxycytidine kinase, more inactivation by cytidine

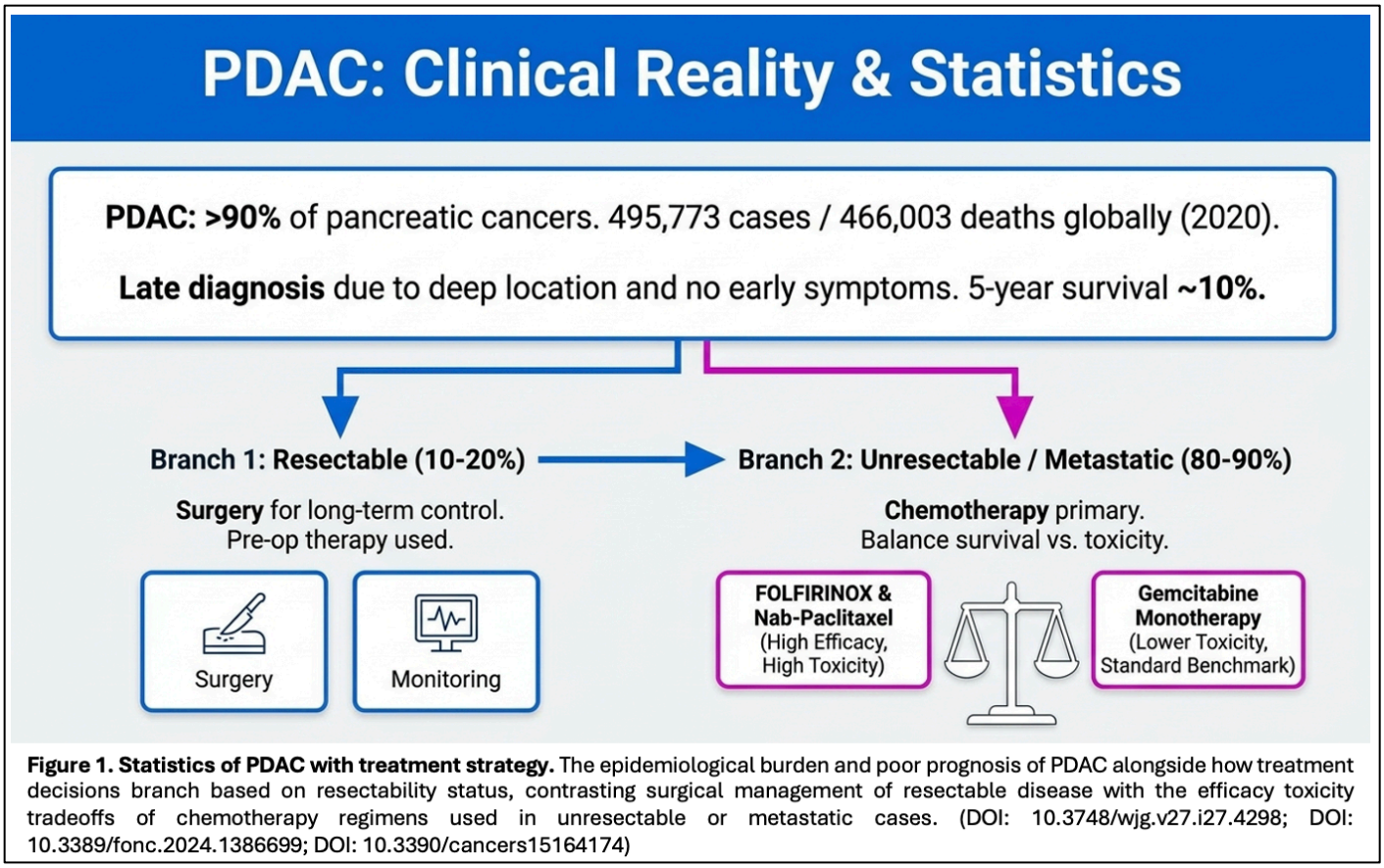

Figure 1. Statistics of PDAC with treatment strategy. The epidemiological burden and poor prognosis of PDAC alongside how treatment decisions branch based on resectability status, contrasting surgical management of resectable disease with the efficacy toxicity tradeoffs of chemotherapy regimens used in unresectable or metastatic cases. (DOI: 10.3748/wjg.v27.i27.4298; DOI: 10.3389/fonc.2024.1386699; DOI: 10.3390/cancers15164174)

deaminase, higher ribonucleotide reductase activity, and the activation of survival pathways such as PI3K/AKT and NF-kB. (6,7) Other contributors are epithelial-mesenchymal transitions, signaling from cytokines produced by surrounding tissue, and major metabolic changes that occur when oxygen and nutrients are limited. (5). Tumor cells may develop resistance to gemcitabine because of their own internal features, but the surrounding tumor microenvironment can also protect them by providing pro-survival signals through stromal cells, extracellular matrix accumulation that limits drug penetration, and low-oxygen conditions, all of which can blunt the cytotoxic effects of Gemcitabine.(8,9) These are a few examples of the complex mechanisms that allow cancer to thrive. Because of this, there is a clear need for therapeutic strategies that sensitize resistant PDAC cells by targeting both internal resistance mechanisms and stromal protection.

Conventional gemcitabine therapy has had limited success in treating PDAC, showing that approaches focused only on stopping tumor growth do not address the main causes of resistance. While combination chemotherapy can help patients live longer and reduce tumor size, it often does not lead to lasting results because PDAC cells quickly adapt through changes in their metabolism and environment that cytotoxic drugs alone cannot fully block. Researchers have become interested in finding treatment targets based on the specific mechanisms that allow PDAC to survive. They are looking at the signaling and metabolic pathways that help tumors survive when faced with low oxygen, lack of nutrients, oxidative stress, and chemotherapy. These pathways could provide more lasting and logical targets for therapy. (10,11) This shift in focus is central to my current study. Since PDAC growth and resistance to treatment depend on these survival and metabolic networks,

targeting them is a logical way to improve how well therapies work. That is why compounds like YXL-182, which block survival signals and metabolic adaptation, are both relevant to the underlying biology and promising as treatments.

1.2 Tumor microenvironment, immune suppression, and metabolic adaptation in PDAC

A key feature of pancreatic ductal adenocarcinoma is its strong desmoplastic reaction, which means the tumor has a thick, fibrous stroma made up of activated cancer-associated fibroblasts (CAFs), pancreatic stellate cells, and many extracellular matrix proteins like collagens, fibronectin, and hyaluronan. (12) This stroma does more than just mark the tumor under a microscope. It changes the tumor's biology by making the tissue stiffer, raising pressure between cells, and squeezing blood vessels, which helps the tumor grow. As illustrated in **Figure 2**, malignant ductal cells, activated CAFs, and excess extracellular matrix remodel the pancreatic tissue architecture, compress local blood vessels, and create a dense desmoplastic barrier. Because of this dense stroma, blood flow and drug delivery are reduced. Less oxygen and nutrients can reach the tumor, and the compressed stroma makes it harder for treatments to get in, leading to lower drug levels inside the tumor and a tough environment with low oxygen and high stress. (13,14) PDAC also progresses because of strong signaling and communication between tumor and stromal cells, which makes the cancer more resistant to treatment. CAFs and other stromal cells help maintain this environment by releasing cytokines, growth factors, metabolites, and enzymes that remodel the extracellular matrix. These factors help tumor cells survive, change shape, avoid the immune system, and resist chemotherapy. (15) {Overall, the PDAC

stroma acts as both a physical barrier and an active force that drives the cancer's aggressiveness and makes treatment more difficult.

One defining feature of PDAC is its immunosuppressive tumor microenvironment, which is characterized by poor effector T-cell infiltration and suppressed antitumor immunity. In many patient tumors, cytotoxic CD8+ T cells are either scarce, kept away from direct contact with tumor cells, or rendered dysfunctional by inhibitory stromal and myeloid cell populations. (16) This is a major factor underlying the limited efficacy of immune checkpoint blockade in patients with PDAC. This immunosuppressive landscape is shaped by multiple cellular populations, including tumor-associated macrophages (TAMs) , myeloid-derived suppressor cells (MDSCs), regulatory T cells (Tregs), and suppressive CAF subsets. (17) TAMs can adopt two broad phenotypes: M1-like (anti-tumor, pro-

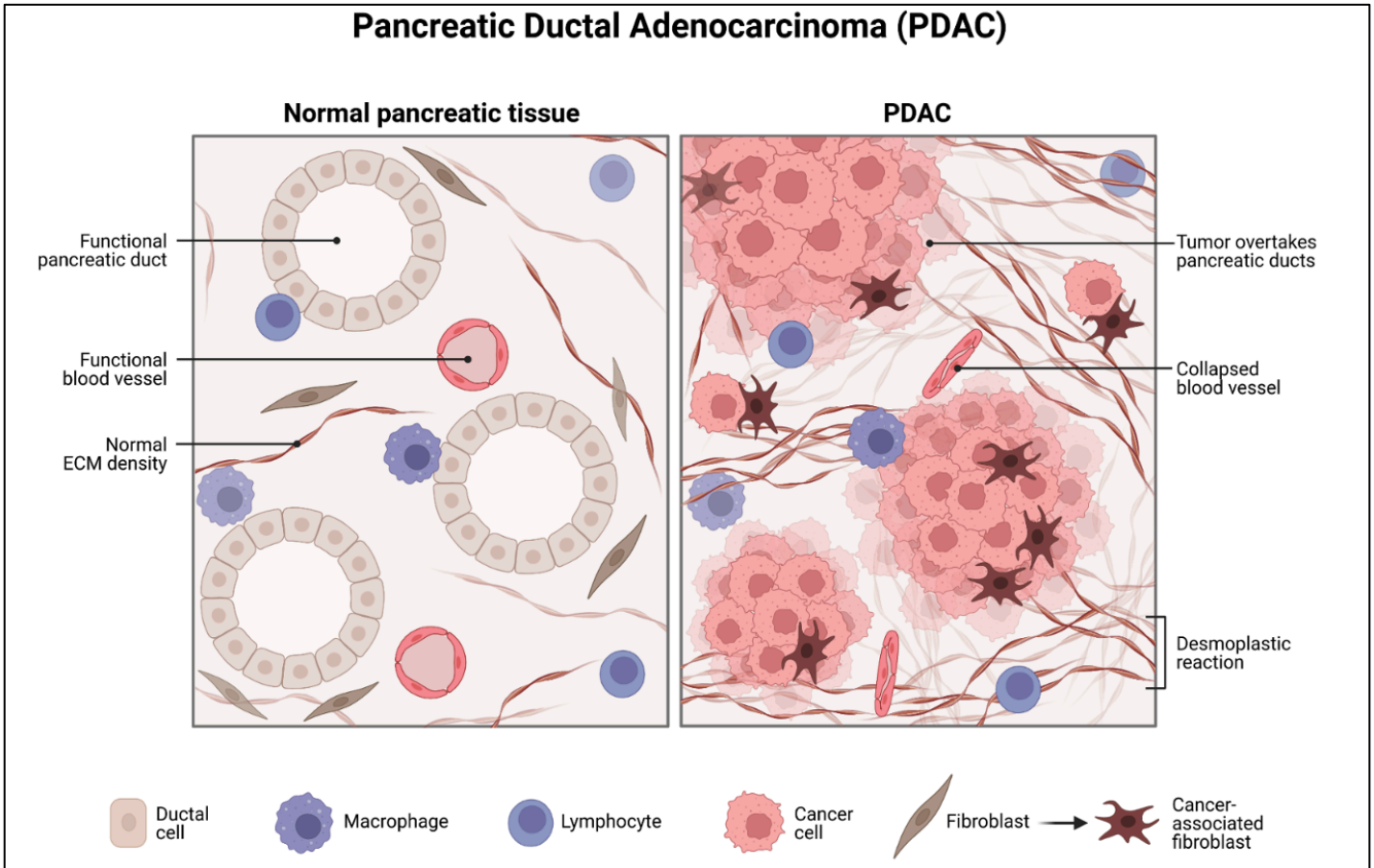

Figure 2. Structural and cellular remodeling of the pancreatic tissue microenvironment during progression to pancreatic ductal adenocarcinoma (PDAC). Normal pancreatic tissue (left) shows intact ductal architecture, functional vasculature, low ECM density, and low populations of macrophages, lymphocytes, and fibroblasts. In PDAC (right), malignant ductal cells replace normal structures while activated cancer-associated fibroblasts (CAFs) deposit excess fibrillar ECM, producing the disease's characteristic desmoplastic reaction. This fibrotic remodeling compresses blood vessels and restricts drug delivery. (doi: 10.1016/j.canlet.2026.218618.) Macrophages and lymphocytes persist but are reprogrammed to support tumor progression rather than antitumor immunity, illustrating the stroma's dual role as a physical and biological barrier to therapy. Created with BioRender.com (2026).

inflammatory) and M2-like (pro-tumor, immunosuppressive). (18) In PDAC, TAMs are predominantly polarized toward an M2-like phenotype that promotes tumor growth, angiogenesis, and immune dysfunction, whereas MDSCs suppress T-cell activation through nutrient depletion, reactive oxygen species production, and the expression of checkpoint ligands. (19,20) Tregs further reinforce this immunosuppressive environment through the secretion of inhibitory cytokines such as IL-10 and TGF-ββ. (21) For these reasons, PDAC is considered an immunologically “cold” tumor, meaning it lacks robust effector T-cell infiltration and remains poorly responsive to immunotherapy. Together, these factors restrict immune infiltration and blunt antitumor responses.

The evolution of PDAC is driven by dynamic bidirectional crosstalk between tumor cells and the surrounding stromal and immune compartments. Tumor cells produce cytokines, chemokines, exosomes and metabolites that attract and re-program fibroblasts, macrophages, neutrophils and MDSCs. These stromal and immune cells reciprocally promote tumor survival, invasion and immune escape through their own secretory programs. (16) The most important mediators of this crosstalk are inflammatory cytokines such as IL-6, TGF-ββ, IL-10, CCL2 and CXCL12. These factors drive epithelial-mesenchymal transition, tumor cell plasticity, fibroblast activation, monocyte recruitment, suppressive macrophage polarization and T-cell dysfunction, building a self-reinforcing inflammatory niche that favors tumor persistence. Thus, inflammatory signaling pathways such as JAK/STAT, TGF-ββ, Notch, Wnt, and hypoxia-inducible factor signaling are important for PDAC survival and maintenance of immune evasion. (13) These pathways combine tumor-intrinsic oncogenic programs with stromal and immune inputs, enabling PDAC cells to adapt to stress, remodel their microenvironment, and resist therapy.

The PDAC microenvironment is characterized by nutrient deprivation, poor perfusion, metabolic stress, and hypoxia, conditions that necessitate substantial metabolic adaptation to support tumor growth and chemoresistance. To survive under these conditions, PDAC cells undergo metabolic rewiring that enables flexible use of mitochondrial respiration, glycolysis, redox buffering, and alternative nutrient acquisition pathways. (22,23) While PDAC has traditionally been associated with increased glycolysis, recent evidence shows that mitochondrial metabolism remains essential in many tumors. PDAC cells can transition between glycolytic and oxidative metabolic states in response to

nutrient availability, oncogenic drivers, stromal interactions, and therapeutic interventions, underscoring the metabolic plasticity of this malignancy. (24) Redox homeostasis also plays a central role in PDAC cell survival. Factors such as low oxygen, mitochondrial activity, oncogenic signaling, and treatment-related stress increase reactive oxygen species (ROS), requiring PDAC cells to maintain antioxidant defenses that limit oxidative damage while preserving redox signaling that supports survival and adaptation. (13)

Studies have shown that certain pancreatic ductal adenocarcinoma tumors depend on OXPHOS, particularly those classified as aggressive, stem-like, and therapy resistant. Tumors with high OXPHOS activity exhibit enhanced mitochondrial respiratory capacity and depend on functional mitochondria to sustain ATP production, maintain redox homeostasis, and withstand conventional cytotoxic therapies. (25) Mitochondrial adaptation supports the survival of resistant pancreatic ductal adenocarcinoma tumors. Following chemotherapy, these tumor cells demonstrate elevated mitochondrial respiration, enhanced antioxidant defenses, and increased metabolic flexibility. Such adaptations allow drug-tolerant cells to persist and contribute to tumor recurrence. (26) These findings support the therapeutic targeting of metabolic plasticity in PDAC. If resistant tumors depend on mitochondrial respiration or OXPHOS-associated antioxidant systems, agents that effect mitochondrial function may sensitize aggressive tumors to treatment, particularly in combination with standard therapies such as gemcitabine.

Immune suppression and metabolic adaptations in PDAC are highly interconnected processes. Hypoxia, nutrient deprivation, and metabolic interactions between tumor and

stromal cells modify the behavior of cancer cells, fibroblasts, and immune populations. These changes establish a microenvironment that impairs antitumor immunity and promotes therapy resistance. (27) This conceptual framework is directly relevant to the present study, which links therapeutic resistance to STAT3-mediated mitochondrial dysfunction, mitochondrial reactive oxygen species (mitoROS), and OXPHOS dependency in PDAC. These pathways are identified as potential vulnerabilities for intervention with YXL-182. (25) In summary, these findings show that successful treatments need to address not just tumor-intrinsic signaling, but also the stromal, immune, and metabolic networks that contribute to resistance.

1.3 STAT3 as a central regulator of tumor survival and resistance

Signal transducer and activator of transcription 3 (STAT3) is a member of the STAT family, a group of conserved cytoplasmic transcription factors in mammalian cells. The STAT family consists of STAT1, STAT2, STAT3, STAT4, STAT5a, STAT5b; where together they which mediate signaling pathways involved in development, immunity, and cancer related processes. (28) STAT3 plays a central mediator role in tumor-promoting tumor signaling that regulates cell survival, proliferation, differentiation, and angiogenesis. (28) Structurally, STAT3 contains several conserved domains, including the N-terminal, DNA-binding, SH2, linker, coiled-coil, and C-terminal domains, each contributing to a certain activation or function. (29) The coiled-coil and SH2 domains are critical for receptor binding, tyrosine phosphorylation, dimerization, and subsequent transcriptional activation. (30)

In normal cells, STAT3 activation is regulated by upstream receptors that include JAK and EGFR. Conversely, persistent STAT3 activation is commonly observed in cancer and

correlates with poor prognosis, immune evasion, and continuous oncogenic signaling. (31,32) As illustrated in **Figure 3,** cytokine binding induces receptor dimerization and JAK-mediated phosphorylation, which recruits and phosphorylates STAT3. Phosphorylated STAT3 then dimerizes, translocates to the nucleus, and activates the transcription of genes involved in proliferation, survival, angiogenesis, invasion, migration, and cancer stemness. In addition to its canonical role, STAT3 can also exerts non-canonical functions. Unphosphorylated STAT3 has the ability to activate alternative transcriptional programs, with serine 727 (S727) phosphorylation is linked to context-dependent regulation of transcriptional activity and mitochondrial STAT3 functions influencing oxidative phosphorylation, reactive oxygen species (ROS) homeostasis, and cellular metabolism. (33) The diverse functions of STAT3 makes itself a central signaling hub that regulates nuclear, metabolic, and microenvironmental adaptations. The JAK/STAT3 pathway represents a promising therapeutic target in pancreatic ductal adenocarcinoma, as aberrant STAT3 signaling is associated with poor prognosis, tumor progression, chemoresistance, and immune suppression in various cancer types.

Over-activation of STAT3 is a defining feature of PDAC, which often results from oncogenic KRAS signaling, inflammatory cytokines, receptor tyrosine kinase pathways, and paracrine factors originating within the tumor microenvironment. (34,35) STAT3 overexpression is observed throughout the course of pancreatic tumorigenesis, from early pancreatic intraepithelial neoplasia (PanIN) lesions to invasive PDAC, displaying its critical role in both tumor initiation and progression.(36) STAT3 is crucial for promoting proliferation, survival, invasion, metastasis, stemness, and stromal remodeling in pancreatic ductal

adenocarcinoma. By inducing genes involved in cell-cycle progression, anti-apoptotic signaling, extracellular matrix interactions, and epithelial-mesenchymal transition (EMT), STAT3 contributes to the emergence of an aggressive tumor phenotype and sustains malignant growth under adverse microenvironmental conditions. Elevated levels of phosphorylated STAT3 are clinically associated with more aggressive disease features and poorer prognoses in pancreatic cancer. (37). Taken together, substantial preclinical evidence has implicated STAT3 in pancreatic ductal adenocarcinoma progression as a central signaling molecule.

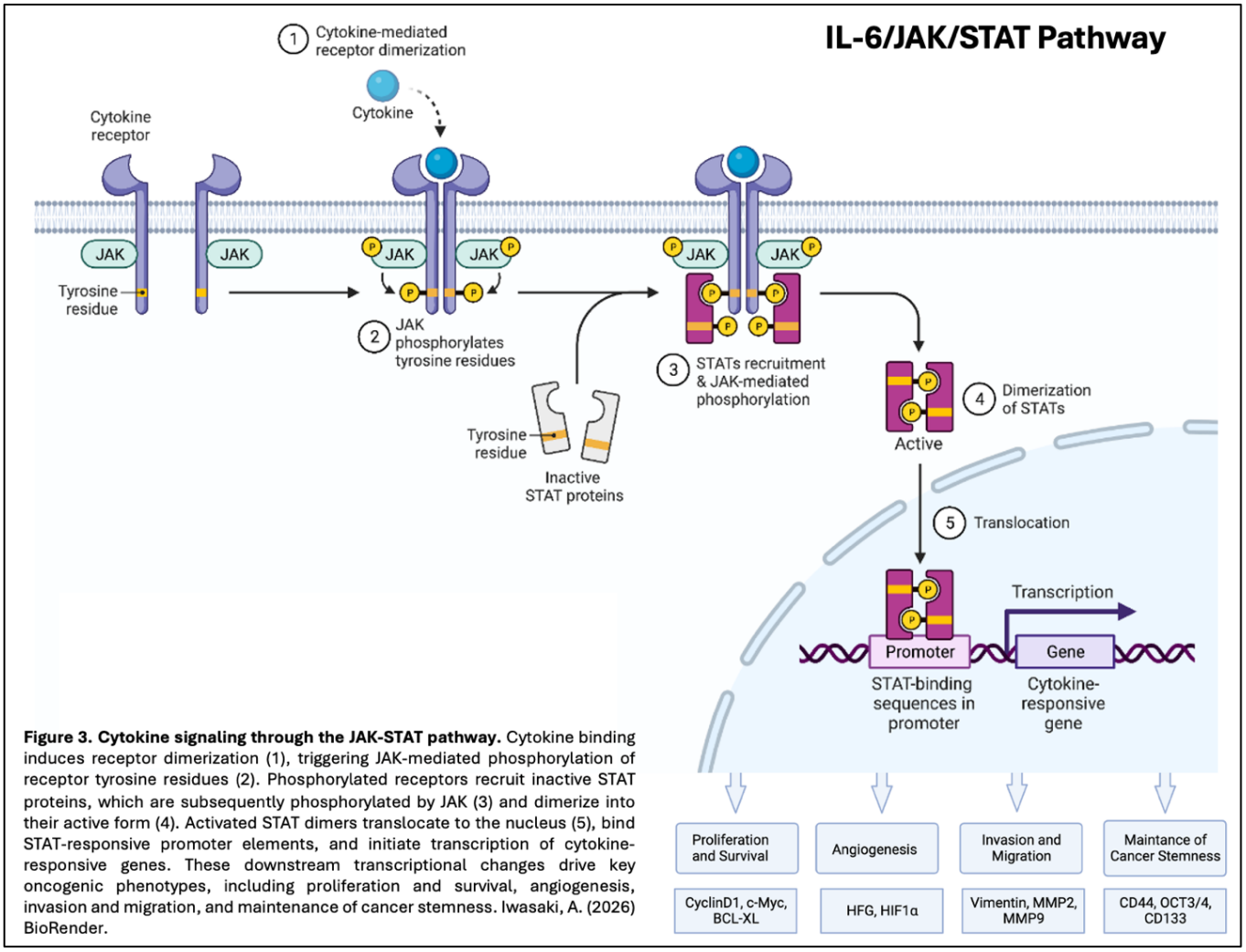

Figure 3. Cytokine signaling through the JAK-STAT pathway. Cytokine binding induces receptor dimerization (1), triggering JAK-mediated phosphorylation of receptor tyrosine residues (2). Phosphorylated receptors recruit inactive STAT proteins, which are subsequently phosphorylated by JAK (3) and dimerize into their active form (4). Activated STAT dimers translocate to the nucleus (5), bind STAT-responsive promoter elements, and initiate transcription of cytokine-responsive genes. These downstream transcriptional changes drive key oncogenic phenotypes, including proliferation and survival, angiogenesis, invasion and migration, and maintenance of cancer stemness. Iwasaki, A. (2026) BioRender.

STAT3 serves as a key mediator of therapeutic resistance in pancreatic ductal adenocarcinoma. Its activation enhances resistance to cytotoxic chemotherapy, targeted therapies, and microenvironmental stress by initiating pro-survival transcriptional programs that inhibit apoptosis and sustain tumor cell viability during treatment. (38,39) STAT3 functions as a central mediator of therapeutic resistance in PDAC. Activation of STAT3 increases resistance to cytotoxic chemotherapy, targeted therapies, and environmental stress by initiating pro-survival transcriptional programs that inhibit apoptosis and maintain tumor cell viability during treatment. (40) STAT3 also plays a critical role in mediating gemcitabine resistance. Studies have indicated that STAT3 inhibition increases gemcitabine sensitivity in pancreatic cancer cells by suppressing epithelial-mesenchymal transition, limiting immune escape, and amplifying oxidative stress-induced damage. Targeting the S1PR1/STAT3 axis has shown to reduce desmoplasia and increase chemosensitivity to gemcitabine in PDAC. (41) In several preclinical models, pharmacological inhibition of STAT3, combined with gemcitabine, results in greater tumor regression, increased apoptosis, and improved survival compared with gemcitabine monotherapy. These findings support STAT3 blockade as a rational approach to enhance chemotherapy efficacy in PDAC. (40,42) Collectively, these findings position STAT3 as a mechanistic driver of both intrinsic and acquired gemcitabine resistance in PDAC and highlights STAT3 targeting as a clinically relevant chemo sensitization strategy.

In addition to its direct effects on tumor cells, STAT3 acts as a central regulator of immune suppression in PDAC. STAT3 activation is mediated by signaling molecules such as interleukin-6 (IL-6), interleukin-10 (IL-10), interleukin-22 (IL-22), CXCL12, and other

inflammatory mediators. Such interactions establish feed-forward signaling loops that sustain tumor-promoting inflammation and suppress effective antitumor immune responses. (35) STAT3 signaling promotes immune evasion via multiple mechanisms, such as inducing programmed death-ligand 1 (PD-L1), enhancing the activity of suppressive myeloid cells, modulating cancer-associated fibroblast (CAF) phenotypes, and generating cytokine environments that suppress cytotoxic T-cell function. (43) In pancreatic ductal adenocarcinoma, these mechanisms sustain an immunologically "cold" tumor microenvironment, characterized by diminished antigen presentation, exclusion or dysfunction of effector lymphocytes, and a predominance of suppressive stromal and myeloid cell populations. (20) STAT3 serves as a critical mediator connecting tumor cell signaling with stromal activation, inflammation, and immune evasion in pancreatic ductal adenocarcinoma.

Recent research has focused on the role of STAT3 in metabolic adaptations. Beyond its established function in regulating the transcription of genes associated with glycolysis, survival, and growth, STAT3 has also been implicated in mitochondrial function, redox balance, and OXPHOS. Suggesting that STAT3 not only contributes to tumor cell fitness at both the transcriptional and metabolic levels. (44,45) The distinction between transcriptional and mitochondrial STAT3 functions is important. The Canonical Y705 phosphorylation activates STAT3 via dimerization, nuclear localization, and target gene expression, whereas S727 phosphorylation has been linked to mitochondrial localization and regulation of electron transport chain activity, ATP production, and ROS production. The roles of pS727 and mitochondrial STAT3 in resistant phenotypes are especially relevant to

PDAC. Tumors exhibiting resistance frequently rely on metabolic plasticity, redox regulation, and mitochondrial adaptation. Mitochondrial STAT3 is believed to promote cell survival during chemotherapy by maintaining oxidative phosphorylation (OXPHOS) efficiency and reducing lethal oxidative stress. In contrast, disruption of these functions may expose a therapeutic vulnerability. (46,47) This mechanistic perspective is especially relevant for studies examining OXPHOS, mitoROS, and mitochondrial dysfunction associated with STAT3-directed therapies.

Given its role in tumor growth, immune suppression, metabolic adaptation, and drug resistance, STAT3 has long been considered an undruggable therapeutic target. Earlier strategies to target STAT3 have included inhibition of upstream kinases such as Janus kinases (JAKs), blockade of receptor-mediated cytokine signaling, application of antisense oligonucleotides, and deployment of small molecules targeting the STAT3 SH2 domain, Y705 phosphorylation, dimerization, or DNA binding. (48) However, drugging STAT3 effectively has proven difficult. Challenges include the absence of deep catalytic pockets typical of enzymes, ,incomplete suppression of non-canonical STAT3 functions, and the limited clinical success or tolerability of several prior STAT3-directed agents, including compounds that failed because of insufficient efficacy or unacceptable toxicity. Despite these limitations, the need for improved STAT3 inhibitors remains compelling. The present findings further emphasize the ongoing necessity for therapeutic development.

My research outline shows that YXL-182 suppresses p-STAT3(Y705), interacts directly with STAT3, lowers downstream targets like MMP-9 and cyclin D1, and affects mitochondrial and OXPHOS-related biology in PDAC cells and tumor models. This section connects the

general literature to my research by presenting STAT3 as a target. Inhibiting STAT3 could weaken survival signaling, help overcome chemoresistance, and disrupt metabolic changes linked to resistant PDAC. Because STAT3 also affects tumor immune function, we created a STAT3 inhibitor that builds up in mitochondria to target OXPHOS and metabolic activity while also influencing immune responses. OXPHOS is often increased in PDAC and drives chemoresistance, so it is an important target. We developed a STAT3 inhibitor that works well both in living models and in cell cultures of PDAC, especially when combined with gemcitabine. The next step is to make a nanoparticle for encapsulation, study its pharmacokinetics, and compare the benefits of combination therapy to single-agent treatment for better tumor targeting and to address other features of chemoresistance in the tumor environment.

1.4 Therapeutic innovation through delivery platforms and mechanistic targeting

In PDAC, therapeutic efficacy usually depends on more than drug potency alone due to the. Tumors dense stroma, poor perfusion, and limited bioavailability undermining the treatment despite strong in vitro activity. To be effective, therapy should combine tumor specific cytotoxicity with an understanding of target biology, tissue penetration, delivery efficiency, and resistance mechanisms from both the cancer and its environment, instead of just increasing conventional chemotherapy. (49,50) Mechanistically targeted therapies address some of these limitations by disrupting specific biological dependencies that resistant tumors actively exploit for survival and adaptation. Instead of generally increasing cell damage, these treatments block key communication points, cell development pathways, or weak spots in metabolism that are especially active in resistant disease

conditions. (51,52) STAT3 represents a particularly attractive target in PDAC because it coordinates inflammatory signaling, survival pathways, immune suppression, and metabolic adaptation, establishing it as a major regulator and considered a non-druggable target response. (36,53)

Nanoplatforms offer new opportunities to enhance the effectiveness of targeted and cytotoxic drugs. In PDAC, nanocarriers can be designed to remain within tumors, deliver medication precisely, bypass tumor defenses, and release their payload at the optimal time. This strategy improves drug safety and efficacy by reducing off-target effects and minimizing side effects. (54,55) Nanoparticles can additional be used to co-deliver chemotherapeutic or immunomodulator therapies; offering a practical route to develop combinational therapies against stromal rich, therapy resistant tumors. (50,56) Evidence has indicated that to achieve a lasting benefit in PDAC, it will require targeting both the tumor intrinsic and microenvironmental resistance mechanisms. This strategy integrates tumor cell elimination, immune activation, immune activation, and suppression of compensatory survival pathways. (49,53)

Next, Chapter 2 introduces a platform-based approach that looks at how nanoplatforms can improve delivery and help make combination therapies work better in hard-to-treat environments. Chapter 3 presents the development and mechanistic characterization of YXL-182, a novel mitochondria-accumulating STAT3 inhibitor, evaluated in vitro and in vivo in PDAC. Chapter 4 extends this work by proposing the encapsulation of YXL-182 into lipid nanoparticles to counter chemotherapeutic delivery challenges specific to PDAC , including poor aqueous solubility, rapid systemic clearance, and limited tumor

penetration through the dense desmoplastic stroma. Together, these chapters demonstrate an integrated strategy in which delivery platform innovation and STAT3 directed, OXPHOS-linked targeting jointly address chemoresistance and metabolic adaptation in PDAC.

1.5.1 Central hypothesis

This dissertation proposes that since STAT3 plays a critical role in pancreatic ductal adenocarcinoma. Inhibition of STAT3 may suppress survival signaling, overcome resistance to gemcitabine, and disrupt metabolic adaptations that facilitate drug tolerance. YXL-182 accumulates in mitochondria and impairs metabolic processes associated with oxidative phosphorylation. Given that OXPHOS is frequently upregulated in certain PDAC cases and contributes to therapeutic resistance, targeting mitochondrial STAT3 and related pathways may represent an effective strategy. Experimental data demonstrate that YXL-182 binds to STAT3, reduces p-STAT3 levels, modulates downstream targets such as MMP-9 and cyclin D1, and alters mitochondrial and OXPHOS activity in both PDAC cell lines and animal tumor models. These findings indicate that future research should investigate the effects of YXL-182 on the immune system and evaluate nanoparticle-based delivery approaches to enhance its efficacy in PDAC and related malignancies.

1.5.2 Overall objective of the dissertation

The primary objective of this dissertation is to elucidate the biological and therapeutic challenges underlying the poor survival and limited treatment efficacy of pancreatic ductal adenocarcinoma, with particular emphasis on the STAT3 signaling pathway, a master regulator implicated in tumor proliferation, survival, immune evasion, and

metabolic adaptation. Because PDAC tumors frequently rely on oxidative phosphorylation and metabolic rewiring to sustain growth and resist chemotherapy, this dissertation investigates STAT3 driven OXPHOS dependency as a therapeutic vulnerability. To address this target, we developed a small-molecule STAT3 inhibitor engineered to accumulate within the mitochondria and evaluated its efficacy and mechanism of action through both in vitro and in vivo studies. Because the dense, immunosuppressive PDAC tumor microenvironment further limits the effectiveness of conventional chemotherapy, this work also considers strategies to overcome these delivery barriers, concluding with future directions toward encapsulating the inhibitor in a lipid nanoparticle platform to improve tumor-targeted delivery and combinatorial therapeutic potential.

1.5.3 Specific aims and guiding questions

This dissertation is structured around four principal aims. The first aim is to demonstrate that YXL-182 targets STAT3 in PDAC by quantifying its binding affinity relative to a reference inhibitor, evaluating its effects on cell death and long-term survival in PDAC and other tumor cell lines, and confirming its mechanism of action through STAT3 pathway inhibition and induction of apoptosis. The second aim is to establish that YXL-182 accumulates in mitochondria and disrupts mitochondrial STAT3 and OXPHOS. This will be accomplished by tracking intracellular localization, analyzing mitochondrial structure, measuring reactive oxygen species and membrane potential, and assessing effects on p-STAT3 S727, STAT3 distribution, and respiratory chain proteins. The third aim is to delineate how YXL-182 induces mitochondrial mediated cell death by quantifying changes in BCL-2 family proteins, caspase-3 , correlating loss of mitochondrial membrane potential

and increased ROS with activation of apoptotic pathways. The fourth aim is to evaluate the efficacy and safety of YXL-182 in combination with gemcitabine, targeting drug-tolerant cells in vivo. This includes assessing the impact on PDAC cells and drug-tolerant populations, monitoring tumor size, survival, and STAT3/apoptosis markers in murine models, and analyzing blood and serum chemistry to confirm safety at therapeutic doses.

1.5.4 Significance and translational relevance

This research is significant for PDAC as it addresses multiple factors contributing to treatment failure, including STAT3 signaling, alterations in mitochondrial and OXPHOS metabolism, resistance to gemcitabine, and the tumor microenvironment. This dissertation contributes to the broader field of therapeutic development for resistant solid tumors by integrating mechanistic insights with practical design strategies, including combination therapies and prospective nanoplatform delivery. The nanoplatform research underscores the necessity of overcoming tumor microenvironment barriers, optimizing drug pharmacokinetics, and modulating immune responses. The YXL-182 investigations demonstrate the development of an inhibitor that targets a critical signaling pathway involved in cellular survival, metabolic regulation, and immune suppression. Collectively, these approaches illustrate a synergistic strategy wherein novel delivery methods and STAT3 inhibition are combined to address resistance in challenging solid tumors, providing both conceptual frameworks and actionable steps for future therapies in PDAC and other refractory cancers.

Previous sections have established that STAT3 functions as a central signaling hub that promotes tumor survival, suppresses immune responses, and facilitates metabolic

alterations in pancreatic ductal adenocarcinoma . Pharmacological inhibition of STAT3, constitutes the primary focus of this dissertation, represents a rational therapeutic strategy. However, targeting STAT3 in isolation is insufficient to overcome the dense stromal matrix and immunosuppressive microenvironment characteristic of PDAC. Durable therapeutic outcomes will likely require the integration of targeted signaling inhibition with innovative drug delivery systems and immune modulation techniques. Chapter 2 examines this concept by reviewing nanoplatform-based delivery systems and immunomodulatory strategies, including major immunotherapy modalities, nanoparticle engineering, and approaches to modulate suppressive cell populations such as tumor associated macrophages and regulatory T cells. This chapter extends the STAT3 rationale outlined previously and provides a broader context for considering targeted agents such as YXL-182 (discussed in Chapter 3) in conjunction with, or as part of, advanced delivery and immune-modulating strategies to improve therapeutic outcomes in treatment resistant PDAC.

References

1. Hu JX, Zhao CF, Chen WB, Liu QC, Li QW, Lin YY, et al. Pancreatic cancer: A review of epidemiology, trend, and risk factors. World J Gastroenterol. 2021 Jul 21;27(27):4298–321. doi:10.3748/wjg.v27.i27.4298
2. Bugazia D, Al-Najjar E, Esmail A, Abdelrahim S, Abboud K, Abdelrahim A, et al. Pancreatic ductal adenocarcinoma: the latest on diagnosis, molecular profiling, and systemic treatments. Front Oncol. 2024 Jul 1;14. doi:10.3389/fonc.2024.1386699
3. Jain AJ, Maxwell JE, Katz MHG, Snyder RA. Surgical Considerations for Neoadjuvant Therapy for Pancreatic Adenocarcinoma. Cancers. 2023 Jan;15(16):4174. doi:10.3390/cancers15164174
4. Lellouche L, Palmieri LJ, Dermine S, Brezault C, Chaussade S, Coriat R. Systemic therapy in metastatic pancreatic adenocarcinoma: current practice and perspectives. Ther Adv Med Oncol. 2021 Jan 1;13:17588359211018539. doi:10.1177/17588359211018539
5. Koltai T, Reshkin SJ, Carvalho TMA, Di Molfetta D, Greco MR, Alfarouk KO, et al. Resistance to Gemcitabine in Pancreatic Ductal Adenocarcinoma: A Physiopathologic and Pharmacologic Review. Cancers. 2022 Jan;14(10):2486. doi:10.3390/cancers14102486
6. Herro R, Croft M. The control of tissue fibrosis by the inflammatory molecule LIGHT (TNF Superfamily member 14). Pharmacol Res. 2016 Feb 1;104:151–5. doi:10.1016/j.phrs.2015.12.018
7. Nakano Y, Tanno S, Koizumi K, Nishikawa T, Nakamura K, Minoguchi M, et al. Gemcitabine chemoresistance and molecular markers associated with gemcitabine transport and metabolism in human pancreatic cancer cells. Br J Cancer. 2007 Feb;96(3):457–63. doi:10.1038/sj.bjc.6603559
8. Carvalho TMA, Di Molfetta D, Greco MR, Koltai T, Alfarouk KO, Reshkin SJ, et al. Tumor Microenvironment Features and Chemoresistance in Pancreatic Ductal Adenocarcinoma: Insights into Targeting Physicochemical Barriers and Metabolism as Therapeutic Approaches. Cancers. 2021 Jan;13(23):6135. doi:10.3390/cancers13236135
9. Liang C, Shi S, Meng Q, Liang D, Ji S, Zhang B, et al. Complex roles of the stroma in the intrinsic resistance to gemcitabine in pancreatic cancer: where we are and where we are going. Exp Mol Med. 2017 Dec;49(12):e406–e406. doi:10.1038/emm.2017.255
10. Derle A, De Santis MC, Gozzelino L, Ratto E, Martini M. The role of metabolic adaptation to nutrient stress in pancreatic cancer. Cell Stress. 2(12):332–9. doi:10.15698/cst2018.12.166 PubMed PMID: 31225458; PubMed Central PMCID: PMC6551672.
11. Encarnación-Rosado J, Kimmelman AC. Harnessing metabolic dependencies in pancreatic cancers. Nat Rev Gastroenterol Hepatol. 2021 Jul;18(7):482–92. doi:10.1038/s41575-021-00431-7
12. Perez VM, Kearney JF, Yeh JJ. The PDAC Extracellular Matrix: A Review of the ECM Protein Composition, Tumor Cell Interaction, and Therapeutic Strategies. Front Oncol. 2021 Oct 6;11. doi:10.3389/fonc.2021.751311

13. Gautam SK, Batra SK, Jain M. Molecular and metabolic regulation of immunosuppression in metastatic pancreatic ductal adenocarcinoma. Mol Cancer. 2023 Jul 24;22(1):118. doi:10.1186/s12943-023-01813-y
14. Hosein AN, Brekken RA, Maitra A. Pancreatic cancer stroma: an update on therapeutic targeting strategies. Nat Rev Gastroenterol Hepatol. 2020 Aug;17(8):487–505. doi:10.1038/s41575-020-0300-1
15. Desbois M, Wang Y. Cancer-associated fibroblasts: Key players in shaping the tumor immune microenvironment. Immunol Rev. 2021;302(1):241–58. doi:10.1111/imr.12982
16. Huber M, Brehm CU, Gress TM, Buchholz M, Alashkar Alhamwe B, von Strandmann EP, et al. The Immune Microenvironment in Pancreatic Cancer. Int J Mol Sci. 2020 Jan;21(19):7307. doi:10.3390/ijms21197307
17. Guo J, Wang S, Gao Q. An integrated overview of the immunosuppression features in the tumor microenvironment of pancreatic cancer. Front Immunol. 2023 Sep 12;14. doi:10.3389/fimmu.2023.1258538
18. Pan Y, Yu Y, Wang X, Zhang T. Tumor-Associated Macrophages in Tumor Immunity. Front Immunol. 2020 Dec 3;11. doi:10.3389/fimmu.2020.583084
19. Li K, Shi H, Zhang B, Ou X, Ma Q, Chen Y, et al. Myeloid-derived suppressor cells as immunosuppressive regulators and therapeutic targets in cancer. Signal Transduct Target Ther. 2021 Oct 7;6(1):362. doi:10.1038/s41392-021-00670-9
20. Ullman NA, Burchard PR, Dunne RF, Linehan DC. Immunologic Strategies in Pancreatic Cancer: Making Cold Tumors Hot. J Clin Oncol. 2022 Aug 20;40(24):2789–805. doi:10.1200/JCO.21.02616
21. Ho MP, Jung M, Ung W, Skouradaki E, Baritaki S, Bonavida B. TGF-β–YY1 signaling as a key driver of immune evasion in pancreatic cancer: Therapeutic implications. Cytokine Growth Factor Rev. 2026 Apr 1;88:58–66. doi:10.1016/j.cytogfr.2026.01.005
22. Huang X, Li M, Hou S, Tian B. Role of the microbiome in systemic therapy for pancreatic ductal adenocarcinoma (Review). Int J Oncol. 2021 Dec 1;59(6):1–14. doi:10.3892/ijo.2021.5281
23. Safa AR. Drug and apoptosis resistance in cancer stem cells: a puzzle with many pieces. Cancer Drug Resist. 2022 Aug 2;5(4):850–72. doi:10.20517/cdr.2022.20 PubMed PMID: 36627897; PubMed Central PMCID: PMC9771762.
24. Valle S, Alcalá S, Martin-Hijano L, Cabezas-Sáinz P, Navarro D, Muñoz ER, et al. Exploiting oxidative phosphorylation to promote the stem and immunoevasive properties of pancreatic cancer stem cells. Nat Commun. 2020 Oct 16;11(1):5265. doi:10.1038/s41467-020-18954-z
25. Masoud R, Reyes-Castellanos G, Lac S, Garcia J, Dou S, Shintu L, et al. Targeting Mitochondrial Complex I Overcomes Chemoresistance in High OXPHOS Pancreatic Cancer. Cell Rep Med. 2020 Nov 17;1(8). doi:10.1016/j.xcrm.2020.100143 PubMed PMID: 33294863.
26. Liu X, Baer JM, Stone ML, Knolhoff BL, Hogg GD, Turner MC, et al. Stromal reprogramming overcomes resistance to RAS-MAPK inhibition to improve pancreas cancer responses to cytotoxic and immune therapy. Sci Transl Med. 2024 Oct 23;16(770):eado2402. doi:10.1126/scitranslmed.ado2402

27. Wu H, Fu M, Wu M, Cao Z, Zhang Q, Liu Z. Emerging mechanisms and promising approaches in pancreatic cancer metabolism. Cell Death Dis. 2024 Aug 1;15(8):553. doi:10.1038/s41419-024-06930-0
28. Loh CY, Arya A, Naema AF, Wong WF, Sethi G, Looi CY. Signal Transducer and Activator of Transcription (STATs) Proteins in Cancer and Inflammation: Functions and Therapeutic Implication. Front Oncol. 2019 Feb 21;9. doi:10.3389/fonc.2019.00048
29. Sgrignani J, Garofalo M, Matkovic M, Merulla J, Catapano CV, Cavalli A. Structural Biology of STAT3 and Its Implications for Anticancer Therapies Development. Int J Mol Sci. 2018 Jun;19(6):1591. doi:10.3390/ijms19061591
30. Zhang T, Kee WH, Seow KT, Fung W, Cao X. The Coiled-Coil Domain of Stat3 Is Essential for Its SH2 Domain-Mediated Receptor Binding and Subsequent Activation Induced by Epidermal Growth Factor and Interleukin-6. Mol Cell Biol. 2000 Oct 15;20(19):7132–9. doi:10.1128/MCB.20.19.7132-7139.2000 PubMed PMID: 10982829.
31. He Z, Song B, Zhu M, Liu J. Comprehensive pan-cancer analysis of STAT3 as a prognostic and immunological biomarker. Sci Rep. 2023 Mar 28;13(1):5069. doi:10.1038/s41598-023-31226-2
32. Rébé C, Ghiringhelli F. STAT3, a Master Regulator of Anti-Tumor Immune Response. Cancers. 2019 Sep;11(9):1280. doi:10.3390/cancers11091280
33. Yang R, Rincon M. Mitochondrial Stat3, the Need for Design Thinking. Int J Biol Sci. 2016 Feb 29;12(5):532–44. doi:10.7150/ijbs.15153
34. Corcoran RB, Contino G, Deshpande V, Tzatsos A, Conrad C, Benes CH, et al. STAT3 Plays a Critical Role in KRAS-Induced Pancreatic Tumorigenesis. Cancer Res. 2011 Jul 14;71(14):5020–9. doi:10.1158/0008-5472.CAN-11-0908
35. Li N, Grivennikov SI, Karin M. The Unholy Trinity: Inflammation, Cytokines, and STAT3 Shape The Cancer Microenvironment. Cancer Cell. 2011 Apr 12;19(4):429–31. doi:10.1016/j.ccr.2011.03.018 PubMed PMID: 21481782.
36. Hamel Z, Sanchez S, Standing D, Anant S. Role of STAT3 in pancreatic cancer. Explor Target Anti-Tumor Ther. 2024 Jan 17;5(1):20–33. doi:10.37349/etat.2024.00202
37. Huang C, Huang R, Chang W, Jiang T, Huang K, Cao J, et al. The Expression and Clinical Significance of pSTAT3, VEGF and VEGF-C in Pancreatic Adenocarcinoma. Neoplasma. 2012;59(01):52–61. doi:10.4149/neo_2012_007
38. Gritsko T, Williams A, Turkson J, Kaneko S, Bowman T, Huang M, et al. Persistent Activation of Stat3 Signaling Induces Survivin Gene Expression and Confers Resistance to Apoptosis in Human Breast Cancer Cells. Clin Cancer Res. 2006 Jan 1;12(1):11–9. doi:10.1158/1078-0432.CCR-04-1752
39. Thongchot S, Ferraresi A, Vidoni C, Salwa A, Vallino L, Kittirat Y, et al. Preclinical evidence for preventive and curative effects of resveratrol on xenograft cholangiocarcinogenesis. Cancer Lett. 2024 Feb 1;582:216589. doi:10.1016/j.canlet.2023.216589
40. Wu X, Tang W, Marquez RT, Li K, Highfill CA, He F, et al. Overcoming chemo/radio-resistance of pancreatic cancer by inhibiting STAT3 signaling. Oncotarget. 2016 Feb 12;7(10):11708–23. doi:10.18632/oncotarget.7336
41. Lankadasari MB, Aparna JS, Mohammed S, James S, Aoki K, Binu VS, et al. Targeting S1PR1/STAT3 loop abrogates desmoplasia and chemosensitizes pancreatic cancer to gemcitabine. Theranostics. 2018 Jun 13;8(14):3824–40. doi:10.7150/thno.25308

42. Oweida AJ, Mueller AC, Piper M, Milner D, Van Court B, Bhatia S, et al. Response to radiotherapy in pancreatic ductal adenocarcinoma is enhanced by inhibition of myeloid-derived suppressor cells using STAT3 anti-sense oligonucleotide. Cancer Immunol Immunother. 2021 Apr 1;70(4):989–1000. doi:10.1007/s00262-020-02701-w
43. Zou S, Tong Q, Liu B, Huang W, Tian Y, Fu X. Targeting STAT3 in Cancer Immunotherapy. Mol Cancer. 2020 Sep 24;19(1):145. doi:10.1186/s12943-020-01258-7
44. Poli V, Camporeale A. STAT3-Mediated Metabolic Reprograming in Cellular Transformation and Implications for Drug Resistance. Front Oncol. 2015 Jun 8;5. doi:10.3389/fonc.2015.00121
45. Yu H, Lee H, Herrmann A, Buettner R, Jove R. Revisiting STAT3 signalling in cancer: new and unexpected biological functions. Nat Rev Cancer. 2014 Nov;14(11):736–46. doi:10.1038/nrc3818
46. Rincon M, Pereira FV. A New Perspective: Mitochondrial Stat3 as a Regulator for Lymphocyte Function. Int J Mol Sci. 2018 Jun;19(6):1656. doi:10.3390/ijms19061656
47. Wegrzyn J, Potla R, Chwae YJ, Sepuri NBV, Zhang Q, Koeck T, et al. Function of Mitochondrial Stat3 in Cellular Respiration. Science. 2009 Feb 6;323(5915):793–7. doi:10.1126/science.1164551
48. Johnson DE, O'Keefe RA, Grandis JR. Targeting the IL-6/JAK/STAT3 signalling axis in cancer. Nat Rev Clin Oncol. 2018 Apr;15(4):234–48. doi:10.1038/nrclinonc.2018.8
49. Ho WJ, Jaffee EM, Zheng L. The tumour microenvironment in pancreatic cancer — clinical challenges and opportunities. Nat Rev Clin Oncol. 2020 Sep;17(9):527–40. doi:10.1038/s41571-020-0363-5
50. Olajubutu O, Ogundipe OD, Adebayo A, Adesina SK. Drug Delivery Strategies for the Treatment of Pancreatic Cancer. Pharmaceutics. 2023 May;15(5):1318. doi:10.3390/pharmaceutics15051318
51. Khan T, Nagarajan M, Kang I, Wu C, Wangpaichitr M. Targeting Metabolic Vulnerabilities to Combat Drug Resistance in Cancer Therapy. J Pers Med. 2025 Feb;15(2):50. doi:10.3390/jpm15020050
52. Wolpaw AJ, Dang CV. Exploiting Metabolic Vulnerabilities of Cancer with Precision and Accuracy. Trends Cell Biol. 2018 Mar 1;28(3):201–12. doi:10.1016/j.tcb.2017.11.006
53. Jin H, Wang L, Bernards R. Rational combinations of targeted cancer therapies: background, advances and challenges. Nat Rev Drug Discov. 2023 Mar;22(3):213–34. doi:10.1038/s41573-022-00615-z
54. Jia M, Zhang D, Zhang C, Li C. Nanoparticle-based delivery systems modulate the tumor microenvironment in pancreatic cancer for enhanced therapy. J Nanobiotechnology. 2021 Nov 22;19(1):384. doi:10.1186/s12951-021-01134-6
55. Pontón I, Sánchez-García D. Nanocarriers for Combination Therapy in Pancreatic Ductal Adenocarcinoma: A Comprehensive Review. Nanomaterials. 2025 Jan;15(15):1139. doi:10.3390/nano15151139
56. Su X, Wang Z, Duan S. Targeted drug delivery systems for pancreatic ductal adenocarcinoma: overcoming tumor microenvironment challenges with CAF-specific nanoparticles. J Natl Cancer Cent. 2023 Dec 1;3(4):306–9. doi:10.1016/j.jncc.2023.10.001

57. Conroy T, Bachet JB, Ayav A, Huguet F, Lambert A, Caramella C, et al. Current standards and new innovative approaches for treatment of pancreatic cancer. Eur J Cancer. 2016 Apr 1;57:10–22. doi:10.1016/j.ejca.2015.12.026 PubMed PMID: 26851397.
58. Wang XR, Jiang ZB, Xu C, Meng WY, Liu P, Zhang YZ, et al. Andrographolide suppresses non-small-cell lung cancer progression through induction of autophagy and antitumor immune response. Pharmacol Res. 2022 May 1;179:106198. doi:10.1016/j.phrs.2022.106198

Chapter 2:
Nanoplatforms for Drug Delivery and Immunomodulation

Abstract

Nanoplatforms have transformed cancer treatment by improving drug delivery and enabling more precise targeting of malignancies; however, limitations in formulation optimization, tumor penetration, and clinical translation remain significant challenges. Nanoparticles have shown promise in enhancing drug delivery and improving immune activation, with the potential for numerous modifications to tailor them for specific environments or targets. Integrating nanoplatforms offers a promising avenue to overcome these hurdles, enhancing treatment outcomes and reducing adverse effects. By improving drug delivery, targeting, and immune modulation, nanoplatforms can unlock the full potential of combinatorial therapies. This review explores the role of nanoplatforms in addressing these limitations and enhancing cancer treatment outcomes with chemotherapies and immunotherapies, examining various types of nanoplatforms. Understanding the mechanisms of immunomodulation through nanoplatform delivery is crucial. We discuss how these nanoplatforms interact with the tumor microenvironment, modulate tumor-associated macrophages and regulatory T cells, activate immune cells directly, enhance antigen presentation, and promote immunological memory. Further benefits include combination approaches integrating nanoplatforms with chemotherapy, radiotherapy, and phototherapy. This review aims to provide insights into the potential of nanoplatforms to enhance cancer therapies when paired with chemotherapies or immunotherapies, paving the way for more effective and personalized treatment strategies.

Key Words: Nanoplatforms, Combination therapy, Drug delivery, Immune activation, Tumor microenvironment, Nanomedicine, Cancer immunotherapy

2. Introduction

2.1.1 Overview of Nanoplatforms in Cancer Therapy

The occurrence and development of cancer is a multi-factor, multi-stage process involving numerous genetic, epigenetic, and environmental factors. Current cancer treatments, including radiotherapy, chemotherapy, and surgery, target both cancerous and healthy cells, leading to significant side effects. These conventional approaches, while often effective, come with several drawbacks, such as nausea, vomiting, hair loss, anemia, and even death (1,2). Nanotechnology has emerged as a promising strategy to overcome these limitations by improving how anticancer agents are delivered, retained, and released within tumors (3). Rather than relying on a drug's intrinsic potency, nanoplatforms can also be engineered to enhance solubility, prolong circulation time, increase tumor-selective accumulation, and reduce off-target toxicity. Nanoplatforms used in oncology span several major carrier classes, as illustrated in Figure 3: lipid-based nanoparticles (e.g., liposomes, solid lipid nanoparticles), polymeric nanoparticles (e.g., PLGA-based systems), inorganic nanoparticles (e.g., gold and silica nanoparticles), and protein-based carriers (e.g., albumin-bound formulations) (4). These platforms can be broadly grouped by function: drug-delivery vehicles designed primarily to improve pharmacokinetics and tumor penetration of cytotoxic or targeted agents, and immunomodulatory nanoplatforms designed to additionally engage or reprogram the immune system alongside drug delivery. Immunomodulatory nanoplatforms represent an important subset of this field. Because immunotherapy agents such as antibody therapeutics (ex. anti-HER2 and anti-CD20 antibodies), tumor vaccines, cytokines (ex. IFN, IL-2), and immune checkpoint inhibitors

(anti-PD-1/PD-L1, anti-CTLA-4) have transformed treatment across numerous malignancies, nanoparticle carriers have increasingly been used to improve their delivery, reduce systemic toxicity, and enhance immune cell targeting (5)(6)(7)(8)(9). For example, nanoparticles can co-deliver tumor antigens and immune adjuvants directly to antigen-presenting cells or carry adoptive cell therapy adjuncts that support engineered T-cell persistence, extending the reach of cellular and non-cellular immunotherapy strategies described in prior work (10)(11)(12). These applications illustrate that nanoplatforms are not simply passive carriers, but active enablers of both direct tumor-cell killing and immune-mediated antitumor responses.

2.1.2 Challenges in Current Drug Delivery Approaches

Despite this progress, current cancer therapies face several delivery-related challenges. In clinical trials, only 20–30% of patients achieve clinical responses to immune checkpoint inhibitors, reflecting limited treatment efficacy (13). Tumor heterogeneity, immune escape mechanisms, and individual patient variability in genome, epigenome, and immune status all contribute to inconsistent therapeutic outcomes (14)(18). Drug resistance further compromises efficacy across chemotherapy, radiotherapy, targeted therapy, and immunotherapy alike (15)(16). Immune-related adverse events (irAEs), including cytokine release syndrome and neurotoxicity, add additional risk when immune-activating agents are administered systemically without targeted delivery (17). As therapy progresses, prolonged drug exposure and accumulation drive co-evolution of the tumor and immune microenvironment, further eroding treatment efficacy over time (19).

With the development of nanotechnology, biological nanomaterials have received extensive attention as a strategy to directly address these delivery-related barriers (20). Nanomaterial-based drug carriers aim to overcome the limitations of conventional therapy by enhancing drug effects on target tissues, lowering systemic toxicity, and improving pharmacokinetics. When combined with conventional or immune-based therapies, nanoplatforms offer higher treatment efficiency, deeper tissue penetration, greater tumor specificity, and reduced toxic side effects, while also improving local and metastatic tumor control (21,22). Nanomaterials can further enhance the unique mechanisms of immunotherapeutic agents — for instance, through ligand-mediated binding and activation of immune cells or cytoplasmic delivery of immune-modulating drugs — and can be engineered to control the release or activation timing of therapeutic payloads (23). As nanotechnology and immunological understanding continue to advance in parallel, their convergence is positioned to drive significant breakthroughs in the diagnosis, treatment, and prevention of tumors.

2.1.2.1 PDAC-Specific Barriers to Drug Delivery and Immunotherapy

Pancreatic ductal adenocarcinoma presents particularly severe barriers to therapeutic delivery because a dense desmoplastic stroma, extensive extracellular matrix deposition, elevated interstitial fluid pressure, vascular compression, and poor tissue perfusion characterize its tumor microenvironment. These features restrict intratumoral drug distribution and can prevent systemically administered therapies from reaching therapeutically effective concentrations throughout the tumor. The fibrotic PDAC stroma is

largely maintained by cancer-associated fibroblasts and pancreatic stellate cells, which deposit extracellular matrix components such as collagen, fibronectin, and hyaluronan. (157,158)

Besides blocking drug access, the PDAC microenvironment also causes low oxygen, lack of nutrients, metabolic stress, and weakens the immune response. (159) These conditions help tumor cells adapt and resist chemotherapy, and they make it harder for cytotoxic T cells to enter and work in the tumor. PDAC tumors often have tumor-associated macrophages, myeloid-derived suppressor cells, regulatory T cells, and certain fibroblasts that together help the tumor avoid the immune system and make immunotherapy less effective (160,161)

Because of these challenges, there is a strong reason to use multifunctional nanoplatforms for PDAC. These nanoplatforms can do more than just carry drugs—they can help drugs stay stable, improve delivery inside the tumor, release drugs in response to low oxygen or acidic conditions, and deliver multiple agents that target both tumor cells and the cells in the tumor environment that suppress the immune system. To be effective, nanomedicines for PDAC will probably need to overcome both the tumor's own drug resistance and the barriers created by its microenvironment.

2.1.3 Nanotechnology-Based Solutions to Delivery and Immunotherapy Limitations

Recent advances in nanotechnology offer targeted solutions to the key delivery and efficacy challenges outlined above. First, to address immune evasion and tumor heterogeneity, nanoparticles can be engineered to co-deliver tumor antigens and immune

adjuvants directly to antigen-presenting cells, enhancing tumor recognition and stimulating robust antitumor immune responses. Lipid nanoparticles (LNPs), for example, can encapsulate both antigens and immunostimulatory molecules, improving dendritic cell activation and T-cell priming; gold nanoparticles (AuNPs) have similarly been shown to enhance immune activation by improving antigen delivery to dendritic cells and boosting antibody production (24). Second, to reduce systemic toxicity and irAEs, nanoplatforms enable targeted delivery of therapeutic agents to tumor tissue through surface modifications such as PEGylation or ligand conjugation. PEG-coated liposomes functionalized with folate ligands, for instance, selectively target folate receptors on tumor cells, increasing local drug accumulation while minimizing off-target exposure (25). Third, to improve low response rates, nanomaterials enhance drug accumulation and retention within tumors via the enhanced permeability and retention (EPR) effect, while enabling controlled, sustained release that increases local drug concentration and therapeutic efficacy (26). Abraxane, a nanoparticle albumin-bound paclitaxel formulation, illustrates this principle clinically — improving drug solubility, reducing toxicity, and enhancing tumor targeting through the EPR effect (27)(28).

Finally, to combat drug resistance, nanoparticles can be designed to bypass efflux-pump-mediated resistance or co-deliver combinations of agents (e.g., chemotherapeutics with siRNA) that suppress resistance pathways, thereby restoring or enhancing treatment effectiveness. Collectively, these nanotechnology-based strategies directly address the major barriers of poor tumor penetration, systemic toxicity, low response rates, and drug resistance — providing a rational, mechanistic basis for integrating nanoplatforms as a

delivery-focused, immunomodulation-capable framework for next-generation cancer therapy, including the STAT3-directed and OXPHOS-linked targeting strategies examined later in this thesis.

2.2 Types of Nanoplatforms

2.2.1 Lipid Nanoparticles

Nanoparticles (NPs) have emerged as versatile platforms for drug delivery and cancer treatment, offering unique advantages in targeting, efficacy, and reduced side effects. This section explores three significant categories of nanoparticles: LNPs, Metal nanoparticles (MNPs), and Polymer nanoparticles (PNPs), and Organic nanoparticles (ONP), as illustrated in Figure 2a. Each type possesses distinct properties and applications in cancer therapy, from enhancing drug delivery to stimulating immune responses. LNPs are spherical lipid structures made from amphiphilic lipids. Due to their large aqueous compartments, liposome-based LNPs are often used as nanosized drug delivery vehicles and are perhaps the most frequent LNP platform used for cancer treatment.(29) Common substances encapsulated in liposomes include biomolecules like nucleic acids (30) ; chemotherapeutics such as doxorubicin (31), paclitaxel (32), and gemcitabine (33); and immune checkpoint inhibitors. (34) (35) LNPs offer several advantages in cancer therapy, including improved drug stability, enhanced tumor targeting through the enhanced permeability and retention (EPR) effect, reduced systemic toxicity, and the ability to carry both hydrophilic and hydrophobic drugs, making them highly versatile for different therapeutic applications.(36)

Lipid nanoparticles are important for the future development of YXL-182, a small-molecule STAT3 inhibitor that builds up in mitochondria and was studied in Chapter 3. While YXL-182 showed activity in preclinical tests as a free compound, its use as a therapy may be limited by issues common to small molecules, such as being cleared from the body too quickly, poor water solubility, unwanted effects on other targets, and trouble reaching the poorly supplied PDAC tumor environment.

Using a lipid nanoparticle formulation could make YXL-182 more stable, improve how it moves through the body, increase its concentration in PDAC tumors, and lower side effects. Lipid nanoparticles could also allow YXL-182 to be given together with gemcitabine or immune-activating agents, which could combine blocking STAT3 signaling with making chemotherapy more effective or boosting the immune response. (162,163)

This approach is a possible next step for this research. Encapsulating YXL-182 could help it get past the delivery challenges in PDAC while still allowing it to target both regular and mitochondrial STAT3 signaling.

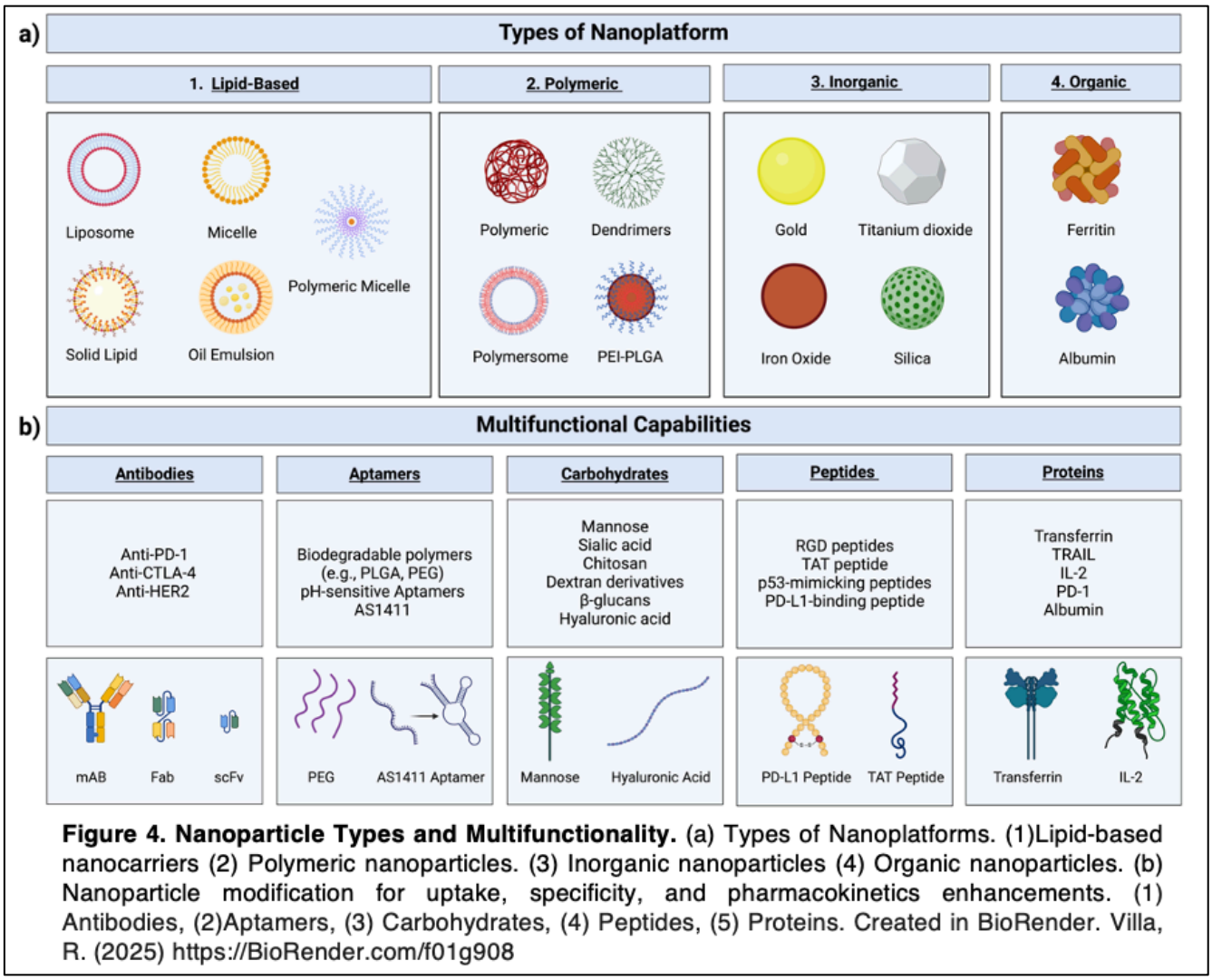

Figure 4. Nanoparticle Types and Multifunctionality. (a) Types of Nanoplatforms. (1)Lipid-based nanocarriers (2) Polymeric nanoparticles. (3) Inorganic nanoparticles (4) Organic nanoparticles. (b) Nanoparticle modification for uptake, specificity, and pharmacokinetics enhancements. (1) Antibodies, (2)Aptamers, (3) Carbohydrates, (4) Peptides, (5) Proteins. Created in BioRender. Villa, R. (2025) https://BioRender.com/f01g908

2.2.2 Metal Nanoparticles

MNPs can be synthesized from various metals, each exhibiting unique properties. (37) Among these, gold, silver, and iron nanoparticles have emerged as the most widely studied and applied in multiple fields, particularly within nanoplatforms for drug delivery.(38,39) Due to their small size, MNPs exhibit strong enhanced permeability and retention (EPR) effects. Among these, gold nanoparticles (AuNPs) are particularly notable for their versatile surface modification capabilities. The first AuNPs used as drug delivery

vehicles were reported by Paciottii et al. 2004 and used for the targeted delivery of covalently attached tumor necrosis factor (TNF) to MC-38 colon carcinoma tumors in mice models. Concerning immune stimulation, AuNPs have been shown to enhance immune activation via more effective delivery of antigens to antigen-presenting cells, such as DCs, and enhance antibody production. (24,40) Silver nanoparticles (AgNPs) are another type of MNP used for drug delivery and have noted cytotoxicity against mammalian cell types, highlighting their therapeutic potential as anticancer agents. (41) Another set of MNPs with its characteristics are Iron-oxide nanoparticles (IONPs), which possess magnetic properties. (42) They are compatible with Magnetic Resonance Imaging (MRI) for monitoring immune cell migration and trafficking. (43) Because of IONPs' magnetic sensitivity, a magnetic field can aid their localization to specific tissues. (39)

2.2.3 Polymer Nanoparticles

Polymer nanoparticles are particles made from a variety of polymers, both synthetic and natural, such as polyethylene glycol (PEG) or polylactide-co-glycolide (PLGA). (44) Dendrimers are a popular class of PNPs made from a series of repeating units or monomers and are defined as 'highly branched, spherical macromolecules. (45) Dendrimer-encapsulated nanoparticles (DENs) usually refer to structures made from polyamide amine (PAMAM), polypropylene imine (PPI), polylysine (PPL), and polyester building blocks. (46) Polyethylene dendrimers have been used as delivery agents with covalently bound doxorubicin. (47) Polymeric nanoparticles offer several advantages for drug delivery, including controllable size, shape, and surface charge

2.2.4 Organic Nanoparticles

Natural PNPs are made from naturally occurring polymers such as peptides and proteins and offer the distinct advantage of being biocompatible and biodegradable nanomaterials. Protein nanocages are an example of natural PNPs and are a class of delivery vehicles that rely on using proteins as (self-assembling) molecular building blocks. Due to many heat shock proteins (HSPs) being overexpressed in cancerous cells, HSPs have been isolated and used to make the nanocage scaffold, and because nanocages have a particular propensity to localize to dendritic cells, the provided cancer antigens isolated from cancerous tissue help to initiate a stronger immunological response by the host. Commonly used proteins for generating protein nanocages include albumin and ferritin. (48,49) Albumin-based nanoparticles benefit from high biocompatibility, long circulation half-life, and the ability to target tumors via gp60 and SPARC receptors, making them highly effective for drug delivery and reducing off-target toxicity. (50)(51) Ferritin nanocages, on the other hand, can specifically target tumor cells through transferrin receptor 1, and their hollow structure allows for efficient encapsulation and delivery of a variety of therapeutic agents, with minimal immunogenic response. (52)(53) The use of these organic protein-based nanocarriers not only improves drug solubility and stability but also enables precise tumor targeting and reduced systemic side effects, making them highly promising platforms for cancer therapy.

While the structural and physicochemical properties of these nanoplatforms provide fundamental advantages for drug delivery, their true value in cancer immunotherapy stems from how these properties translate to enhanced immunomodulatory functions. Each nanoplatform category interacts uniquely with the immune system to overcome specific

barriers in cancer immunotherapy. Lipid nanoparticles excel in delivering immune-activating payloads like nucleic acids that stimulate pattern recognition receptors, while their ability to co-deliver antigens and adjuvants creates potent cancer vaccines. (54) Metal nanoparticles, particularly AuNPs, not only serve as delivery vehicles but actively modulate dendritic cell maturation and antigen presentation, crucial steps in T cell priming. The inherent cytotoxicity of AgNPs contributes to immunogenic cell death, releasing tumor-associated antigens that further stimulate immune responses. (55) Meanwhile, IONPs combine magnetic targeting with immunomodulatory capabilities, enabling both spatial control of therapy and enhanced T cell activation. [44] The following sections explore how these intrinsic properties of each nanoplatform directly enhance anti-cancer immune responses through specific mechanistic pathways.

2.3. Advantages of Nanoplatforms

2.3.1 Nanoplatform Modifications

Improving immunotherapy has been a constant goal for many researchers as immunotherapy treatment has shown remarkable success in treating various types of cancers with more manageable side effects. Nanoplatforms are being engineered with modifications to enhance targeting, overcome biological barriers, and provide multifunctional capabilities, significantly improving drug delivery compared to traditional immunotherapies. (56)(57) Introducing nanoplatforms with Immune therapies unlocks new avenues and applications for therapeutic approaches. PEG, a hydrophilic polymer, is widely used in pharmaceutical formulations, improving drug stability and circulation time, and reduces overall immune responses through a process known as "PEGylation". (58) (59). For

example, PEG-coated liposomes attached with folate ligands specifically target folate receptors on tumor cells, increasing drug accumulation at the tumor site while minimizing off-target effects. (60)(61)

Another common surface modification involves using pectin, a natural polysaccharide, which has been applied to gold AuNPs for targeted delivery of doxorubicin to hepatocyte (HepG2) cells. These pectin-coated AuNPs demonstrated enhanced cellular uptake via clathrin-mediated endocytosis and showed significantly higher cytotoxicity against HepG2 cells than non-targeted formulations. (62) Similarly, AgNPs modified with the cell-penetrating peptide TAT have been shown to increase the localization of doxorubicin in MCF-7 xenograft tumors in mice, with 6.7 ± 2.4% of the injected dose accumulating in tumor tissue compared to significantly lower accumulation in non-targeted systems. (63) These examples illustrate how surface modifications such as PEGylation, ligand conjugation, and functional coatings enhance nanoparticle targeting by improving drug accumulation at tumor sites and reducing systemic toxicity compared to conventional delivery systems. Transferrin-functionalized nanoparticles, which bind to transferrin receptors commonly overexpressed in cancer cells, have also demonstrated significant improvements in targeting and drug delivery. Transferrin-conjugated nanographene oxide (Tf-NGO) nanoplatforms loaded with platinum complexes exhibited a 2.5-fold increase in cellular uptake and drug retention in MCF-7 tumor spheroids compared to free platinum complexes, significantly improving anticancer efficacy by inhibiting tumor cell migration and invasion. (25) (64)

Similarly, antibody-functionalized nanoparticles offer precise targeting capabilities. Monoclonal antibody-functionalized magnetic nanoparticles (MgNPs) loaded with doxorubicin demonstrated selective accumulation in Met/HGFR-positive tumors, dispersing throughout the tumor mass more effectively than non-functionalized MgNP. This enhanced targeting increased drug retention within the tumor and reduced systemic toxicity, with a 1.8-fold greater dispersion within Met/HGFR-positive xenograft tumors compared to bare MNPs, highlighting their potential for precise drug delivery. (65)(66) Red blood cell membrane-coated nanoparticles also mimic natural "self" markers like CD47 to evade immune detection and extend circulation time. A study demonstrated that Fe3O4 nanoparticles coated with red blood cell membranes (Fe3O4@RBC NPs) exhibited significantly extended circulation half-life of RBC-NPs was calculated to be 39.6 hours, compared to 15.8 hours for PEG-coated nanoparticles. (67) This biomimetic approach leverages the CD47 protein on RBC membranes as a "don't eat me" signal to macrophages, effectively escaping immune clearance and prolonging circulation. (68) These examples underscore the effectiveness of ligand-based functionalization in improving drug accumulation, retention, and therapeutic outcomes in cancer treatment. These modifications enable active targeting by leveraging the interaction between ligands and specific surface receptors, providing superior drug delivery efficiency and therapeutic efficacy compared to passive targeting or unmodified systems.

2.3.2 Stimuli Response

Stimuli-responsive designs allow for further refined targeting by releasing drugs in response to specific conditions like acidic pH or hypoxia, conditions found within the tumor. (69) An example includes pH-sensitive chitosan-coated nickel nanotubes that release drugs

selectively in acidic tumor environments, achieving 2.5 times higher drug release compared to neutral pH. (70) The Li et al. group developed a Trojan-Horse nanoparticle (pPhD NP), which responds to the acidic tumor microenvironment by shedding their PEG coating, which crosslinks the nanoparticle, resulting in a size reduction from 79 nm to accommodate hundreds of ultra-small (approximately 4 nm) drug-loaded nanoparticles, facilitating cellular uptake. (71) Size-transformable bicomponent peptide nanoparticles developed by Ma et al. respond to both the acidic tumor microenvironment and near-infrared laser irradiation, inducing a size-shrinkage effect from their initial size of approximately 120 nm to smaller particles of around 40 nm upon entering the tumor microenvironment, significantly enhancing tumor penetration. (72) Transformable nanoparticles, which change size or shape during delivery, address the paradox of larger particles being retained longer in circulation but struggling to penetrate tumors. As shown in Figure 2b, nanoparticle modifications—including antibodies, aptamers, carbohydrates, peptides, and proteins—enhance uptake, specificity, and pharmacokinetics, offering tailored solutions for therapeutic applications. These systems maintain optimal drug ratios and release profiles, improving bioavailability and overcoming resistance mechanisms in cancer cells. Innovations in targeting and multifunctionality mark a significant advancement over traditional drug delivery systems by enhancing specificity and efficacy utilizing these platforms.

Stimuli-responsive nanoplatforms could be especially useful for treating PDAC, since this disease often involves low oxygen, oxidative stress, acidic areas, and changes in the extracellular matrix. These conditions can be used to trigger the targeted release of YXL-

182 once nanoparticles build up in the tumor. For instance, systems that respond to pH or reactive oxygen species can help prevent early drug release in the bloodstream and increase release in stressed PDAC tissue. (164) Systems that respond to matrix-remodeling enzymes may also help in desmoplastic tumors, where fibroblasts and tumor cells change the extracellular matrix. (165) These strategies may boost local delivery of YXL-182 and lower the risk of the drug affecting healthy tissue.

2.4 Mechanisms of Immunomodulation:

2.4.1 Tumor-associated macrophages (TAMs) and Regulatory T cells (T-reg)

The immune system can be classified as innate or adaptive immunity to monitor abnormal cell growth, such as cancerous cell development. Innate immunity is the first line of defense and employs macrophages, dendritic cells, and natural killer cells to detect and respond rapidly to tumor-associated antigens. (73) Immunogenic cell death (ICD) bridges innate and adaptive immunity in cancer therapy by releasing danger-associated molecular patterns (DAMPs) like calreticulin, ATP, and HMGB1, which activate the immune system against cancer. (74) These signals enhance the recruitment and maturation of dendritic cells, mainly antigen-presenting cells, to present tumor antigens and promote adaptive immunity with more targeted responses. (75) Despite the delicate immune surveillance networks, tumors still can escape from the T cell activity by expressing immune checkpoints, such as PD1/PDL1 and CTLA-1, promoting the activation of T regulatory cells, myeloid-derived suppressor cells (MDSCs), and some inhibitory cytokines like TGF-β and IL-10. (76)

(77) (78) (79) Thus, manipulating nanoparticles to polarize TAM from M2 to M1 showed great potential for reprogramming an immunosuppressive tumor micro-environment (TME).

A group developed mesoporous Prussian blue nanoparticles modified with hyaluronic acid on their surface (LMWHA-MPB). It could be used as an in-situ macrophages converter to remodel pro-tumor M2 to anti-tumor M1 type. LMWHA-MPB selectively accumulates in tumor sites and generates plenty of oxygen, alleviating tumor hypoxia via the catalytic decomposition of endogenous hydrogen peroxide. (80) M2-like macrophage-targeting nanoparticle (PNP@R@M-T), encapsulated with a peptide sequence M2pep and potent driver of macrophage reprogramming resiquimod (R848), and the surface modified with abundant CD47 (don't eat me signal) and B16-OVA melanoma cell membrane to extend the accumulation at tumor sites. As a result, it showed more selectively delivered drugs to 58% of M2-like TAMs compared to 39% of M1-like TAMs and 32% of dendritic cells. It dramatically reprogrammed the M2-like TAMs, reduced tumor size, and prolonged survival. (81) These innovative nanoparticle-based approaches demonstrate significant potential for reprogramming tumor-associated macrophages from the pro-tumor M2 phenotype to the anti-tumor M1 phenotype, with other benefits including targeted delivery, reduced systemic toxicity, and enhanced anti-tumor immune responses.

2.4.2 Direct Immune Cell Activation

Nanoplatforms have also been employed as immunostimulants to directly activate immune cells, such as natural killer (NK) cells, cytotoxic T cells, and DCs. As innate immune cells, NK cells can detect abnormal cell proliferation and secrete cytotoxic granules to increase cell permeability and activate the apoptotic pathway without dependent antigen

presentation. (82) (83) (84) A group developed lipid nanoparticles containing siRNAs targeting SHP-1, Cb1-b, and c-Cbl to enhance NK cell activation. These nanoparticles reversed the inhibition of NK cell toxicity, provided target specificity for NK92 NKp46high and YTS-2DL1 NK cells, and downregulated intrinsic inhibitory signals, unleashing NK cell activation without inducing aberrant activity. (85) Besides NK cells, DCs, the primary antigen-presenting cells (APCs) in cancer, serve as another critical bridge between innate and adaptive immunity. It could be activated by toll-like receptor (TLR) stimulation and promote pro-inflammatory responses, such as the secretion of IL-12 to reactivate NK cells leading to tumor-killing activity. (86) Perry et al. used particle replication in nonwetting templates (PRINT) nanoparticles to deliver CpG, a TLR9 agonist, which enhances pro-inflammatory cytokine expression in lung tumor models. The PRINT-CpG exhibited local therapeutic efficacy through the retention of CpG within the lungs and enhanced the expression of pro-inflammatory cytokines IL-6, IL-12 p40, TNF-α, and IFN-γ in the tumor site and with no influence of cytokine expression in the serum. (87)

Given the increasing attention to immunotherapy, modulating cytotoxic T cells is necessary since their activation, persistence, and exhaustion status directly determine the efficacy of tumor eradication and the ability to overcome immunosuppressive tumor microenvironments. (88) To elevate the therapeutic efficacy of adoptive T cell transfer therapy and avoid T cell exhaustion in the immunosuppressive TME, Kang et al. created T cell-membrane-coated nanoparticles (TCMNPs) to target tumor cells and restore cytotoxic functions in CTLs by blocking immune checkpoint PD-L1 interaction. Additionally, unlike the adoptive T-cell therapy, the anti-tumoral effects of TCMNPs are tumor antigen-nonspecific

responses, showing anti-tumoral effects on multiple types of tumors. (89) Chimeric antigen receptor (CAR)-T cell transfer therapy has also shown promising potential for tumor treatment but faces challenges in solid tumors due to immunosuppression, antigen heterogeneity, and physical barriers, potentially causing cytokine release syndrome and off-tumor toxicity. (90)

To combat this problem, Zhang et al. developed targeted nanocarriers that deliver a combination of tumor-targeting peptide iRGD loaded with PI3K inhibitor and α-GalCer agonist of therapeutic T cells, allowing the removal of protumor cell populations and simultaneously stimulating antitumor effector cells. After the repeated infusions of the nanoparticles before the CAR-T cell therapy, the nanoparticle treatment enabled tumor-specific CAR-T cells to home to the lesion; triggering tumor regression in the 4T1 breast cancer murine model, which didn't show responsiveness to conventional infusion of CAR-T cells. (91) By directly activating immune cells such as NK cells, DCs, and cytotoxic T cells, these nanoplatforms can overcome immunosuppressive barriers in the tumor microenvironment. Furthermore, their ability to improve the efficacy of adoptive cell transfer therapies, including CAR-T cell therapy, highlights the versatility and promise of nanoplatform-based approaches in expanding cancer treatment strategies.

2.4.3 Antigen-presenting Enhancement

Recent advancements in nanotechnology have led to the development of innovative nanoparticle-based strategies that enhance cancer immunotherapy by improving the delivery and efficacy of immune-modulating agents. A recent study developed multilevel lipid rewiring nanoparticles for tumor-associated dendritic cell (TADC) revitalization, which

specifically bind to the lipid transport receptor Msr1 on the TADC surface and restrict the extracellular lipid uptake, cytoplasmic de novo lipid biosynthesis, and nuclear lipogenic gene transcription. As a result, the slimming of TADCs induces their maturation and reconstructs their function in inflammatory cytokine production, cytotoxic T cell recruitment, the inhibition of tumor growth in 4T1-bearing mice and further overcomes the tumor resistance to immune checkpoint blockade therapy. (92) Levy's et. al 2021 group developed immune-agonistic nanoparticles (iaNPs) combining TLR9, STING, and RIG-I agonists with melanoma-specific peptides to enhance interferon production and APC activation. This iaNPs improved cancer immunotherapy by protecting agonists, increasing systemic half-life, and reducing tumor burden in melanoma models. (93) The encapsulated peptides sensitized T-cells to target melanoma cells, increasing cytokine secretion and tumor cell killing. Vaccines represent an antigen-specific strategy in cancer treatment designed to stimulate the immune system to recognize and target tumor-specific or tumor-associated antigens.

Still, intrinsic suppressive mechanisms like SOCS1 upregulation in dendritic cells (DCs) often limit their efficacy. (94) Nanoparticles can optimize antigen delivery and APC activation, enhancing adaptive immune responses. Yu et al. developed lipid nanoparticles to deliver SOCS1 siRNA into DCs, improving their antigen presentation and pro-inflammatory factor secretion. This results in potent tumor prevention and suppression in melanoma-bearing mice. This SOCS1 silencing resulted in enhanced DC function, including increased expression of co-stimulatory molecules CD80 and CD86, enhanced secretion of pro-inflammatory cytokines IL-12 and TNF-α, and improved antigen presentation capacity,

resulting in potent tumor prevention. (95) This approach demonstrates the potential of using LNP-mediated siRNA delivery to engineer more potent DCs for cancer immunotherapy, highlighting the versatility of nanoplatforms in advancing cancer treatment strategies.

2.4.4 Immunological Memory

Tumor metastasis and recurrence remain significant challenges in current clinical cancer treatment. While immune checkpoint inhibitors have shown clinical efficacy across various cancer types, they are ineffective in many patients, with only 20–40% achieving long-term survival three years post-treatment. (96) Therefore, the impact of immunotherapies on specific antitumor T helper cells that possess antigen-specific immune responses and immunogenic memory has become a focal point of intensive research. Neek et al. combined protein nanoparticle vaccines with immune checkpoint inhibitors to improve antitumor efficacy in the B16-F10 melanoma model. The E2-derived nanoparticle (25 nm diameter) simultaneously delivered CpG and a gp100 melanoma antigen epitope. CpG-gp-E2 nanoparticles increased antigen-specific IFN-γ secretion, delayed tumor development, and prolonged survival. They augmented tumor-infiltrating CD8 T cells, decreased MHC-I expression on tumor surfaces, and elicited a more efficient and durable immune response than anti-PD1 or CpG alone. (97) Cold tumors are another clinical challenge, with limited immune activity within the tumor microenvironment. They typically have low levels of tumor-infiltrating lymphocytes, low expression of MHC class I and immune checkpoints like PD-L1, and a low tumor mutational burden. (98) This lack of immune cell infiltration and activation renders cold tumors resistant to many immunotherapy approaches, as illustrated in **Figure 4:** Key Pathways of Tumor-Mediated Immune Suppression.

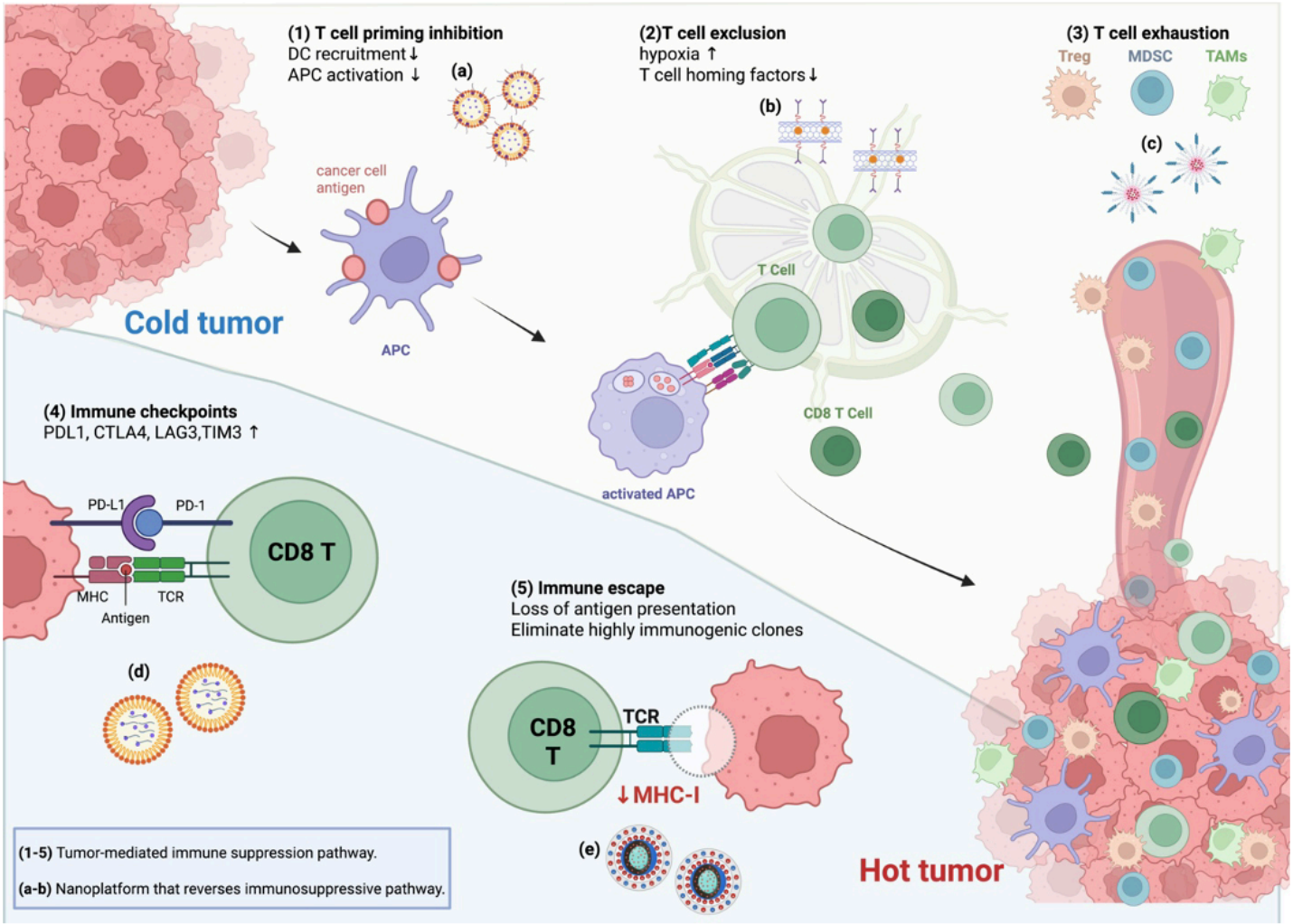

Figure 5. Key pathways of tumor-mediated immune suppression and representative nanoplatform strategies that counteract these mechanisms. (1) Inhibition of T cell priming, preventing the initiation of an effective immune response; (2) T cell exclusion, physically preventing T cells from reaching the tumor; (3) T cell exhaustion, leading to a loss of T cell function; (4) Activation of immune checkpoints, suppressing T cell activity; and (5) Immune escape, allowing the tumor to evade immune detection and destruction. (a) PLGA nanoparticles encapsulating ovalbumin (OVA) antigen and TLR ligands have been shown to enhance DC activation, cross-presentation, and potentiate CD8+ T cell responses. (b) Copper(II) metal-organic framework (MOF) nanosheet enhanced with platinum nanoparticles and folate (Cu-TCPP(Al)-Pt-FA) target the tumor microenvironment, deplete glutathione, relieve hypoxia, and enhance cytotoxic T lymphocyte (CTL) infiltration. (c) Mannose-modified polymeric micelles delivering mRNA encoding IRF-5 and IKKβ specifically target M2 tumor-associated macrophages (TAMs), reprogramming them toward an M1 phenotype and enhancing antitumor immunity. (d) PLGA nanoparticles encapsulating PD-L1, and PD-1 siRNA restore CD8+ T cell function and promote cytotoxic T cell responses, outperforming antibody-based treatments in preclinical models. (e)Charge-switchable nanoparticles co-loaded with JQ1, and doxorubicin (DOX) induce ICD and inhibit the PD-L1 pathway, boosting chemo-immunotherapy efficacy and increasing CTL infiltration. Created in BioRender. Mahri, S. (2025) https://BioRender.com/m5r7rsn

2.5 Combination Approaches with Nanoplatforms:

2.5.1 Combination with Chemotherapy

Chemotherapy has been a foundational treatment in oncology for years. Recent studies have highlighted the ability of specific chemotherapeutic agents to induce immunogenic cell death (ICD), a process that leads to the release of tumor antigens and damage-associated molecular patterns (DAMPs), which activate immune effector cells. (99) (100) (101) (102) While chemotherapy-induced ICD can generate local immune activation, it often fails to trigger a robust systemic antitumor immune response. This limitation can be attributed to multiple factors, including the TME and insufficient antigen presentation. In addition, chemotherapy can induce immune resistance by upregulating immune checkpoint molecules such as programmed cell death protein ligand 1(PD-L1) and interfering with the differentiation and function of immune cells, which further suppresses the immune response.(103) (104) To overcome these challenges, the co-delivery of chemotherapeutic agents and immunomodulators using NPs has emerged as a potential solution. (105) (106) (107) By delivering both agents simultaneously to the tumor site, this combinatorial approach has the potential to produce synergistic effects, effectively killing cancer cells and activating the immune system, thereby enhancing overall therapeutic efficacy.

A recent study introduced self-delivery nano-PROTACs (DdLD NPs) for colorectal cancer treatment. (108) The DdLD NPs are formed through the self-assembly of doxorubicin (DOX), dBET57 (a BRD4 degrader), and DSPE-PEG2000, allowing for the efficient co-delivery of both the chemotherapeutic agent and immunomodulator to the tumor site. The combination of DOX and dBET57 induces tumor cell death, promotes ICD, and inhibits

tumor glycolysis and lower PD-L1 expression through BRD4 degradation, effectively avoiding adaptive immune resistance. PD-L1 is a critical immune checkpoint protein expressed on tumor cells that enables tumors to evade immune surveillance. By reducing PD-L1 expression, DdLD NPs restore T cell activation and antitumor immunity, effectively enhancing the immune system's ability to target and destroy cancer cells. Additionally, the induction of ICD by DOX facilitates the release of tumor-associated antigens, which are taken up by dendritic cells to prime cytotoxic T cells. This synergistic mechanism not only disrupts tumor survival pathways but also amplifies immune responses, demonstrating the immunotherapeutic potential of DdLD NPs. These self-delivery DdLD NPs systemically activated antitumor immunity, significantly suppressing both primary and metastatic colorectal cancer progression. By combining direct tumor killing with immune modulation, this nanoplatform offers a promising approach for chemoimmunotherapy.

Studies indicate that accumulating tumor-associated macrophages correlates with poor clinical outcomes. In response, Song et al. developed tumor microenvironment-sensitive cluster nanoparticles (BLZ-945SCNs/Pt) for spatial targeting of TAMs and tumor cells. (109) BLZ-945SCNs/Pt were self-assembled from a Pt-prodrug-conjugated amphiphilic copolymer with the colony-stimulating factor 1 (CSF-1R) BLZ-945 receptor inhibitor encapsulated within the nanoparticles. Upon reaching the tumor site, the SCNs undergo a pH-triggered transition that leads to the rapid release of BLZ-945 in the perivascular regions, where TAMs are predominantly located. This targeted release inhibits the CSF-1/CSF-1R signaling pathway and facilitates the depletion of TAMs. The Pt-prodrug, carried by small nanoparticles, is released in deeper tumor tissues, efficiently killing cancer

cells. Treatment with BLZ-945SCNs/Pt not only induces cancer cell death but also modulates the tumor immune environment, ultimately achieving a synergistic chemoimmunotherapy effect.

2.5.2 Combination with Phototherapy

Phototherapy, including photodynamic therapy (PDT) and photothermal therapy (PTT), employs light and photosensitizers (PS) to kill tumor cells. (110) (111) PDT generates reactive oxygen species (ROS) upon laser irradiation, while PTT uses light-induced heat to induce cell death. (112) As a minimally invasive and localized therapy, PDT has been clinically applied to treat head, neck, bladder, and skin cancers (10.1038/s41571-020-0410-2). Although PTT has not yet been used in clinics, several PTT agents, including gold-based nanoparticles, are currently being evaluated in clinical trials. (113) Beyond their direct cytotoxic effects, PDT and PTT can also induce ICD. (114) (115) Moreover, ROS generated during PDT has been shown to polarize macrophages toward the M1 phenotype, supporting antitumor immunity. (116) (117) The heat generated by PTT increases the blood flow and disrupts tumor vasculature, leading to increased permeability and enhanced immune cell infiltration into the TME. (112) (113) Therefore, to further improve the therapeutic efficacy of phototherapy, a promising strategy is the co-delivery of PS and immunomodulatory agents using nanoplatforms. This combination ensures precise tumor targeting and localized activation of both PS and the immune system, effectively eliminating the primary tumor while amplifying the antitumor immune response. Additionally, it induces long-term immunity, potentially preventing metastasis and tumor recurrence. (118)

Nano-super artificial dendritic cells (saDC@Fs-NPs) were reported to facilitate tumor photodynamic immunotherapy (10.1002/adma.202208555). The outer membrane of saDC@Fs-NPs, derived from 4T1 cells, presents peptide-major histocompatibility complex I and CD86 to activate T-cells directly. Including anti-LAG3 antibodies on the membrane helps reverse T-cell exhaustion, thus boosting the ability of the immune system to recognize and attack tumor cells. Meanwhile, the inner PS of the saDC@Fs-NPs enhances the release of DAMPs through PDT-induced ICD, transforming "cold tumors" into "hot tumors" and improving the tumor immune's microenvironment. This study demonstrates the potential of using nano-engineered dendritic cells to enhance the efficiency of cancer photodynamic immunotherapy. PTT alone has limited clinical therapeutic benefits, primarily due to the upregulation of key immunosuppressive pathways, such as PD-L1 and indoleamine 2,3-dioxygenase 1 (IDO-1). To address this limitation, Lei et al. developed a bispecific nano modulator to enhance the efficacy of PTT. (119) The nano modulator is self-assembled from indocyanine green (ICG), a BRD4 inhibitor (JQ1), and an IDO-1 inhibitor (BMS986205) without any excipients. The ICG functions as a PS for PTT, while JQ1 downregulates PD-L1 expression, and BMS inhibits IDO-1 activity. The bispecific nano modulator efficiently induces PTT and ICD upon laser irradiation. The nano modulator reverses PTT-mediated upregulation of PD-L1 and IDO-1, thereby enhancing CD8+ T cell infiltration and increasing levels of TNF-α and IFN-γ in tumors.

2.5.3 Combination with Radiotherapy

Radiotherapy (RT) is one of the most widely used and effective treatment modalities for cancer, with nearly 50% of patients receiving RT as part of their treatment. (120) (121)

Research has demonstrated that RT can reshape the TME and modulate the immune response. However, these effects are generally insufficient to elicit a systemic immune response. RT can also promote immunosuppressive mechanisms, such as the increased level and infiltration of regulatory T cells (Tregs). (122) (123) Thus, RT is often ineffective against metastasis and fails to prevent tumor recurrence. Clinical trials have explored multimodal approaches to improve tumor response, including RT and immunotherapy. (Keam et al.) (125) Clinical data have not shown statistically significant improvements in tumor response with radio-immunotherapy compared to monotherapy. (126) (127) Several factors contribute to these limited outcomes, including off-target effects of immune adjuvants and radioactive agents and the development of innate and adaptive resistance. Nanoplatforms, integrated active targeting, and controlled drug release hold promise for overcoming these challenges.

For instance, Yanxian et al. developed core cross linked di-selenide nanoparticles (dSeNPs) as carriers for radio-responsive delivery of the toll-like receptors 7/8 agonist (R848). (128) The R848@dSeNPs were synthesized by cross-linking an amphiphilic block copolymer with di-selenide linkers, encapsulating R848 inside the nanoparticles. These nanoparticles exhibited dose- and time-dependent radiosensitivity, enabling X-ray irradiation-based, spatiotemporal control over the release of R848. In vivo studies showed that the local, radio-responsive release of R848 significantly enhanced the synergistic efficacy of combined radioimmunotherapy by promoting macrophage polarization, dendritic cell maturation, and cytotoxic T cell activation, ultimately improving tumor treatment outcomes. In another work, MnO2 nanoparticles loaded with anti-programmed death ligand

1 (αPDL1@MnO2) have been reported to strengthen RT-induced systemic antitumor immune responses. (129) The released Mn2+ ions from αPDL1@MnO2 under acidic tumor pH can activate the stimulator of the interferon genes (STING) pathway, facilitating the secretion of IFN-β and maturation of BMDCs. Additionally, the release of αPDL1 from αPDL1@MnO2 nanoparticles further promotes the intertumoral infiltration of cytotoxic T lymphocytes (CTLs).

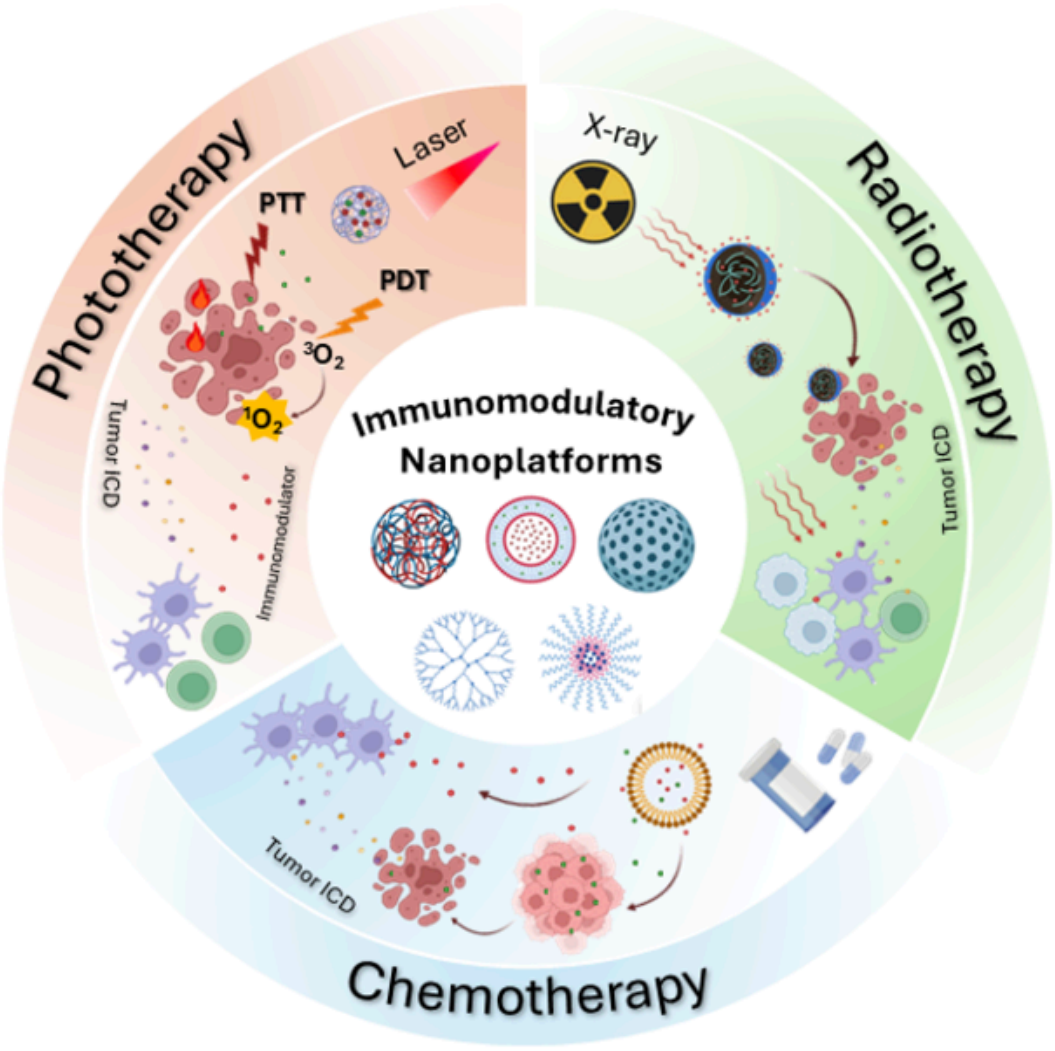

Figure 6. This illustration showcases the various approaches to combinational tumor therapy—chemotherapy, radiotherapy, and phototherapy—using nanoplatforms.

The combination of αPDL1@MnO2 and RT inhibited the growth of primary tumors and triggered systemic antitumor immunity, resulting in a pronounced abscopal effect that effectively inhibits tumor metastasis. In summary, combining nanoplatforms with traditional therapies offers synergistic effects to overcome limitations in cancer treatment, as visualized in Figure 4, which showcases diverse combinational approaches to tumor therapy.

2.6 Clinical Studies

Combining nanoplatforms with immunotherapy shows promise in various cancer treatments, and several clinical trials assessing the safety and efficacy of these combinations are underway. Unlike preclinical studies, these combinations are given as separate drugs and never integrated into the same nanoplatform. Clinical outcomes have been varied, with some combinations showing significant benefits while others have raised safety concerns or failed to show statistical significance. Recent compilations of clinical trials using nanoparticles and Immunotherapeutic are found here. (130) (131) Most strategies rely on the combination of a well-established nanomedicine such as Abraxane (albumin-paclitaxel) or Doxil (Liposomal doxorubicin) with checkpoint inhibitors (e.g., atezolizumab, pembrolizumab, durvalumab, Nivolumab, Ipilimumab). Novel nanomedicines, such as nano vaccines and radiosensitizers (NBTXR3), have also been evaluated.

Combining Abraxane with checkpoint inhibitors is most prevalent in clinical trials. In the phase 3 NeoTRIP Michelangelo trial (NCT02620280 (132)), combining Abraxane,

atezolizumab, and carboplatin as neoadjuvant therapy showed no improvement in the pathological complete response (pCR) rate compared to Abraxane and carboplatin alone, with an overall pCR rate of 48.6% vs. 44.4% ($p = 0.48$). Moreover, the addition of atezolizumab was also associated with a higher incidence of serious adverse events. Although the trial did not show a significant improvement in 5-year event-free survival or pCR rates overall, where patients with high densities of CD8+ TCF1+ Ki67+ cells derived greater benefit from atezolizumab. This may suggest that nanoparticles and immunotherapies may enhance antitumor immunity by targeting specific immune cell populations in the tumor microenvironment. (133) (134) Pembrolizumab, in combination with Abraxane, was investigated in the PEANUT study (NCT03464734) with urothelial carcinoma patients who had progressed after one or two prior chemotherapy regimens, including platinum-based therapy. The study reported promising outcomes, with progression-free survival (PFS) of 5.9 months and an overall response rate (ORR) of 38.6%. (135)

Nanoplatforms like ANKTIVA (N-803), a NANT Cancer Vaccine (NCV), combines a low-dose chemotherapy with adenoviral and yeast-based cancer antigen vaccines, natural killer cell platforms, and the IL-15 superagonist N-803. The NCV approach has shown significant potential in inducing immunogenic cell death and long-term T-cell memory, with clinical studies demonstrating complete remission across multiple tumor types, including pancreatic, breast, colorectal, and head and neck cancers. (NCT03022825) For instance, in the phase 2b QUILT 3.055 trial (NCT03228667), ANKTIVA combined with checkpoint inhibitors (KEYTRUDA or OPDIVO) showed a 57% 12-month overall survival rate in non-small cell lung cancer (NSCLC) patients who had progressed on prior immunotherapy, which

prompted the initiation of global phase 3 trials (ResQ301/ResQ302) to confirm these results. (136) (137) This nanoplatform activates NK cells and memory T cells, effectively resensitizing tumors to immune attack and enhancing long-term survival outcomes. Additionally, its ability to activate the cGAS-STING pathway and induce immunogenic cell death further amplifies antitumor immunity, demonstrating its potential as a next-generation immunotherapy platform. (138)

The combination of ipilimumab and nivolumab has been explored in breast and pancreatic cancers. Adding ipilimumab and nivolumab to chemotherapy only (Doxil, cyclophosphamide) increased toxicity without efficacy gains, though sequential use was tolerable with some response in Phase IIb in patients with metastatic hormone receptor-positive breast cancer. (ICON trial, NCT03409198) (139) The trial highlighted that tumor lymphocyte infiltration is predictive of chemotherapy efficacy in breast cancer. Low-dose cyclophosphamide further reduced immunosuppressive regulatory T cells (Tregs), enhancing immune activation increasing median progression-free survival (PFS) to 5.1 months in the immune-chemo group versus 3.6 months in the chemo-only group. By inducing ICD, the chemotherapy amplified the release of tumor antigens, creating a more favorable microenvironment for nivolumab and ipilimumab to activate T cells effectively. [127]

Finally, NBTXR3, a hafnium oxide-based nanoparticle, has been investigated with immunotherapies such as nivolumab and pembrolizumab across various cancers. Intertumoral injection of NBTXR3 combined with radiotherapy and anti-PD-1 therapy has demonstrated feasibility, safety, and promising early efficacy in patients with head and neck

squamous cell carcinoma (HNSCC) and lung and liver metastases (NCT03589339). NBTXR3 enhanced radiation-induced tumor antigen release, expanding the T-cell repertoire and triggering both local and systemic immune responses. These findings highlight the potential of nanoparticle-based strategies to enhance the effects of radiotherapy when paired with immune checkpoint inhibitors. Additionally, NBTXR3 is being further explored in combination with ipilimumab/nivolumab or pembrolizumab alongside radiation therapy for metastatic HNSCC and advanced solid malignancies with lung and liver metastases (NCT04862455, NCT05039632). Several NBTXR3 clinical studies amplified RT energy deposition within tumor cells, leading to improved tumor killing without increasing toxicity to surrounding healthy tissues. The nanoparticles facilitated tumor antigen release, promoting T-cell activation and systemic immune responses (abscopal effect). In anti-PD-1 non-responders, NBTXR3/RT/anti-PD-1 therapy resulted in tumor regression in 6 out of 7 patients who had progressed on prior ICIs. (141) (142) (143)

While nanoplatform-based immunotherapies have shown promise, it is important to acknowledge the significant failure rates observed in clinical trials. Approximately 40% of phase III oncology trials, including those involving immunotherapies and nanomedicines, fail to demonstrate the expected therapeutic benefit, with the majority of failures attributed to a lack of efficacy rather than safety concerns. (146) For nanomedicines specifically, while early-phase trials show high success rates (~94% for phase I), this drops dramatically to ~48% for phase II and a mere ~14% for phase III trials, primarily due to efficacy limitations. (147) (148) (149) A notable example is the voluntary withdrawal of the Abraxane/atezolizumab combination for triple-negative breast cancer in 2021 after

accelerated FDA approval, as more mature data failed to demonstrate statistically significant improvement in progression-free survival. (NCT02425891) (150) Similarly, the phase III NeoTRIP trial combining Abraxane with atezolizumab showed no significant improvement in pathological complete response rates (48.6% vs. 44.4%, p = 0.48) over chemotherapy alone, while increasing adverse events. (132) These failures highlight the challenges in translating preclinical success to clinical benefit, emphasizing the need for better patient selection strategies, improved trial design, and deeper understanding of the complex interactions between nanoplatforms and the immune system to optimize clinical outcomes.

2.7 Conclusion

Nanoplatforms have revolutionized cancer treatment by improving drug delivery and enabling more precise targeting of malignant cells. Nanoplatforms still offers a promising avenue to overcome these hurdles by improving drug delivery, targeting, and immune modulation. This review explores these nanoplatforms interactions within the tumor microenvironment and their synergistic effects with therapies like chemotherapy, radiotherapy, and phototherapy to enhance antitumor immunity. Current chemotherapies and immunotherapies are challenged by limited patient response rates. (13) While current challenges like limited efficacy and drug resistance, nanoplatforms represent a powerful and versatile strategy for advancing cancer immunotherapy, offering multifaceted benefits in drug delivery, immune modulation, and personalized targeting. This review highlighted the utilization of nanoplatforms within the TME and their synergistic effects with conventional therapies such as chemotherapy, radiotherapy, and phototherapy to amplify antitumor

immunity. By addressing the challenges of faced in current therapies, nanoplatforms represent a versatile and promising approach to advancing cancer treatment. The integration of nanotechnology into immunotherapy holds great potential for improving therapeutic outcomes while minimizing toxicity, paving the way for more effective and individualized cancer treatments.

2.8 Future Perspectives

For PDAC, nanoplatforms offer more than just better drug delivery. The disease's dense tissue, poor blood flow, metabolic challenges, and immune suppression make it hard for treatments to work well. Nanoplatforms can help drugs reach tumors more effectively and support combination treatments that target both cancer cells and the tumor's immune environment. This idea is central to Chapter 3, which looks at YXL-182, a STAT3 inhibitor that builds up in mitochondria and blocks STAT3 signaling and related functions in PDAC. Encapsulating YXL-182 in a lipid nanoparticle could improve how the drug moves through the body, how well it reaches tumors, and how it works with other treatments like gemcitabine or immunotherapies. Overall, the nanoplatform strategies discussed here support using STAT3 targeting as part of a broader treatment plan for PDAC.

The future of nanoplatform-based cancer therapy lies in developing personalized strategies tailored to individual patient characteristics, such as genetic profiles and tumor microenvironment composition, to optimize outcomes and minimize adverse effects. (21) For example, stimuli-responsive nanoparticles with active targeting ligands can overcome current limitations like off-target effects and limited tumor penetration.(151) This includes designing multifunctional nanoparticles for synergistic delivery of therapies and engineering

platforms that penetrate tumors while evading immune detection. (152) Research should prioritize promoting long-term immunological memory to prevent tumor recurrence while accelerating clinical translation through combination therapies that integrate chemotherapeutics with immunomodulators or paired with phototherapy and radiotherapy with immune activation. Advancements in nanoplatform design will enable precise drug release, enhanced tumor targeting, and better modulation of the tumor microenvironment, leading to more effective, personalized treatments.

Overcoming current limitations like off-target effects, limited tumor penetration, and immune evasion through stimuli-responsive release, active targeting ligands, and immune cloaking will further improve efficacy and specificity by exploring novel biocompatible and biodegradable nanomaterials. (153) Additionally, the integration of artificial intelligence (AI) into nanomedicine further enhances these advancements by enabling real-time optimization of drug delivery systems based on patient-specific data, such as genomic profiles and tumor characteristics. (154) (155) AI-driven algorithms can dynamically adjust nanoparticle formulations and release kinetics to maximize therapeutic efficacy while minimizing adverse. (156) As research advances, innovations in bioinspired nanoplatforms, biocompatible materials, and AI-driven drug delivery systems are set to transform cancer immunotherapy, overcoming current challenges while paving the way for more personalized and effective treatment strategies.

References

1. Altun İ, Sonkaya A. The Most Common Side Effects Experienced by Patients Were Receiving First Cycle of Chemotherapy. *Iran J Public Health*. 2018;47:1218–1219.
2. Ukidve A, Cu K, Kumbhojkar N, et al. Overcoming biological barriers to improve solid tumor immunotherapy. *Drug Deliv Transl Res*. 2021;11:2276–2301.
3. Immunotherapy for Cancer - NCI.April 29, 2015. Available at: https://www.cancer.gov/about-cancer/treatment/types/immunotherapy. Accessed February 12, 2025.
4. Galluzzi L, Vacchelli E, Pedro J-MB-S, et al. Classification of current anticancer immunotherapies. *Oncotarget*. 2014;5:12472–12508.
5. Liu L, Chen J. Therapeutic antibodies for precise cancer immunotherapy: current and future perspectives. *Med Rev*. 2:555–569.
6. Zahavi D, Weiner L. Monoclonal Antibodies in Cancer Therapy. *Antibodies*. 2020;9:34.
7. Yan F, Cowell LG, Tomkies A, et al. Therapeutic Vaccination for HPV-Mediated Cancers. *Curr Otorhinolaryngol Rep*. 2023;11:44–61.
8. Pardoll DM. The blockade of immune checkpoints in cancer immunotherapy. *Nat Rev Cancer*. 2012;12:252–264.
9. Buchbinder EI, Desai A. CTLA-4 and PD-1 Pathways: Similarities, Differences, and Implications of Their Inhibition. *Am J Clin Oncol*. 2016;39:98–106.
10. Rosenberg SA, Restifo NP, Yang JC, et al. Adoptive cell transfer: a clinical path to effective cancer immunotherapy. *Nat Rev Cancer*. 2008;8:299–308.
11. Morgan RA, Chinnasamy N, Abate-Daga D, et al. Cancer regression and neurological toxicity following anti-MAGE-A3 TCR gene therapy. *J Immunother Hagerstown Md 1997*. 2013;36:133–151.
12. Maude SL, Laetsch TW, Buechner J, et al. Tisagenlecleucel in Children and Young Adults with B-Cell Lymphoblastic Leukemia. *N Engl J Med*. 2018;378:439–448.
13. Peterson C, Denlinger N, Yang Y. Recent Advances and Challenges in Cancer Immunotherapy. *Cancers*. 2022;14:3972.
14. Hegde PS, Chen DS. Top 10 Challenges in Cancer Immunotherapy. *Immunity*. 2020;52:17–35.
15. Vasan N, Baselga J, Hyman DM. A view on drug resistance in cancer. *Nature*. 2019;575:299–309.
16. Dobosz P, Stępień M, Golke A, et al. Challenges of the Immunotherapy: Perspectives and Limitations of the Immune Checkpoint Inhibitor Treatment. *Int J Mol Sci*. 2022;23:2847.
17. Emens LA, Romero PJ, Anderson AC, et al. Challenges and opportunities in cancer immunotherapy: a Society for Immunotherapy of Cancer (SITC) strategic vision. *J Immunother Cancer*. 2024;12:e009063.
18. Jones PA, Issa J-PJ, Baylin S. Targeting the cancer epigenome for therapy. *Nat Rev Genet*. 2016;17:630–641.
19. Zhu L, Wu J, Gao H, et al. Tumor immune microenvironment-modulated nanostrategy for the treatment of lung cancer metastasis. *Chin Med J (Engl)*. 2023;136:2787–2801.
20. Zou J, Zhang Y, Pan Y, et al. Advancing nanotechnology for neoantigen-based cancer theranostics. *Chem Soc Rev*. 2024;53:3224–3252.

21. Sui X, Jin T, Liu T, et al. Tumor Immune Microenvironments (TIMEs): Responsive Nanoplatforms for Antitumor Immunotherapy. *Front Chem*. 2020;8.
22. Zhang N, Zhou J, Li S, et al. Advances in Nanoplatforms for Immunotherapy Applications Targeting the Tumor Microenvironment. *Mol Pharm*. 2024;21:410–426.
23. Irvine DJ, Dane EL. Enhancing cancer immunotherapy with nanomedicine. *Nat Rev Immunol*. 2020;20:321–334.
24. Lehmann CHK, Heger L, Heidkamp GF, et al. Direct Delivery of Antigens to Dendritic Cells via Antibodies Specific for Endocytic Receptors as a Promising Strategy for Future Therapies. *Vaccines*. 2016;4:8.
25. Hong L, Li W, Li Y, et al. Nanoparticle-based drug delivery systems targeting cancer cell surfaces. *RSC Adv*. 2023;13:21365–21382.
26. Song W, Musetti SN, Huang L. Nanomaterials for cancer immunotherapy. *Biomaterials*. 2017;148:16–30.
27. Zhao M, Lei C, Yang Y, et al. Abraxane, the Nanoparticle Formulation of Paclitaxel Can Induce Drug Resistance by Up-Regulation of P-gp. *PLoS ONE*. 2015;10:e0131429.
28. Ibrahim NK, Desai N, Legha S, et al. Phase I and Pharmacokinetic Study of ABI-007, a Cremophor-free, Protein-stabilized, Nanoparticle Formulation of Paclitaxel1. *Clin Cancer Res*. 2002;8:1038–1044.
29. Jiang W, von Roemeling CA, Chen Y, et al. Designing nanomedicine for immuno-oncology. *Nat Biomed Eng*. 2017;1:1–11.
30. Sayour EJ, Grippin A, De Leon G, et al. Personalized Tumor RNA Loaded Lipid-Nanoparticles Prime the Systemic and Intratumoral Milieu for Response to Cancer Immunotherapy. *Nano Lett*. 2018;18:6195–6206.
31. Lee C-Y, Tsai T, Peng P-C, et al. Fabrication of Doxorubicin-Loaded Lipid-Based Nanocarriers by Microfluidic Rapid Mixing. *Biomedicines*. 2022;10:1259.
32. Zhen Y, Ewert KK, Fisher WS, et al. Paclitaxel loading in cationic liposome vectors is enhanced by replacement of oleoyl with linoleoyl tails with distinct lipid shapes. *Sci Rep*. 2021;11:7311.
33. Tamam H, Park J, Gadalla HH, et al. Development of Liposomal Gemcitabine with High Drug Loading Capacity. *Mol Pharm*. 2019;16:2858–2871.
34. Buchbinder EI, Desai A. CTLA-4 and PD-1 Pathways: Similarities, Differences, and Implications of Their Inhibition. *Am J Clin Oncol*. 2016;39:98–106.
35. Chen L, Han X. Anti-PD-1/PD-L1 therapy of human cancer: past, present, and future. *J Clin Invest*. 2015;125:3384–3391.
36. Waheed I, Ali A, Tabassum H, et al. Lipid-based nanoparticles as drug delivery carriers for cancer therapy. *Front Oncol*. 2024;14.
37. Burlec AF, Corciova A, Boev M, et al. Current Overview of Metal Nanoparticles' Synthesis, Characterization, and Biomedical Applications, with a Focus on Silver and Gold Nanoparticles. *Pharm Basel Switz*. 2023;16:1410.
38. Burlec AF, Corciova A, Boev M, et al. Current Overview of Metal Nanoparticles' Synthesis, Characterization, and Biomedical Applications, with a Focus on Silver and Gold Nanoparticles. *Pharm Basel Switz*. 2023;16:1410.

39. Singh P, Pandit S, Balusamy SR, et al. Advanced Nanomaterials for Cancer Therapy: Gold, Silver, and Iron Oxide Nanoparticles in Oncological Applications. *Adv Healthc Mater*. 2025;14:e2403059.
40. Michelini S, Barbero F, Prinelli A, et al. Gold nanoparticles (AuNPs) impair LPS-driven immune responses by promoting a tolerogenic-like dendritic cell phenotype with altered endosomal structures. *Nanoscale*. 2021;13:7648–7666.
41. Kovács D, Igaz N, Gopisetty MK, et al. Cancer Therapy by Silver Nanoparticles: Fiction or Reality? *Int J Mol Sci*. 2022;23:839.
42. Gobbo OL, Sjaastad K, Radomski MW, et al. Magnetic Nanoparticles in Cancer Theranostics. *Theranostics*. 2015;5:1249–1263.
43. Chung S, Revia RA, Zhang M. Iron oxide nanoparticles for immune cell labeling and cancer immunotherapy. *Nanoscale Horiz*. 2021;6:696–717.
44. Zielińska A, Carreiró F, Oliveira AM, et al. Polymeric Nanoparticles: Production, Characterization, Toxicology and Ecotoxicology. *Molecules*. 2020;25:3731.
45. Patri AK, Majoros IJ, Baker JR. Dendritic polymer macromolecular carriers for drug delivery. *Curr Opin Chem Biol*. 2002;6:466–471.
46. Pérez-Ferreiro M, M. Abelairas A, Criado A, et al. Dendrimers: Exploring Their Wide Structural Variety and Applications. *Polymers*. 2023;15:4369.
47. Zhang M, Zhu J, Zheng Y, et al. Doxorubicin-Conjugated PAMAM Dendrimers for pH-Responsive Drug Release and Folic Acid-Targeted Cancer Therapy. *Pharmaceutics*. 2018;10:162.
48. Zhang S, Chen M, Geng Z, et al. Potential Application of Self-Assembled Peptides and Proteins in Breast Cancer and Cervical Cancer. *Int J Mol Sci*. 2023;24:17056.
49. Mainini F, Bonizzi A, Sevieri M, et al. Protein-Based Nanoparticles for the Imaging and Treatment of Solid Tumors: The Case of Ferritin Nanocages, a Narrative Review. *Pharmaceutics*. 2021;13:2000.
50. Hassanin I, Elzoghby A. Albumin-based nanoparticles: a promising strategy to overcome cancer drug resistance. *Cancer Drug Resist*. 2020;3:930–946.
51. Hoogenboezem EN, Duvall CL. Harnessing Albumin as a Carrier for Cancer Therapies. *Adv Drug Deliv Rev*. 2018;130:73–89.
52. Lee NK, Cho S, Kim I-S. Ferritin – a multifaceted protein scaffold for biotherapeutics. *Exp Mol Med*. 2022;54:1652–1657.
53. Deng G, Li Y, Liang N, et al. Ferritin in cancer therapy: A pleiotropic tumoraffin nanocage-based transport. *Cancer Med*. 2023;12:11570–11588.
54. Li F, Zhang X-Q, Ho W, et al. mRNA lipid nanoparticle-mediated pyroptosis sensitizes immunologically cold tumors to checkpoint immunotherapy. *Nat Commun*. 2023;14:4223.
55. Sargsian A, Koutsoumpou X, Girmatsion H, et al. Silver nanoparticle induced immunogenic cell death can improve immunotherapy. *J Nanobiotechnology*. 2024;22:691.
56. Waheed S, Li Z, Zhang F, et al. Engineering nano-drug biointerface to overcome biological barriers toward precision drug delivery. *J Nanobiotechnology*. 2022;20:395.

57. P j N, Patil SR, Veeraraghavan VP, et al. Oral cancer stem cells: A comprehensive review of key drivers of treatment resistance and tumor recurrence. *Eur J Pharmacol*. 2025;989:177222.
58. Jokerst JV, Lobovkina T, Zare RN, et al. Nanoparticle PEGylation for imaging and therapy. *Nanomed*. 2011;6:715–728.
59. Suk JS, Xu Q, Kim N, et al. PEGylation as a strategy for improving nanoparticle-based drug and gene delivery. *Adv Drug Deliv Rev*. 2016;99:28–51.
60. Wu K, Yu B, Li D, et al. Recent Advances in Nanoplatforms for the Treatment of Osteosarcoma. *Front Oncol*. 2022;12.
61. Thomas OS, Weber W. Overcoming Physiological Barriers to Nanoparticle Delivery—Are We There Yet? *Front Bioeng Biotechnol*. 2019;7.
62. Borker S, Pokharkar V. Engineering of pectin-capped gold nanoparticles for delivery of doxorubicin to hepatocarcinoma cells: an insight into mechanism of cellular uptake. *Artif Cells Nanomedicine Biotechnol*. 2018;46:826–835.
63. Liu J, Zhao Y, Guo Q, et al. TAT-modified nanosilver for combating multidrug-resistant cancer. *Biomaterials*. 2012;33:6155–6161.
64. Zhu H, Zhou B, Chan L, et al. Transferrin-functionalized nanographene oxide for delivery of platinum complexes to enhance cancer-cell selectivity and apoptosis-inducing efficacy. *Int J Nanomedicine*. 2017;12:5023–5038.
65. Hosu O, Tertis M, Cristea C. Implication of Magnetic Nanoparticles in Cancer Detection, Screening and Treatment. *Magnetochemistry*. 2019;5:55.
66. Oltolina F, Colangelo D, Miletto I, et al. Tumor Targeting by Monoclonal Antibody Functionalized Magnetic Nanoparticles. *Nanomaterials*. 2019;9:1575.
67. Rao L, Bu L-L, Xu J-H, et al. Red Blood Cell Membrane as a Biomimetic Nanocoating for Prolonged Circulation Time and Reduced Accelerated Blood Clearance. *Small*. 2015;11:6225–6236.
68. Luk BT, Zhang L. Cell membrane-camouflaged nanoparticles for drug delivery. *J Controlled Release*. 2015;220:600–607.
69. Rahim MA, Jan N, Khan S, et al. Recent Advancements in Stimuli Responsive Drug Delivery Platforms for Active and Passive Cancer Targeting. *Cancers*. 2021;13:670.
70. Hoop M, Mushtaq F, Hurter C, et al. A smart multifunctional drug delivery nanoplatform for targeting cancer cells. *Nanoscale*. 2016;8:12723–12728.
71. Xue X, Huang Y, Bo R, et al. Trojan Horse nanotheranostics with dual transformability and multifunctionality for highly effective cancer treatment. *Nat Commun*. 2018;9:3653.
72. Ma T, Chen R, Lv N, et al. Size-Transformable Bicomponent Peptide Nanoparticles for Deep Tumor Penetration and Photo-Chemo Combined Antitumor Therapy. *Small*. 2022;18:2106291.
73. Rameshbabu S, Labadie BW, Argulian A, et al. Targeting Innate Immunity in Cancer Therapy. *Vaccines*. 2021;9:138.
74. Ding D, Jiang X. Advances in Immunogenic Cell Death for Cancer Immunotherapy. *Small Methods*. 2023;7:2300354.
75. Fucikova J, Kepp O, Kasikova L, et al. Detection of immunogenic cell death and its relevance for cancer therapy. *Cell Death Dis*. 2020;11:1–13.

76. Lee DY, Im E, Yoon D, et al. Pivotal role of PD-1/PD-L1 immune checkpoints in immune escape and cancer progression: Their interplay with platelets and FOXP3+Tregs related molecules, clinical implications and combinational potential with phytochemicals. *Semin Cancer Biol*. 2022;86:1033–1057.
77. Ravi R, Noonan KA, Pham V, et al. Bifunctional immune checkpoint-targeted antibody-ligand traps that simultaneously disable TGFβ enhance the efficacy of cancer immunotherapy. *Nat Commun*. 2018;9:741.
78. Tian E-M, Yu M-C, Feng M, et al. RORγt agonist synergizes with CTLA-4 antibody to inhibit tumor growth through inhibition of Treg cells via TGF-β signaling in cancer. *Pharmacol Res*. 2021;172:105793.
79. Shevtsov M, Sato H, Multhoff G, et al. Novel Approaches to Improve the Efficacy of Immuno-Radiotherapy. *Front Oncol*. 2019;9.
80. Zhang H, Zhang X, Ren Y, et al. An in situ microenvironmental nano-regulator to inhibit the proliferation and metastasis of 4T1 tumor. *Theranostics*. 2019;9:3580–3594.
81. Zhang Y, Chen Y, Li J, et al. Development of Toll-like Receptor Agonist-Loaded Nanoparticles as Precision Immunotherapy for Reprogramming Tumor-Associated Macrophages. *ACS Appl Mater Interfaces*. 2021;13:24442–24452.
82. Gamen S, Hanson DA, Kaspar A, et al. Granulysin-Induced Apoptosis. I. Involvement of at Least Two Distinct Pathways1. *J Immunol*. 1998;161:1758–1764.
83. Sordo-Bahamonde C, Lorenzo-Herrero S, Payer ÁR, et al. Mechanisms of Apoptosis Resistance to NK Cell-Mediated Cytotoxicity in Cancer. *Int J Mol Sci*. 2020;21:3726.
84. Ramírez-Labrada A, Pesini C, Santiago L, et al. All About (NK Cell-Mediated) Death in Two Acts and an Unexpected Encore: Initiation, Execution and Activation of Adaptive Immunity. *Front Immunol*. 2022;13.
85. Biber G, Sabag B, Raiff A, et al. Modulation of intrinsic inhibitory checkpoints using nano-carriers to unleash NK cell activity. *EMBO Mol Med*. 2022;14:e14073.
86. Hart OM, Athie-Morales V, O'Connor GM, et al. TLR7/8-Mediated Activation of Human NK Cells Results in Accessory Cell-Dependent IFN-γ Production1. *J Immunol*. 2005;175:1636–1642.
87. Perry JL, Tian S, Sengottuvel N, et al. Pulmonary Delivery of Nanoparticle-Bound Toll-like Receptor 9 Agonist for the Treatment of Metastatic Lung Cancer. *ACS Nano*. 2020;14:7200–7215.
88. Raskov H, Orhan A, Christensen JP, et al. Cytotoxic CD8+ T cells in cancer and cancer immunotherapy. *Br J Cancer*. 2021;124:359–367.
89. Kang M, Hong J, Jung M, et al. T-Cell-Mimicking Nanoparticles for Cancer Immunotherapy. *Adv Mater*. 2020;32:2003368.
90. Daei Sorkhabi A, Mohamed Khosroshahi L, Sarkesh A, et al. The current landscape of CAR T-cell therapy for solid tumors: Mechanisms, research progress, challenges, and counterstrategies. *Front Immunol*. 2023;14.
91. Zhang F, Stephan SB, Ene CI, et al. Nanoparticles That Reshape the Tumor Milieu Create a Therapeutic Window for Effective T-cell Therapy in Solid Malignancies. *Cancer Res*. 2018;78:3718–3730.

92. Xu C, Ji X, Zhou Y, et al. Slimming and Reinvigorating Tumor-Associated Dendritic Cells with Hierarchical Lipid Rewiring Nanoparticles. *Adv Mater Deerfield Beach Fla*. 2023;35:e2211415.
93. Levy ES, Chang R, Zamecnik CR, et al. Multi-Immune Agonist Nanoparticle Therapy Stimulates Type I Interferons to Activate Antigen-Presenting Cells and Induce Antigen-Specific Antitumor Immunity. *Mol Pharm*. 2021;18:1014–1025.
94. He M, Chen X, Luo M, et al. Suppressor of cytokine signaling 1 inhibits the maturation of dendritic cells involving the nuclear factor kappa B signaling pathway in the glioma microenvironment. *Clin Exp Immunol*. 2020;202:47–59.
95. Yu Z, Wu M, Huang Y, et al. Single-component lipid nanoparticles for engineering SOCS1 gene-silenced dendritic cells to boost tumor immunotherapy. *Biomater Sci*. 2022;11:263–277.
96. Rogiers A, Boekhout A, Schwarze JK, et al. Long-Term Survival, Quality of Life, and Psychosocial Outcomes in Advanced Melanoma Patients Treated with Immune Checkpoint Inhibitors. *J Oncol*. 2019;2019:5269062.
97. Neek M, Tucker JA, Butkovich N, et al. An Antigen-Delivery Protein Nanoparticle Combined with Anti-PD-1 Checkpoint Inhibitor Has Curative Efficacy in an Aggressive Melanoma Model. *Adv Ther*. 2020;3:2000122.
98. Khosravi G-R, Mostafavi S, Bastan S, et al. Immunologic tumor microenvironment modulators for turning cold tumors hot. *Cancer Commun Lond Engl*. 2024;44:521–553.
99. Ahmed A, Tait SWG. Targeting immunogenic cell death in cancer. *Mol Oncol*. 2020;14:2994–3006.
100. Xi Y, Chen L, Tang J, et al. Amplifying “eat me signal” by immunogenic cell death for potentiating cancer immunotherapy. *Immunol Rev*. 2024;321:94–114.
101. Inoue H, Tani K. Multimodal immunogenic cancer cell death as a consequence of anticancer cytotoxic treatments. *Cell Death Differ*. 2014;21:39–49.
102. Chang X, Bian M, Liu L, et al. Induction of immunogenic cell death by novel platinum-based anticancer agents. *Pharmacol Res*. 2023;187:106556.
103. Ng HY, Li J, Tao L, et al. Chemotherapeutic Treatments Increase PD-L1 Expression in Esophageal Squamous Cell Carcinoma through EGFR/ERK Activation. *Transl Oncol*. 2018;11:1323–1333.
104. Sharma A, Jasrotia S, Kumar A. Effects of Chemotherapy on the Immune System: Implications for Cancer Treatment and Patient Outcomes. *Naunyn Schmiedebergs Arch Pharmacol*. 2024;397:2551–2566.
105. Lim S, Park J, Shim MK, et al. Recent advances and challenges of repurposing nanoparticle-based drug delivery systems to enhance cancer immunotherapy. *Theranostics*. 2019;9:7906–7923.
106. Lang X, Wang X, Han M, et al. Nanoparticle-Mediated Synergistic Chemoimmunotherapy for Cancer Treatment. *Int J Nanomedicine*. 2024;19:4533–4568.
107. Mu W, Chu Q, Liu Y, et al. A Review on Nano-Based Drug Delivery System for Cancer Chemoimmunotherapy. *Nano-Micro Lett*. 2020;12:142.

108. Zhao L-P, Zheng R-R, Rao X-N, et al. Chemotherapy-Enabled Colorectal Cancer Immunotherapy of Self-Delivery Nano-PROTACs by Inhibiting Tumor Glycolysis and Avoiding Adaptive Immune Resistance. *Adv Sci*. 2024;11:2309204.
109. Shen S, Li H-J, Chen K-G, et al. Spatial Targeting of Tumor-Associated Macrophages and Tumor Cells with a pH-Sensitive Cluster Nanocarrier for Cancer Chemoimmunotherapy. *Nano Lett*. 2017;17:3822–3829.
110. Kadkhoda J, Tarighatnia A, Barar J, et al. Recent advances and trends in nanoparticles based photothermal and photodynamic therapy. *Photodiagnosis Photodyn Ther*. 2022;37:102697.
111. Xie Z, Fan T, An J, et al. Emerging combination strategies with phototherapy in cancer nanomedicine. *Chem Soc Rev*. 2020;49:8065–8087.
112. Overchuk M, Weersink RA, Wilson BC, et al. Photodynamic and Photothermal Therapies: Synergy Opportunities for Nanomedicine. *ACS Nano*. 2023;17:7979–8003.
113. Han HS, Choi KY. Advances in Nanomaterial-Mediated Photothermal Cancer Therapies: Toward Clinical Applications. *Biomedicines*. 2021;9:305.
114. Guo R, Wang S, Zhao L, et al. Engineered nanomaterials for synergistic photo-immunotherapy. *Biomaterials*. 2022;282:121425.
115. Li W, Yang J, Luo L, et al. Targeting photodynamic and photothermal therapy to the endoplasmic reticulum enhances immunogenic cancer cell death. *Nat Commun*. 2019;10:3349.
116. Li X, Gao J, Wu C, et al. Precise modulation and use of reactive oxygen species for immunotherapy. *Sci Adv*. 2024;10:eadl0479.
117. Zhou W, Yang F, Zhang X. Roles of M1 Macrophages and Their Extracellular Vesicles in Cancer Therapy. *Cells*. 2024;13:1428.
118. Ng CW, Li J, Pu K. Recent Progresses in Phototherapy-Synergized Cancer Immunotherapy. *Adv Funct Mater*. 2018;28:1804688.
119. Zhou L, Feng B, Wang H, et al. A bispecific nanomodulator to potentiate photothermal cancer immunotherapy. *Nano Today*. 2022;44:101466.
120. Song G, Cheng L, Chao Y, et al. Emerging Nanotechnology and Advanced Materials for Cancer Radiation Therapy. *Adv Mater*. 2017;29:1700996.
121. Zaorsky NG, Yu JB, McBride SM, et al. Prostate Cancer Radiation Therapy Recommendations in Response to COVID-19. *Adv Radiat Oncol*. 2020;5:659–665.
122. Zhang Z, Liu X, Chen D, et al. Radiotherapy combined with immunotherapy: the dawn of cancer treatment. *Signal Transduct Target Ther*. 2022;7:1–34.
123. Muroyama Y, Nirschl TR, Kochel CM, et al. Stereotactic Radiotherapy Increases Functionally Suppressive Regulatory T Cells in the Tumor Microenvironment. *Cancer Immunol Res*. 2017;5:992–1004.
124. Keam S, Gill S, Ebert MA, et al. Enhancing the efficacy of immunotherapy using radiotherapy. *Clin Transl Immunol*. 2020;9:e1169.
125. Spiotto M, Fu Y-X, Weichselbaum RR. The intersection of radiotherapy and immunotherapy: mechanisms and clinical implications. *Sci Immunol*. 2016;1:EAAG1266.
126. Galluzzi L, Aryankalayil MJ, Coleman CN, et al. Emerging evidence for adapting radiotherapy to immunotherapy. *Nat Rev Clin Oncol*. 2023;20:543–557.

127. Li H, Luo Q, Zhang H, et al. Nanomedicine embraces cancer radio-immunotherapy: mechanism, design, recent advances, and clinical translation. *Chem Soc Rev*. 2023;52:47–96.
128. Wu Y, Qin J, Gu Y, et al. Radioresponsive Delivery of Toll-like Receptor 7/8 Agonist for Tumor Radioimmunotherapy Enabled by Core-Cross-Linked Diselenide Nanoparticles. *ACS Nano*. 2024;18:2800–2814.
129. Deng Z, Xi M, Zhang C, et al. Biomineralized MnO2 Nanoplatforms Mediated Delivery of Immune Checkpoint Inhibitors with STING Pathway Activation to Potentiate Cancer Radio-Immunotherapy. *ACS Nano*. 2023;17:4495–4506.
130. García-Domínguez DJ, López-Enríquez S, Alba G, et al. Cancer Nano-Immunotherapy: The Novel and Promising Weapon to Fight Cancer. *Int J Mol Sci*. 2024;25:1195.
131. Shi Y. Clinical Translation of Nanomedicine and Biomaterials for Cancer Immunotherapy: Progress and Perspectives. *Adv Ther*. 2020;3:1900215.
132. Gianni L, Huang CS, Egle D, et al. Pathologic complete response (pCR) to neoadjuvant treatment with or without atezolizumab in triple-negative, early high-risk and locally advanced breast cancer: NeoTRIP Michelangelo randomized study. *Ann Oncol Off J Eur Soc Med Oncol*. 2022;33:534–543.
133. admin 1. New data from Michelangelo Foundation's NeoTRIP trial discussed during ESMO Congress.Fondazione Michelangelo. November 8, 2023. Available at: https://www.fondazionemichelangelo.org/news-update/new-data-from-michelangelo-foundations-neotrip-trial-discussed-during-esmo-congress/. Accessed April 11, 2025.
134. Dugo M, Huang C-S, Egle D, et al. The Immune-Related 27-Gene Signature DetermaIO Predicts Response to Neoadjuvant Atezolizumab plus Chemotherapy in Triple-Negative Breast Cancer. *Clin Cancer Res Off J Am Assoc Cancer Res*. 2024;30:4900–4909.
135. Giannatempo P, Raggi D, Marandino L, et al. Pembrolizumab and nab-paclitaxel as salvage therapy for platinum-treated, locally advanced or metastatic urothelial carcinoma: interim results of the open-label, single-arm, phase II PEANUT study. *Ann Oncol Off J Eur Soc Med Oncol*. 2020;31:1764–1772.
136. jhollister. Long-Term Survival Data for Non-Small Cell Lung Cancer & Phase 3 Cancer Clinical Trials for ANKTIVA®.ImmunityBio. September 9, 2024. Available at: https://immunitybio.com/immunitybio-presents-positive-long-term-overall-survival-data-in-non-small-cell-lung-cancer-patients-and-announces-registrational-intent-phase-3-trials-with-anktiva-and-checkpoint-immunotherapy/. Accessed April 11, 2025.
137. ImmunityBio follows through in lung cancer.ApexOnco. Available at: https://www.oncologypipeline.com/apexonco/https%3A%2F%2Fwww.oncologypipeline.com%2Fapexonco%2Fimmunitybio-follows-through-lung-cancer. Accessed April 11, 2025.
138. Immunotherapy and Cell Therapy Platforms - Therapies for Cancer.ImmunityBio. Available at: https://immunitybio.com/platforms/. Accessed April 11, 2025.

139. Andresen NK, Røssevold AH, Quaghebeur C, et al. Ipilimumab and nivolumab combined with anthracycline-based chemotherapy in metastatic hormone receptor-positive breast cancer: a randomized phase 2b trial. *J Immunother Cancer*. 2024;12:e007990.
140. Shen C, Frakes JM, Hackman TG, et al. Early signs of efficacy in patients with anti-PD-1 naïve and anti-PD-1 resistant HNSCC treated with NBTXR3/SBRT in combination with nivolumab or pembrolizumab in the phase I trial Study 1100. *J Clin Oncol*. 2024;42:6035–6035.
141. Shen CJ, Jameson KL, Weiss J, et al. NANORAY-1100: A phase I study of NBTXR3 activated by radiotherapy in patients with advanced cancers treated with anti-PD-1 therapy. *J Clin Oncol*. 2020;38:TPS86–TPS86.
142. Shen C, Frakes JM, Niu J, et al. A phase I trial evaluating NBTXR3 activated by radiotherapy in combination with nivolumab or pembrolizumab in patients with advanced cancers. *J Clin Oncol*. 2021;39:2590–2590.
143. Shen C, Frakes J, Niu J, et al. 684 NBTXR3 activated by radiotherapy in combination with nivolumab or pembrolizumab in patients with advanced cancers: results from an ongoing dose escalation phase I trial (Study 1100). *J Immunother Cancer*. 2022;10.
144. Weber JS, Carlino MS, Khattak A, et al. Individualised neoantigen therapy mRNA-4157 (V940) plus pembrolizumab versus pembrolizumab monotherapy in resected melanoma (KEYNOTE-942): a randomised, phase 2b study. *Lancet Lond Engl*. 2024;403:632–644.
145. Sahin U, Oehm P, Derhovanessian E, et al. An RNA vaccine drives immunity in checkpoint-inhibitor-treated melanoma. *Nature*. 2020;585:107–112.
146. Pretorius S, Alberto Grignolo P. Phase III Trial Failures: Costly, But Preventable. 2016;25.
147. He H, Liu L, Morin EE, et al. Survey of Clinical Translation of Cancer Nanomedicines—Lessons Learned from Successes and Failures. *Acc Chem Res*. 2019;52:2445–2461.
148. Li X, Zhou Y, Xu B, et al. Comparison of efficacy discrepancy between early-phase clinical trials and phase III trials of PD-1/PD-L1 inhibitors. *J Immunother Cancer*. 2024;12:e007959.
149. ClinicalDevelopmentSuccessRates2011_2020.pdf.
150. Schmid P, Adams S, Rugo HS, et al. Atezolizumab and Nab-Paclitaxel in Advanced Triple-Negative Breast Cancer. *N Engl J Med*. https://doi.org/10.1056/NEJMoa1809615.
151. Theivendren P, Kunjiappan S, Pavadai P, et al. Revolutionizing Cancer Immunotherapy: Emerging Nanotechnology-Driven Drug Delivery Systems for Enhanced Therapeutic Efficacy. *ACS Meas Sci Au*. 2025;5:31–55.
152. Mu D, He P, Shi Y, et al. Bioinspired Membrane-Coated Nanoplatform for Targeted Tumor Immunotherapy. *Front Oncol*. 2022;11.
153. Dhilip Kumar SS, Abrahamse H. Recent advances in the development of biocompatible nanocarriers and their cancer cell targeting efficiency in photodynamic therapy. *Front Chem*. 2022;10.
154. Vidhya KS, Sultana A, M NK, et al. Artificial Intelligence's Impact on Drug Discovery and Development From Bench to Bedside. *Cureus*. 15:e47486.

155. Liao J, Li X, Gan Y, et al. Artificial intelligence assists precision medicine in cancer treatment. *Front Oncol*. 2023;12:998222.
156. Wang W, Chen K, Jiang T, et al. Artificial intelligence-driven rational design of ionizable lipids for mRNA delivery. *Nat Commun*. 2024;15:10804.

Chapter 3:
Development and Preclinical Evaluation of YXL-182, a Dual-Targeting Inhibitor of Canonical and Mitochondrial STAT3 in PDAC

3.1 Introduction

Pancreatic ductal adenocarcinoma remains difficult to treat because its aggressive biology and dense stromal microenvironment sustain resistance to conventional chemotherapy, underscoring the need for mechanism-based strategies that target both tumor-intrinsic and microenvironment-driven survival programs. (1,2) Among the pathways sustaining this resistance, STAT3 is particularly compelling because it links oncogenic signaling to metabolic adaptation, making it both a biological driver of disease and a candidate therapeutic vulnerability in PDAC. (3)

STAT3's importance in pancreatic cancer stems from its ability to coordinate multiple hallmarks of aggressive disease simultaneously. Beyond promoting cell-cycle progression and survival, STAT3 supports invasive behavior, epithelial-mesenchymal plasticity, and resistance to apoptosis through downstream effectors such as Cyclin D1, MMP-9, BCL2L1, and Survivin. This broad functional reach helps explain why suppressing STAT3 signaling can enhance gemcitabine activity and improve drug delivery in PDAC models by remodeling the tumor microenvironment rather than simply depleting stroma, (4) and why low phospho-STAT3 has been associated with better outcomes in settings where gemcitabine responsiveness is preserved.

Despite this strong rationale, direct inhibition of STAT3 has historically been challenging, since STAT3 functions largely through protein-protein and protein-DNA interactions rather than a well-defined catalytic pocket. Structural and medicinal chemistry studies have identified the SH2 domain as a tractable, mechanistically relevant site for therapeutic targeting, as it is required for phospho tyrosine recognition, dimerization, and downstream signaling. (5,6) More recently, SH2-directed compounds have been shown to

suppress not only Tyr705 phosphorylation and nuclear signaling but also broader STAT3-dependent tumor phenotypes in pancreatic cancer models. (7,8)

This SH2-targeting strategy takes on added significance considering STAT3's non-canonical mitochondrial functions. Ser727-phosphorylated STAT3 contributes to electron transport chain activity, mitochondrial membrane potential, ATP production, and redox homeostasis, helping preserve mitochondrial function under metabolic stress. (9,10) Because PDAC cells frequently rely on oxidative phosphorylation to survive under nutrient-poor, hypoxic, stromal-rich conditions, and because elevated OXPHOS programs are linked to stemness, dormancy, and treatment resistance, compounds capable of disrupting both STAT3 signaling and mitochondrial respiration may offer an advantage over agents that target proliferation-associated pathways alone. SH2-targeted STAT3 inhibitors that suppress both Tyr705- and Ser727-dependent functions have been shown to reduce nuclear transcriptional output while impairing mitochondrial OXPHOS, with dual suppression linked to reduced tumor growth and greater vulnerability under metabolic stress in pancreatic cancer models. (8)

Our work builds on this concept through the characterization of YXL-182, a chalcone-thiol derivative generated by coupling a STAT3-inhibitory scaffold to a mitochondria-targeting coumarin-based moiety. YXL-182 suppresses PDAC cell growth across multiple in vitro models, reduces long-term clonogenic survival, and induces apoptotic cell death as measured by cleaved caspase-3 and Annexin V/PI assays. Mechanistically, YXL-182 directly engages STAT3, reduces Tyr705 phosphorylation, limits nuclear accumulation of activated STAT3, and suppresses downstream targets such as MMP-9 and Cyclin D1, while leaving p-JAK1 relatively unchanged; consistent with pathway inhibition at the level of STAT3 rather than broad upstream kinase suppression.

Beyond this canonical effect, our data point to a second, metabolically relevant layer of activity. Transcriptomic profiling reveals coordinated disruption of genes involved in complex I assembly, complexes III/IV/V, mitochondrial ribosome and import machinery, and redox control, including NDUFAF8, NDUFA1, COX6A1, COX7A2 TOMM7, SDHA. These transcriptional changes are supported by functional evidence of reduced mitochondrial

respiration and ultrastructural findings consistent with mitochondrial injury, including swelling and cristae disruption. Together, these results support a model in which YXL-182 functions as a dual STAT3/OXPHOS modulator that links inhibition of oncogenic transcriptional signaling to bioenergetic collapse.

This dual mechanism carries relevance for combination therapy. Consistent with prior work showing that STAT3 inhibition can improve gemcitabine efficacy in PDAC through effects on tumor cell survival and adaptive resistance pathways. Our data show that YXL-182 enhances gemcitabine responsiveness in vitro and improves tumor control and survival in KPC models when used in combination. A compound that weakens both STAT3-dependent survival signaling and mitochondrial energetic reserve may therefore be especially effective in PDAC, where resistance is sustained by both transcriptional and metabolic adaptation.

In this chapter, we characterize YXL-182 as a dual-mechanism STAT3/OXPHOS inhibitor in PDAC, detailing its direct engagement of STAT3, its disruption of mitochondrial bioenergetics, and its therapeutic efficacy alone and in combination with gemcitabine in vitro and in vivo.

3.2 Methods

Cell Culture

The human pancreatic ductal adenocarcinoma cell lines PANC-1, MIA PaCa-2, and the murine KPC cell line were cultured in Dulbecco's Modified Eagle Medium (DMEM) supplemented with 10% fetal bovine serum (FBS) and 1% penicillin/streptomycin (P/S). The human pancreatic ductal adenocarcinoma cell lines BxPC-3 and AsPC-1 were cultured in RPMI 1640 medium supplemented with 10% FBS and 1% P/S. All cell lines were maintained at 37 °C in a fully humidified atmosphere containing 5% CO2 in air.

Cell Toxicity

Cell viability was assessed using a luminescent ATP-based cytotoxicity assay. Cells were seeded at 3,000 cells per well in 96-well plates and allowed to adhere overnight prior to treatment. Test compounds were then added at the indicated concentrations, and cells were incubated for 48 hours. Following treatment, the medium was removed and replaced with CytoGlo reagent (Promega) according to the manufacturer's instructions, and plates were incubated for 5 min at room temperature. The resulting lysates were transferred to white opaque 96-well plates, and luminescence was measured on a microplate reader to determine relative cell viability. Three replicate wells were used for each condition and six wells for untreated control was used as 100% viability.

Surface plasmon resonance (SPR)

SPR analysis was performed by ChemScene using full-length native STAT3 protein. YXL-182 was tested over a concentration range of 2.1875–140 nM and demonstrated concentration-dependent binding to STAT3, supporting a direct physical interaction.

Cellular Thermal Shift Assay (CETSA)

Target engagement of YXL-182 with STAT3 was assessed using the cellular thermal shift assay, as previously described (doi:10.1038/nprot.2014.138). Cells were harvested by trypsinization, washed with PBS, and resuspended at a defined density in PBS

supplemented with protease and phosphatase inhibitors. Cell suspensions were treated with either YXL-182 and incubated for 2 hours at 37 °C to allow compound-target engagement. Following treatment, cell suspensions were aliquoted (~100 µL per tube) into PCR tubes and each aliquot was heated for 3 min across a temperature gradient of 40–67 °C in ~3 °C increments using a thermal cycler. Immediately after heating, the samples snap-frozen in liquid nitrogen . Cells were lysed by two to three freeze-thaw cycles to release soluble protein while denatured, aggregated protein remained insoluble. Lysates were clarified by centrifugation at high speed of 15,000 × g for 15 min at 4 °C to pellet aggregated protein, and the soluble supernatant fraction was collected. Protein concentration in the soluble fraction was determined by BCA assay, and equal amounts of protein were resolved by SDS-PAGE, transferred to PVDF membranes, and probed by western blot for STAT3, using a loading control antibody GAPDH to confirm equal protein input.

Western blotting

Cells were lysed in ice-cold RIPA buffer supplemented with protease and phosphatase inhibitors, incubated on ice for 20 min, and centrifuged at 14,000 × g for 15 min at 4 °C. Supernatants were collected, and protein concentration was determined using a BCA assay according to the manufacturer's instructions. Equal amounts of protein (typically 0–40 µg per lane) were mixed with 5× Laemmli sample buffer, boiled at 95 °C for 5 min, and resolved by SDS-PAGE. Proteins were then transferred to PVDF membranes using a wet-tank transfer system in Tris-glycine transfer buffer containing 20% methanol; gels and membranes were first equilibrated in transfer buffer for 5 min, assembled into the transfer stack, and transferred at 100 V for 60 min at 4 °C. Following transfer, membranes were briefly rinsed in TBS or TBST (TBS with 0.1% Tween-20) and blocked for 1 hour at room temperature in 5% BSA in TBST. Membranes were incubated with primary antibodies overnight at 4 °C with gentle rocking, then washed three times for 5 min each in TBST and incubated with species-appropriate HRP-conjugated secondary antibodies diluted in blocking buffer for 1 hour at room temperature. After a final series of three washes in TBST, bound antibodies were

detected using enhanced chemiluminescence (ECL) reagents, and chemiluminescent signals were captured using a digital imaging system.

Clonogenic survival

Cells were seeded at a density of 300 cells per well in 6-well plates and allowed to adhere overnight. Cells were then treated with the indicated drug concentrations and incubated for 7 days to allow colony formation. At the assay endpoint, culture medium was removed, and cells were washed twice with PBS. Colonies were fixed and stained with methylene blue on a rocker for 1 hour at room temperature, then washed three times with PBS to remove excess stain. Plates were air-dried, imaged, and colonies were quantified using ImageJ software.

Nuclear fractionation

Nuclear and cytoplasmic protein fractions were isolated using the NE-PER™ Nuclear and Cytoplasmic Extraction Reagents kit (Thermo Fisher Scientific), according to the manufacturer's instructions. Cells were harvested by trypsinization, washed with ice-cold PBS, and pelleted by centrifugation at 500 × g for 5 min. The cell pellet was resuspended in ice-cold Cytoplasmic Extraction Reagent I (CER I) supplemented with protease and phosphatase inhibitors, vortexed vigorously for 15 sec to fully suspend the pellet, and incubated on ice for 10 min. Ice-cold Cytoplasmic Extraction Reagent II (CER II) was then added, and the sample was vortexed for 5 sec, incubated on ice for 1 min, and vortexed again for 5 sec. The lysate was centrifuged at maximum speed (~16,000 × g) for 5 min at 4 °C, and the resulting supernatant, containing the cytoplasmic fraction, was immediately transferred to a clean, pre-chilled tube and kept on ice. The remaining insoluble pellet, containing intact nuclei, was resuspended in ice-cold Nuclear Extraction Reagent (NER) and vortexed for 15 sec. The sample was incubated on ice for a total of 40 min, with vortexing for 15 sec at 10-min intervals throughout the incubation. Following incubation, the sample was centrifuged at maximum speed (~16,000 × g) for 10 min at 4 °C, and the resulting supernatant, containing the nuclear fraction, was collected and transferred to a clean tube. Protein concentration in

each fraction was determined by BCA assay, and cytoplasmic and nuclear extracts were stored at −80 °C until use for downstream western blot analysis.

Mitochondrial Fractionation

Mitochondrial and cytosolic fractions were isolated using the Mitochondria Isolation Kit for Cultured Cells (Thermo Scientific), according to the manufacturer's instructions. Cells (~2 × 10^6 per sample) were harvested and pelleted by centrifugation at ~850 × g for 2 min, and the supernatant was discarded. The cell pellet was resuspended in 600 µL of Mitochondria Isolation Reagent A supplemented with protease inhibitors, vortexed at medium speed for 5 sec, and incubated on ice for exactly 2 min. Next, 10 µL of Mitochondria Isolation Reagent B was added, and the sample was vortexed at maximum speed for 5 sec, then incubated on ice for 5 min with vortexing at maximum speed every minute. Following incubation, 800 µL of Mitochondria Isolation Reagent C (also supplemented with protease inhibitors) was added, and the tube was mixed by inversion. The sample was centrifuged at 700 × g for 10 min at 4 °C to pellet nuclei and unbroken cells, and the supernatant was transferred to a new tube and centrifuged at 12,000 × g for 15 min at 4 °C to pellet the mitochondrial fraction. The resulting supernatant (cytosolic fraction) was collected and stored separately, and the mitochondrial pellet was washed by resuspension in 400 µL of Mitochondria Isolation Reagent C followed by centrifugation at 12,000 × g for 5 min at 4 °C; the supernatant was discarded. The washed mitochondrial pellet was maintained on ice and either used immediately or resuspended in lysis buffer containing protease inhibitors for downstream protein extraction. Protein concentration in both mitochondrial and cytosolic fractions was determined by BCA assay prior to western blot analysis.

RNA isolation and RNA sequencing

Total RNA was isolated using the AllPrep DNA/RNA Micro Kit (QIAGEN, cat. no. 80284) according to the manufacturer’s instructions. Briefly, cells were lysed in Buffer RLT Plus, homogenized, and processed through AllPrep DNA and RNeasy MinElute spin columns to purify total RNA. RNA was eluted in RNase-free water and quantified using a NanoDrop Lite

spectrophotometer (*Thermo Fisher Scientific*). RNA samples meeting quality-control criteria were submitted to Novogene for library preparation, quality assessment, and next-generation RNA sequencing.

Flow cytometry

For flow cytometric analyses, cells were seeded at 3×10^5 cells per well in 6-well plates and allowed to adhere overnight prior to treatment. Following drug incubation, both floating and adherent cells were collected by trypsinization, neutralized with complete medium, and pelleted by centrifugation. Cells were washed twice with cold PBS and fixed by dropwise addition of cold 70% ethanol while vortexing, then stored at the recommended temperature and duration prior to staining. For cell-cycle analysis, fixed cells were washed to remove residual fixative, treated with RNase A, and stained with propidium iodide (PI) in PBS for at least 30 min at room temperature in the dark. Cell suspensions were then passed through 40 µm filter tubes to remove clumps prior to acquisition, and DNA content was analyzed by flow cytometry to determine cell-cycle distribution. For apoptosis analysis, unfixed cells were washed twice in cold PBS, resuspended in binding buffer, and stained with annexin V and PI according to the manufacturer's protocol. Following a brief incubation in the dark at room temperature, samples were analyzed by flow cytometry, and cell populations were quantified as viable, early apoptotic, late apoptotic, or necrotic based on annexin V/PI staining.

qPCR

Total RNA was isolated using TRIZOL reagent (Invitrogen) via the phenol-chloroform extraction method. cDNA was synthesized from 2 µg of total RNA using SuperScript II reverse transcriptase (Invitrogen) in a 20 µL reaction. The resulting cDNA was diluted 1:20 in nuclease-free water, and 4 µL was used per qPCR reaction, performed in triplicate. qPCR was carried out using Power SYBR Green PCR Master Mix (Thermo Fisher) on a CFX96 Real-Time PCR Detection System (Bio-Rad), including a non-template negative control. GAPDH amplification was used to normalize mRNA expression levels.

Transmission Electron Microscopy (TEM)

Panc-1 cells were seeded in 8-well slide plates (30,000 cells per well, Lab-Tek) and treated as indicated for 24 hrs. Samples were fixed with 0.1 M cacodylate buffer containing 2.5% glutaraldehyde plus 2% paraformaldehyde, transferred onto carbon square mesh grids, and observed under a Talos L120C transmission electron microscope.

Caspase-3/7 activity

In caspase 3/7 activity assay, cells in 96-well plates (10,000 cells per well) were treated as indicated, followed by adding AMC caspase-3/7 assay kit (50 µL per well, AnaSpec). The fluorescence intensity (λ_{ex} = 356 nm, λ_{em} = 442 nm) was recorded by a microplate reader. Data were analyzed by FlowJo 7.6.1.

Mitochondrial ROS detection

Mitochondrial superoxide was assessed using MitoROS™ 580 (AAT Bioquest, cat. no. 16052) according to the manufacturer's instructions. Following YXL-182 treatment, cells were incubated with MitoROS™ 580 working solution for 10–30 minutes at 37 °C protected from light, washed twice with PBS, and imaged by fluorescence microscopy.

Animal Model

All animal experiments were conducted in compliance with guidelines and animal protocol (#23784) approved by the Institutional Animal Care and Use Committee at the University of California, Davis. To establish subcutaneous xenograft models, 5×10^6 MIA PaCa-2 cells suspended in a 1:1 mixture of Matrigel (Corning) and PBS were injected subcutaneously into both flanks of NRG mice purchased from The Jackson Laboratory. To establish the orthotopic KPC model, 7.5×10^5 KPC cells were orthotopically implanted into C57BL/6 mice by Inotiv.

In Vivo Antitumor Studies

On subcutaneous PDAC tumor models, mice were randomly assigned to four groups once tumors reached approximately 100 mm^3. Each group received either PBS or YXL-182 daily for four weeks at doses of 50 mg/kg^{-1} or 100 mg/kg-1. Tumor progression was assessed using calipers or a VEVO F2xc ultrasound system. Upon completion of the treatment period, tumors and major organs were harvested for subsequent histological analysis.

Ultrasound

Orthotopic KPC tumor growth was monitored over time using a Vevo F2Xc high-frequency ultrasound imaging system (FUJIFILM VisualSonics). Mice were anesthetized with inhaled isoflurane and positioned identically for each imaging session to ensure consistent tumor visualization. Ultrasound gel was applied to the shaved abdominal area, and tumors were imaged using standard B-mode ultrasound. Tumor boundaries were manually traced in the images, and tumor volumes were measured using the Vevo F2Xc analysis software and ImageJ. Imaging was conducted at specified time points during the study to track changes in tumor burden.

Immunohistochemistry

Tumor sections were deparaffinized and subjected to antigen retrieval in citrate buffer (pH 6.0) for 45 minutes using a Decloaking Chamber (Biocare Medical, USA) at 125 °C. Sections were blocked with normal goat serum and incubated overnight at room temperature in a humidified chamber with rabbit primary antibodies against phospho-STAT3 (Tyr705; D3A7; Cell Signaling Technology, #9145), Ki-67 (Cell Signaling Technology, #12202; 1:1000), or cleaved caspase-3 (Cell Signaling Technology, #9661; 1:500). Sections were then incubated with biotinylated goat anti-rabbit secondary antibody (1:1000; Vector Laboratories, USA). Signal was amplified using the VECTASTAIN Elite ABC Kit and visualized with 3,3'-diaminobenzidine substrate (Vector Laboratories, USA).

Statistical Analysis

Statistical analyses were performed using GraphPad Prism 10. Data are presented as mean ± standard deviation (SD). Comparisons between two groups were performed using unpaired, two-tailed Student's t-tests. Where appropriate, chi-square tests, two-way analysis of variance (ANOVA), and Kaplan–Meier survival analyses were performed. Statistical significance was defined as ns, not significant; p<0.05p; p<0.01;p<0.001; and ****p<0.0001.

3.3 Results and Discussion

3.3.1 YXL-182 directly binds STAT3 and disrupts canonical signaling

To confirm that YXL-182 directly engages STAT3, we performed cellular thermal shift assays (CETSA) and surface plasmon resonance (SPR) binding studies. Together, these assays demonstrated direct physical interaction between YXL-182 and STAT3 protein. When considered alongside the downstream signaling analyses, these data support a direct STAT3-targeted mechanism of action, consistent with SH2-domain-directed inhibition rather than solely indirect or off-target effects.

Structurally, YXL-182 is a chalcone-thiol derivative composed of a STAT3-inhibitory pharmacophore linked to a mitochondria-targeting coumarin scaffold, generating a dual-function, mitochondria-accumulating STAT3 inhibitor (**Figure 7a**). SPR analysis compared the binding affinity of YXL-182 with C-188-9, a STAT3 inhibitor in clinical development. YXL 182 bound STAT3 with a $K_D$of 28.6 nM, compared with 8.36 nM for C-188-9; thus, both compounds exhibited tight low-nanomolar binding affinity (**Figure 7b**). Although C-188-9 showed a lower K_D, the low-nanomolar affinity of YXL-182 supports strong direct engagement of STAT3. CETSA further demonstrated intracellular target engagement, as YXL-182 treatment produced a shift in STAT3 thermal stability between 49 and 52 °C, indicating

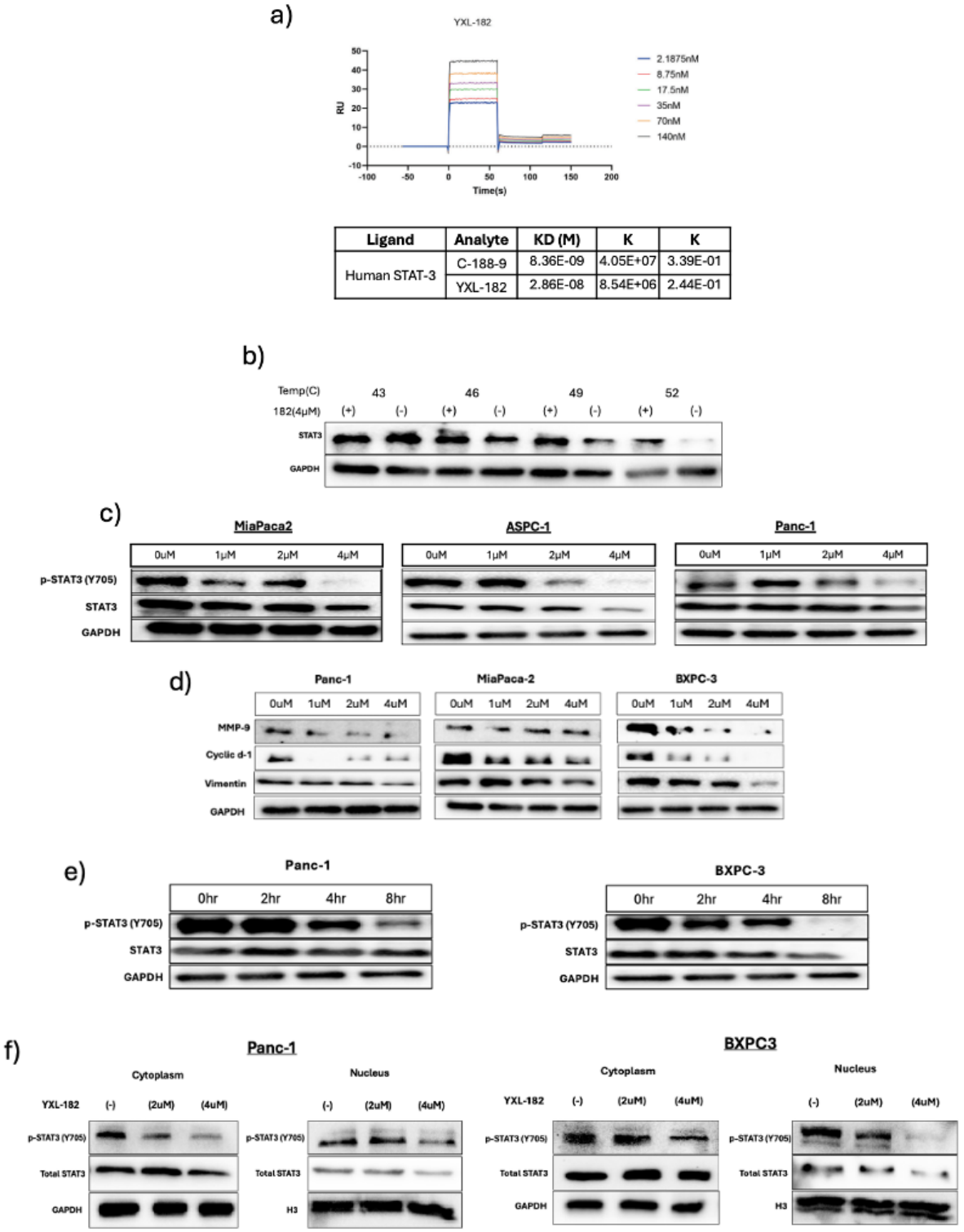

Ligand	Analyte	KD (M)	K	K
Human STAT-3	C-188-9	8.36E-09	4.05E+07	3.39E-01
	YXL-182	2.86E-08	8.54E+06	2.44E-01

Figure 7. YXL-182 directly binds STAT3 and inhibits canonical STAT3 signaling in PDAC cells.
(A) Surface plasmon resonance analysis of YXL-182 and the clinically evaluated STAT3 inhibitor C-188-9 binding to recombinant STAT3 protein. The equilibrium dissociation constants (K_D) were 28.6 nM for YXL-182 and 8.36 nM for C-188-9. (B) Cellular thermal shift assay (CETSA) demonstrating thermal stabilization of STAT3 following YXL-182 treatment, consistent with intracellular STAT3 target engagement. (C) Immunoblot analysis of p-STAT3(Y705) in MIA PaCa-2, AsPC-1, and PANC-1 cells treated with increasing concentrations of YXL-182 for 24 hours. (D) Immunoblot analysis of STAT3-associated downstream proteins MMP-9, cyclin D1, and vimentin in MIA PaCa-2, BxPC-3, and PANC-1 cells following YXL-182 treatment. (E) Time-course analysis of p-STAT3(Y705) inhibition in PANC-1 and BxPC-3 cells treated with 4 μM YXL-182. (F) Nuclear fractionation analysis of p-STAT3(Y705) and total STAT3 in PANC-1 and BxPC-3 cells following YXL-182 treatment, demonstrating reduced nuclear STAT3 accumulation.

that the compound binds STAT3 in cells and not only in a purified biochemical system (**Figure 7c**). We next assessed whether direct target engagement translated into inhibition of canonical STAT3 signaling. Western blot analysis in MIA PaCa-2, AsPC-1, and PANC-1 cells showed dose-dependent reduction of phosphorylated STAT3 (p-STAT3), with complete inhibition observed at 4 μM YXL-182 after 24 hours of treatment (**Figure 7d**). In MIA PaCa-2, BxPC-3, and PANC-1 cells, YXL-182 also reduced expression of the STAT3-associated downstream targets MMP-9, cyclin D1, and vimentin, indicating suppression of STAT3-dependent transcriptional output in addition to reduced STAT3 phosphorylation (**Figure 7e**). Time-course studies in PANC-1 and BxPC-3 cells further showed that 4 μM YXL-182 produced time-dependent p-STAT3 suppression, with complete inhibition by 8 hours (**Figure 7f**).

Finally, nuclear fractionation experiments in PANC-1 and BxPC-3 cells showed that YXL-182 markedly reduced nuclear accumulation of both p-STAT3 and total STAT3 (**Figure 7g**). These data indicate that YXL-182 inhibits several key components of canonical STAT3 signaling, including STAT3 phosphorylation, nuclear localization, and downstream target expression. Collectively, Figure 7 establishes YXL-182 as a direct, high-affinity STAT3 inhibitor with sustained suppression of canonical STAT3 signaling in PDAC cells.

3.3.2 YXL-182 is a potent, broadly active STAT3 inhibitor in PDAC cells

Across multiple PDAC cell lines, YXL-182 reduced cell viability in a dose-dependent manner and suppressed long-term clonogenic survival, indicating growth-inhibitory activity that extended beyond acute cytotoxicity. Consistent with direct STAT3 pathway inhibition, YXL-182 reduced STAT3 Tyr705 phosphorylation without a corresponding decrease in p-JAK1, supporting a mechanism centered on STAT3 rather than generalized upstream JAK suppression. YXL-182 also increased markers of apoptosis, including cleaved caspase-3 and Annexin V/PI positivity, while reducing expression of the STAT3 downstream targets MMP-9 and cyclin D1. Cell-cycle analyses further supported reduced proliferative capacity following YXL-182 treatment.

To determine whether linkage of the STAT3-targeting chalcone-thiol moiety and the mitochondria-targeting coumarin scaffold enhanced biological activity, we first evaluated

each component separately. The chalcone derivative YXL-43 displayed an IC50 of 20.9 μM, whereas the coumarin scaffold 7acc1 displayed an IC50 of 15.9 μM (**Figure 8b**). In contrast, the linked compound YXL-182 exhibited IC50 values below 3 μM across all PDAC cell lines tested: 1.46 μM in PANC-1, 1.69 μM in MIA PaCa-2, 2.40 μM in BxPC-3, 1.26 μM in AsPC-1, and 2.46 μM in KPC cells (**Figure 8c**). The substantially greater potency of YXL-182 relative to either individual component supports the functional advantage of the linked dual-pharmacophore design.

To assess whether this cytotoxicity translated into durable growth suppression, clonogenic assays were performed in PANC-1 and BxPC-3 cells. YXL-182 produced a dose-dependent decrease in colony formation, with near-complete colony reduction at 500 nM (**Figure 8d**). This result indicates that YXL-182 impairs long-term proliferative capacity at concentrations below those needed to achieve acute cytotoxic effects. Cell-cycle analysis in BxPC-3 and AsPC-1 cells further showed an increased G2 population accompanied by a corresponding reduction in the G1 population within 24 hours of treatment **(Figure 8e**). Together, these results show that YXL-182 exerts broad antiproliferative activity in PDAC cells through reduced STAT3 signaling, durable clonogenic suppression, apoptosis induction, and G2-associated cell-cycle arrest.

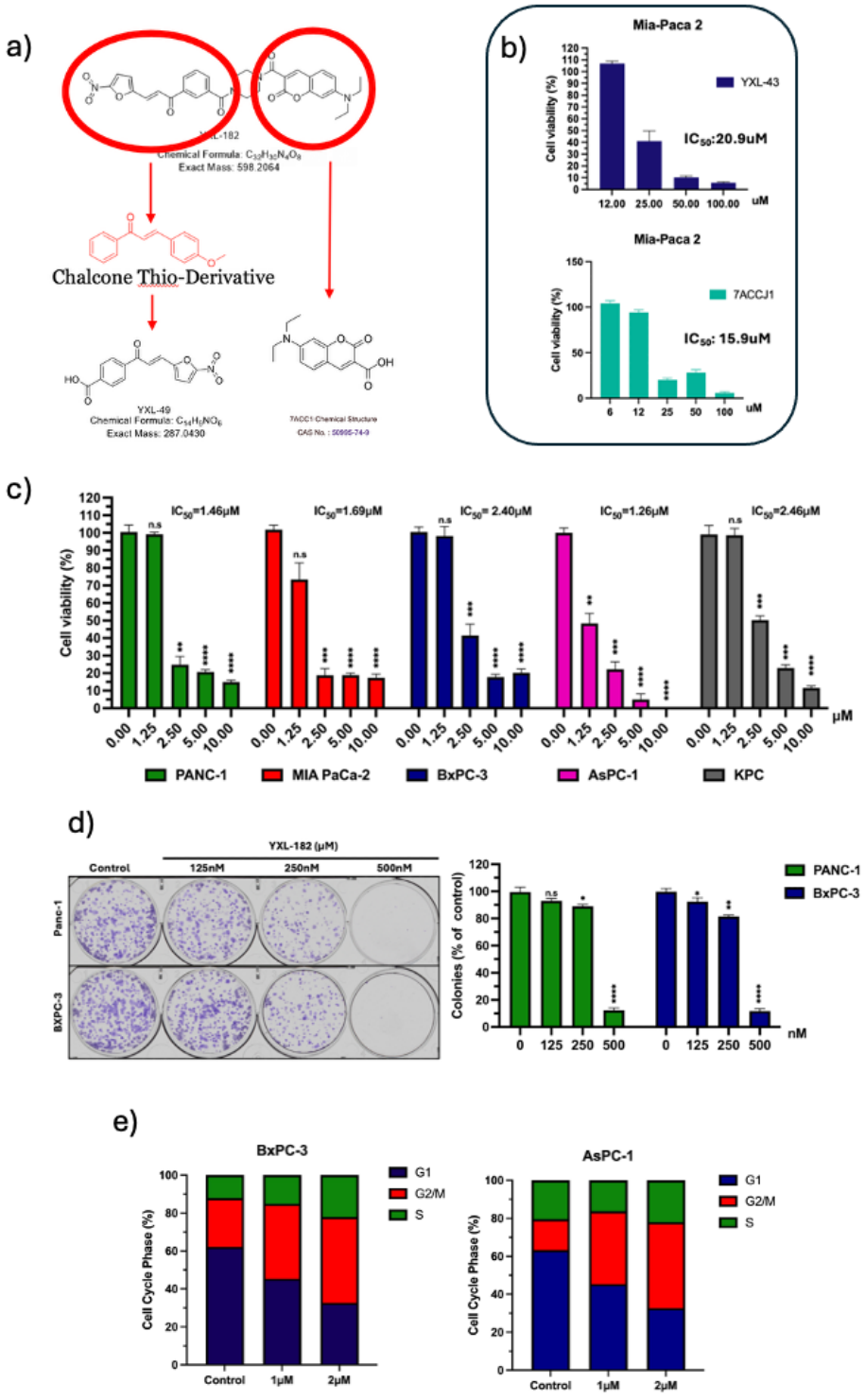

Figure 8. YXL-182 exhibits broad antiproliferative activity in PDAC cells.
(A) Schematic representation of the linked chalcone-thio STAT3-targeting and coumarin-based mitochondria-targeting moieties comprising YXL-182. (B) Cell-viability analysis of the individual YXL-182 structural components, YXL-43 and 7acc1. YXL-43 and 7acc1 displayed IC50 values of 20.9 µM and 15.9 µM, respectively. (C) Dose-response analysis of YXL-182 in PDAC cell lines. IC50 values were 1.46 µM in PANC-1, 1.69 µM in MIA PaCa-2, 2.40 µM in BxPC-3, 1.26 µM in AsPC-1, and 2.46 µM in KPC cells. (D) Clonogenic survival of PANC-1 and BxPC-3 cells treated with increasing concentrations of YXL-182, showing dose-dependent inhibition of colony formation and near complete colony loss at 500 nM. (E) Cell-cycle distribution of BxPC-3 and AsPC-1 cells after 24 hours of YXL-182 treatment, demonstrating increased G2-phase accumulation with a corresponding reduction in the G1 population. Data is presented as the mean of three independent experiments (n = 3).

3.3.3 YXL-182 accumulates in mitochondria and disrupts mitochondrial STAT3 and OXPHOS function

Subcellular localization studies confirmed that YXL-182 accumulates within mitochondria, consistent with its design as a chalcone-thiol derivative coupled to a mitochondria-targeting coumarin-based moiety. Fluorescence colocalization in BxPC-3 cells treated with YXL-182 for 6 hours revealed substantial overlap between the YXL-182 signal and a mitochondrial marker, confirming mitochondrial accumulation within this time frame (**Figure 9a**). To determine whether this localization affected the mitochondrial pool of STAT3, mitochondrial and cytosolic fractions were isolated from PANC-1 and MIA PaCa-2 cells treated with 2 or 4 μM YXL-182. Immunoblotting demonstrated a dose-dependent reduction in mitochondrial p-STAT3(Ser727), a phosphorylation site associated with non-canonical mitochondrial STAT3 activity and distinct from canonical nuclear STAT3 Tyr705 signaling (**Figure 9b**). These findings indicate that YXL-182 reduces the mitochondrial p-STAT3(Ser727) pool and is consistent with disruption of mitochondrial STAT3 signaling.

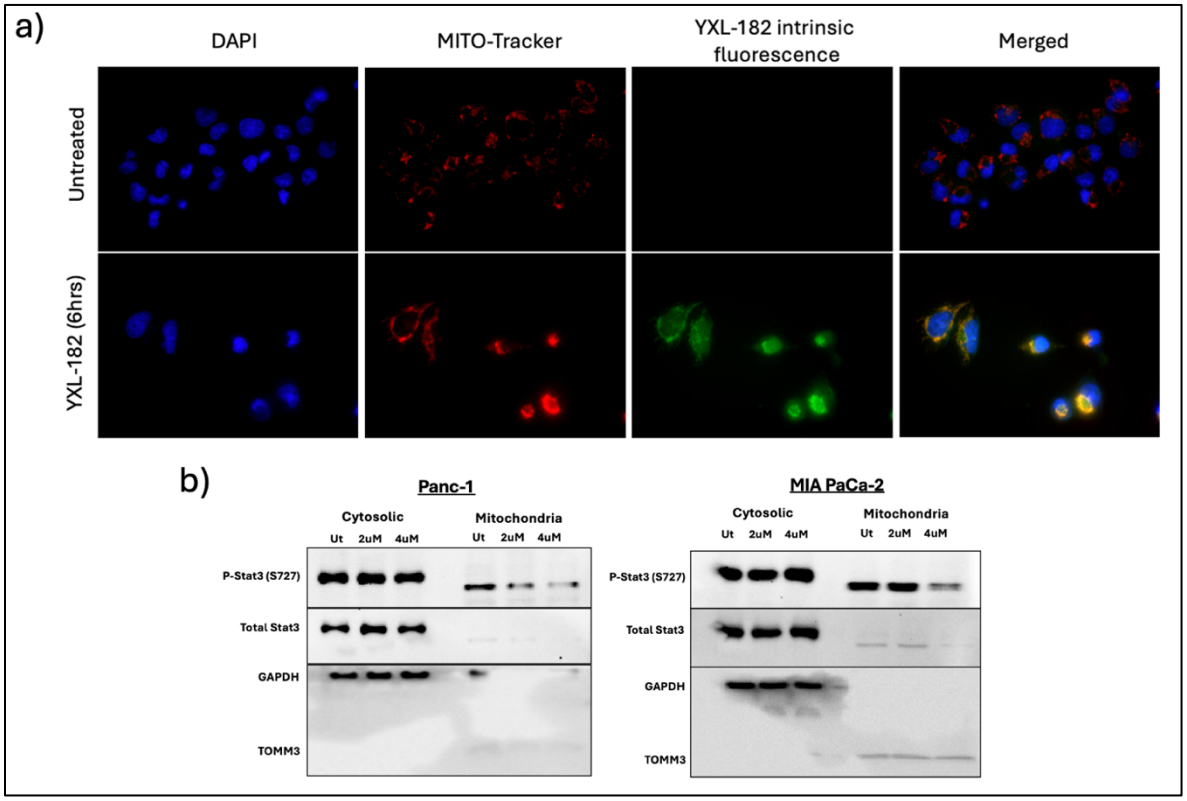

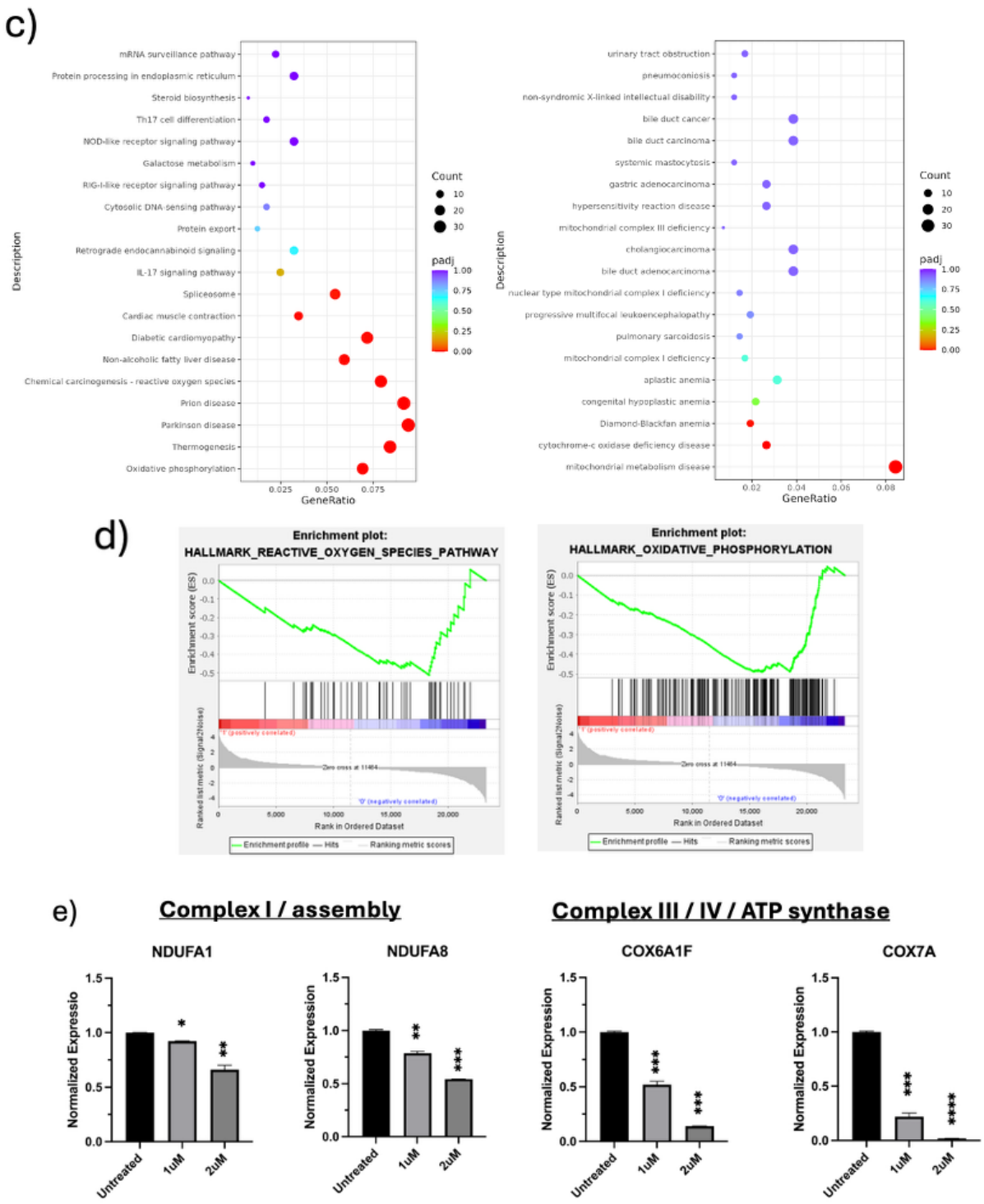

Figure 9. YXL-182 localizes to mitochondria and disrupts mitochondrial STAT3-associated OXPHOS signaling.
(A) Fluorescence colocalization of YXL-182 and a mitochondrial marker in BxPC-3 cells treated for 6 hours, demonstrating mitochondrial accumulation of YXL-182. (B) Mitochondrial and cytosolic fractionation of PANC-1 and MIA PaCa-2 cells treated with 2 or 4 μM YXL-182, followed by immunoblotting for p-STAT3(S727), demonstrating dose-dependent reduction of the mitochondrial p-STAT3(S727) pool. (C) KEGG pathway analysis of differentially expressed genes following treatment with 1 μM YXL-182 for 16 hours, identifying oxidative phosphorylation and mitochondrial dysfunction among the most significantly altered pathways. (D) Gene set enrichment analysis showing downregulation of oxidative phosphorylation and reactive oxygen species-associated gene sets after YXL-182 treatment. (E) qPCR validation of representative mitochondrial genes involved in complex I function (NDUFA1 and NDUFA8), electron transport chain and ATP synthase–associated pathways (COX6A1 and COX7A2), and mitochondrial protein import (TOMM7). Data are presented as the mean of three independent experiments (n=3).

To capture early transcriptional consequences of YXL-182 treatment before substantial cell death occurred, RNA-seq was performed after exposure to a sub-lethal concentration of YXL-182 (1 μM, 16 hours). KEGG pathway analysis of differentially expressed genes identified oxidative phosphorylation and mitochondrial dysfunction among the most significantly affected pathways (**Figure 9c**). GSEA further revealed coordinated downregulation of OXPHOS- and reactive oxygen species-associated gene sets (**Figure 9d**), supporting the conclusion that YXL-182 produces a broad mitochondrial stress response.

Transcriptomic profiling showed coordinated downregulation of genes involved in complex I assembly (NDUFAF8, NDUFA1, and NDUFB4), complexes III/IV and ATP synthase function (UQCR10, COX6A1, COX5B, COX7A2,), mitochondrial ribosome and protein-import machinery (TOMM7), qPCR validated reduced expression of representative mitochondrial genes, including NDUFA1 and NDUFA8, COX6A1 and COX7A2, and TOMM7 (**Figure 9e**). These molecular changes were accompanied by reduced mitochondrial respiration and ultrastructural damage in PANC-1 cells, including mitochondrial swelling and disrupted cristae architecture. Together, the localization, fractionation, transcriptomic, functional, and ultrastructural data support a model in which YXL-182 disrupts mitochondrial STAT3-associated function and broadly impairs OXPHOS-related mitochondrial homeostasis.

3.3.4 YXL-182 induces mitochondria-intrinsic apoptosis

To determine whether YXL-182-mediated mitochondrial disruption translated into apoptotic cell death, we evaluated mitochondrial ROS production, mitochondrial ultrastructure, bioenergetic function, and apoptotic signaling in PDAC cells. In BxPC-3 cells, treatment with 2 μM YXL-182 for 6 hours increased mitochondrial ROS, as detected by fluorescence microscopy (**Figure 10a**). Cellular uptake of YXL-182 was detectable by 4 hours, and p-STAT3 inhibition was observed by 6 hours placing mitochondrial ROS accumulation within the early cellular response to treatment.

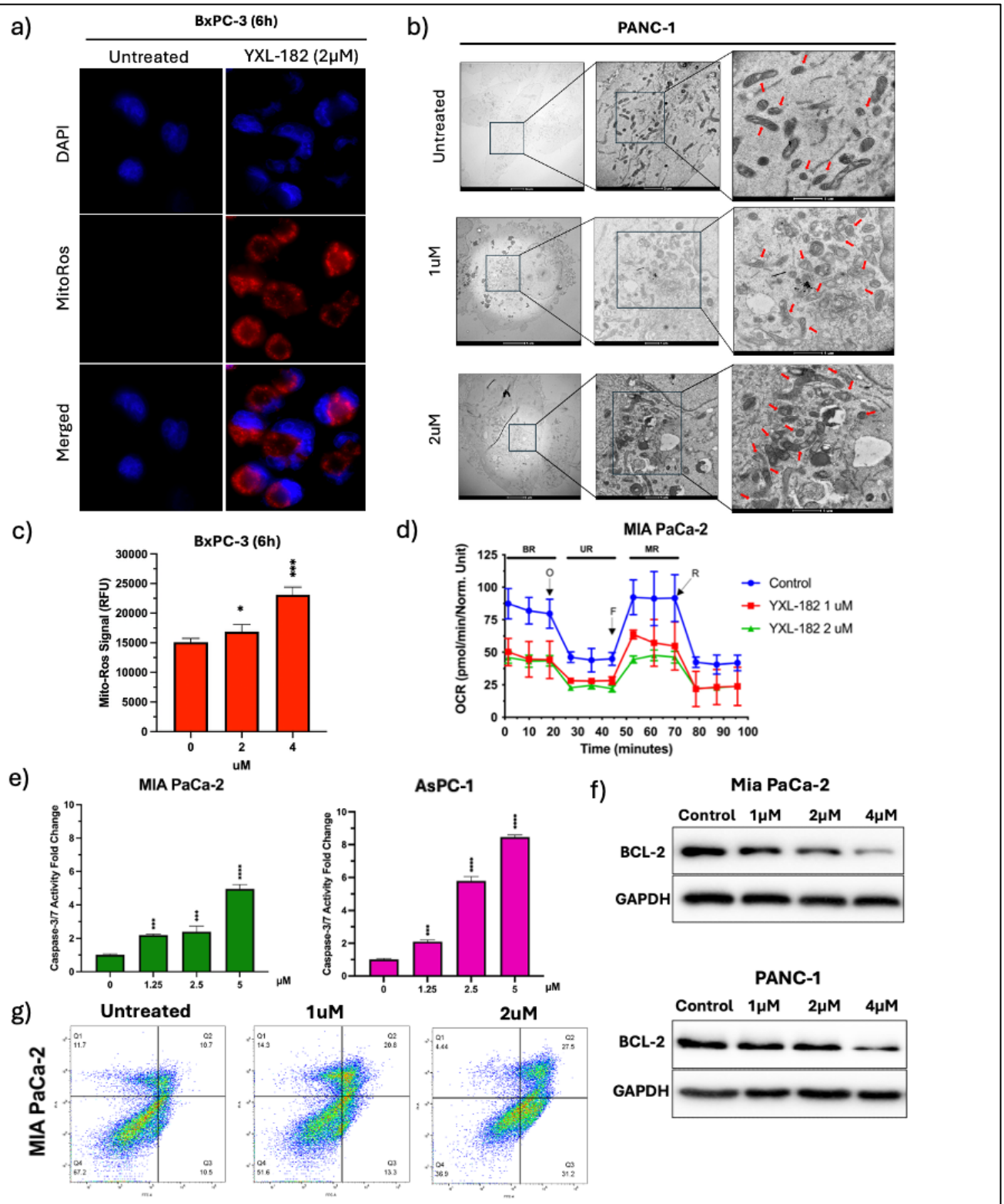

Figure 10. YXL-182 induces mitochondrial dysfunction and intrinsic apoptosis in PDAC cells.
(A) Fluorescence microscopy of BxPC-3 cells treated with 2 μM YXL-182 for 6 hours, showing increased mitochondrial reactive oxygen species signal. (B) Transmission electron microscopy of PANC-1 cells treated with 1 or 4 μM YXL-182 for 24hours, showing dose-dependent mitochondrial swelling, disrupted cristae, and membrane rupture relative to untreated controls. (C) Quantification of mitochondrial ROS following 6-hour YXL-182 treatment. (D) Seahorse Mito Stress Test showing dose-dependent reductions in basal respiration, maximal respiration, and spare respiratory capacity after YXL-182 treatment; 2 μM produced the greatest suppression of oxidative phosphorylation in MIA PaCa-2 with 24 hour drug exposure. (E) Immunoblot analysis of BCL-2 expression in PANC-1 and MIA PaCa-2 cells treated with 4 μM YXL-182 for 24 hours. (F) Caspase-3/7 activity in MIA PaCa-2 and AsPC-1 cells treated with YXL-182 for 24 hours. (G) Annexin V/PI flow-cytometric analysis of MIA PaCa-2 cells treated with 1 or 2 μM YXL-182 for 24 hours. Data is presented as the mean of three independent experiments (n = 3).

Quantification of MitoSOX fluorescence confirmed a dose-dependent increase in mitochondrial ROS, with signal increasing by 10% at 2 μM and 47% at 4 μM after 6 hours (**Figure10c**). Transmission electron microscopy provided structural evidence of mitochondrial injury. Untreated cells displayed predominantly elongated mitochondria with intact lamellar cristae. In contrast, 1 μM YXL-182 induced mitochondrial swelling, disrupted cristae architecture, and occasional membrane rupture. At 4 μM, most mitochondria exhibited extensive swelling, near-complete loss of cristae, and membrane rupture (**Figure 10b**). These findings demonstrate a dose-dependent progression from early mitochondrial stress to severe structural disruption.

To check whether the observed mitochondrial disruption was accompanied by impaired mitochondrial energy production, we performed a Seahorse Mito Stress Test to measure oxygen consumption rate in real time. YXL-182 reduced basal respiration, maximal respiration, and spare respiratory capacity in a dose-dependent manner, with 2 μM producing the greatest suppression across all parameters **(Figure 10d**). These data indicate that YXL-182 limits both basal oxidative phosphorylation and the capacity of PDAC cells to increase respiration in response to metabolic stress. We next assessed whether this mitochondrial dysfunction was associated with activation of intrinsic apoptosis. Caspase-3/7 activity increased in both MIA PaCa-2 and AsPC-1 cells after 24 hours of YXL-182 treatment. In MIA PaCa-2 cells, caspase-3/7 activity increased 2.1-fold, 2.3-fold, and 4.8-fold at 1.25, 2.5, and 5 μM, respectively. AsPC-1 cells showed a stronger response, with 2-fold, 5.8-fold, and 8-fold increases at the same concentrations (**Figure 10f**). In parallel, western blot analysis showed reduced BCL-2 expression in PANC-1 and MIA PaCa-2 cells after treatment with 4 μM YXL-182 for 24 hours (**Figure 10e**). Because BCL-2 is an anti-apoptotic protein that protects cells from mitochondrial apoptosis, its reduction is consistent with a shift toward apoptotic susceptibility. Finally, Annexin V/PI staining in MIA PaCa-2 cells confirmed dose-dependent apoptotic cell death. The viable cell population decreased from 67.2% in untreated cells to 51.6% at 1 μM and 36.9% at 2 μM YXL-182, whereas combined early and late apoptotic populations increased from 21.2% to 34.1% and 58.7%, respectively (**Figure 10g**). Collectively, these results support a model in which YXL-

182 induces mitochondrial ROS accumulation, bioenergetic failure, structural mitochondrial injury, BCL-2 downregulation, and caspase-dependent intrinsic apoptosis in PDAC cells.

3.3.5 YXL-182 is tolerated in vivo and enhances gemcitabine activity

To establish a tolerable dose range for in vivo studies, we evaluated YXL-182 as a single agent in NRG mice bearing subcutaneous MIA PaCa-2 xenografts. Because YXL-182 is hydrophobic, an oral formulation was developed to improve solubility and permit daily oral-gavage dosing. In maximum tolerated dose studies, YXL-182 was well tolerated at 50 and 100 mg/kg, with no overt signs of acute toxicity or treatment-associated body-weight loss (**Figure 11c**). These findings established that the formulation supported repeated dosing at therapeutically relevant concentrations.

We next compared the antitumor activity of YXL-182 with C-188, a clinically evaluated STAT3 inhibitor, in the MIA PaCa-2 xenograft model. At 60 mg/kg, YXL-182 showed greater tumor-growth suppression than C-188 (**Figure 11a**). Body weights remained stable throughout treatment in both single-agent groups, further supporting the tolerability of YXL-182 at the active dose (**Figure 11b**). Thus, the observed tumor-growth effect was not accompanied by an apparent systemic toxicity signal based on body-weight monitoring. To determine whether tumor control translated into improved survival, we performed Kaplan–Meier analysis in tumor-bearing animals treated with vehicle, C-188, or YXL-182. Vehicle-treated animals had the shortest survival, with all animals reaching endpoint by approximately day 42. C-188 produced a modest survival benefit that was not statistically

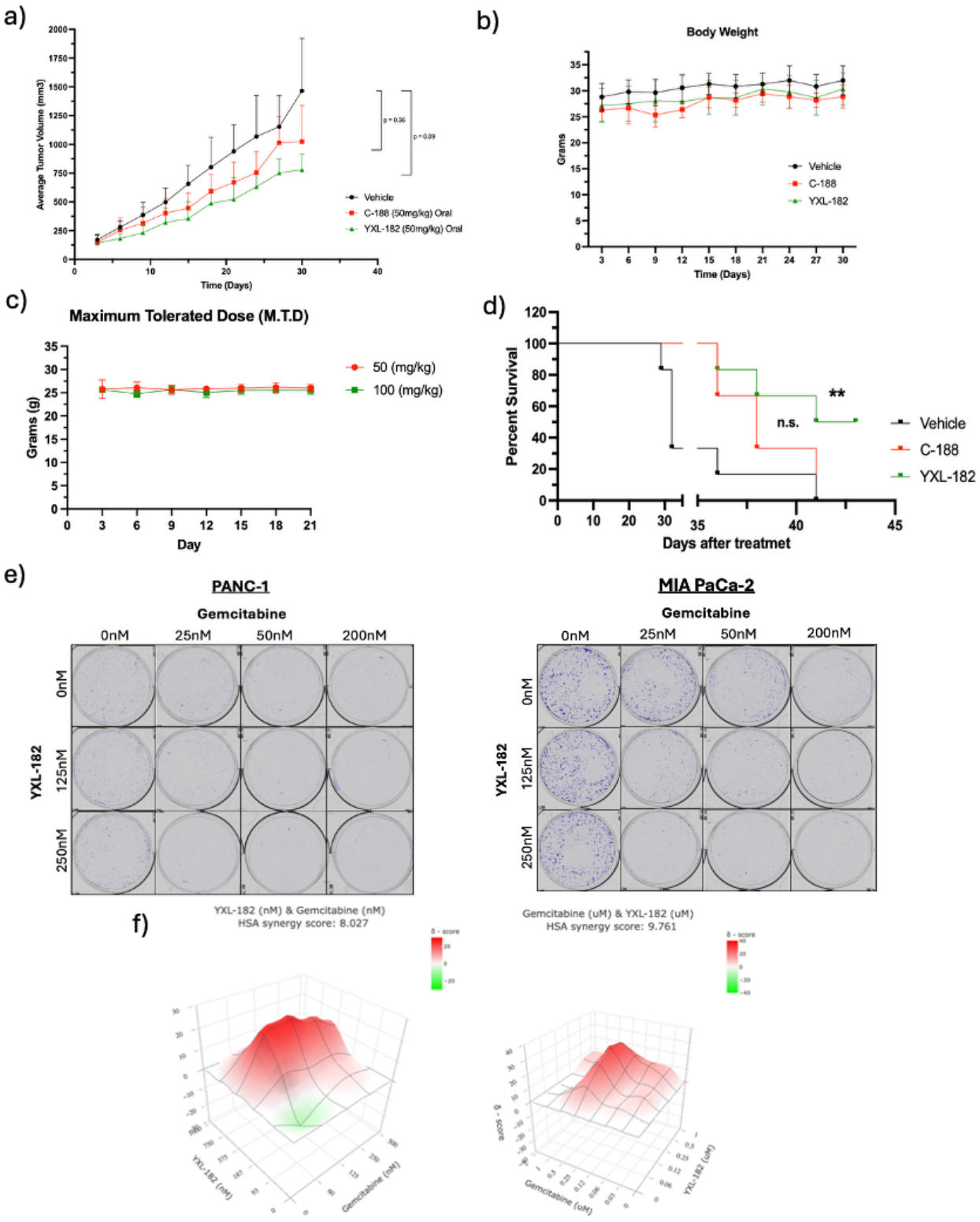

Figure 11. YXL-182 is tolerated in vivo, produces antitumor activity, and enhances gemcitabine response in PDAC models.
(A) Tumor-growth analysis in NRG mice bearing subcutaneous MIA PaCa-2 xenografts treated with YXL-182 or the clinical-stage STAT3 inhibitor C-188. YXL-182 produced greater tumor-growth suppression than C-188 when administered once daily at 50 mg/kg by oral gavage. Tumor-growth data are shown for six mice per treatment group (n=6). (B) Body weight was monitored throughout the xenograft study in mice receiving YXL-182 or C-188 monotherapy. Data are shown for eight mice per treatment group (n=8). (C) Maximum tolerated dose assessment of orally administered YXL-182. Mice treated daily with 50 or 100 mg/kg YXL-182 showed no overt toxicity or treatment-associated weight loss. (D) Kaplan–Meier survival analysis of tumor-bearing animals treated with vehicle, C-188, or YXL-182. Vehicle-treated animals reached endpoint by day 42. C-188 did not significantly improve survival, whereas YXL-182 significantly prolonged survival, with 50% of animals alive at study end. (E) Clonogenic assays in PANC-1 and MIA PaCa-2 cells treated with YXL-182, gemcitabine, or the combination. (F) Three-dimensional HSA synergy landscapes for the YXL-182/gemcitabine combination in PANC-1 and MIA PaCa-2 cells. Overall, HSA synergy scores were 8.027 in PANC-1 cells and 9.761 in MIA PaCa-2 cells, indicating positive combination activity.

significant relative to vehicle. In contrast, YXL-182 significantly prolonged survival compared with vehicle, with 50% of treated animals remaining alive at the end of the observation period (**Figure 11d**).

Together, the tumor-growth and survival data indicate that YXL-182 provides in vivo antitumor activity and a survival benefit in this PDAC model. Because gemcitabine is a standard therapy for PDAC but is limited by the development of resistance, we next tested whether YXL-182 could enhance gemcitabine activity. Clonogenic assays in PANC-1 and MIA PaCa-2 cells showed that the YXL-182/gemcitabine combination reduced colony formation more effectively than either single agent (**Figure 11e**). In PANC-1 cells, 125–250 nM YXL-182 enhanced gemcitabine-mediated clonogenic suppression across the tested gemcitabine concentrations, with near-complete colony loss at 200 nM gemcitabine. In MIA PaCa-2 cells, the combination substantially reduced colony formation at 25–50 nM gemcitabine and nearly eliminated colonies at 200 nM gemcitabine. Dose-matrix studies quantitatively confirmed a positive drug interaction. Using the highest single agent model, the YXL-182/gemcitabine combination produced overall HSA synergy scores of 8.027 in PANC-1 cells and 9.761 in MIA PaCa-2 cells (**Figure 11f**). These findings demonstrate that YXL-182 enhances gemcitabine activity in two PDAC cell models. In the context of the preceding data, the combination response is consistent with the possibility that simultaneous STAT3 inhibition and mitochondrial OXPHOS disruption may reduce the metabolic adaptability that contributes to chemotherapy resistance.

3.3.6 YXL-182 enhances gemcitabine efficacy in vitro and in orthotopic KPC models

Building on the mechanistic, in vitro combination, and safety data described above, we next evaluated whether YXL-182 could enhance gemcitabine efficacy in an immunocompetent orthotopic C57BL/6 KPC PDAC model. Combination treatment with YXL-182 and gemcitabine was well tolerated throughout the study. Mice receiving YXL-182 at 100 mg/kg, either alone or in combination with 50 mg/kg gemcitabine, maintained stable body weight during the dosing period, with no evidence of treatment-associated weight loss or overt toxicity (**Figure 12a**). These findings indicate that the enhanced antitumor activity of

the combination was not accompanied by an apparent increase in systemic toxicity based on body-weight monitoring.

We next evaluated whether YXL-182 improved therapeutic response to gemcitabine in vivo. Kaplan–Meier survival analysis showed that vehicle-treated animals had the shortest survival, with all mice reaching endpoint by approximately day 34. YXL-182 and gemcitabine monotherapy modestly extended survival, with all animals reaching endpoint by approximately days 50 and 46, respectively. In contrast, combination treatment produced the greatest survival benefit, with approximately 57% of animals remaining alive at day 60 (**Figure 12b**). Thus, the combination improved survival relative to either monotherapy in the orthotopic KPC model.

Consistent with the survival outcome, longitudinal tumor measurements showed progressive tumor growth in vehicle-treated mice, reaching approximately 47 mm^3 by week 4. YXL-182 and gemcitabine monotherapy each reduced tumor growth, with mean tumor volumes of approximately 22–23 mm^3 at week 4. The combination group achieved the strongest tumor-growth control, with mean tumor volume remaining below 20 mm^3 at the final time point and significantly lower than vehicle and the single-agent treatment groups, as indicated **in Figure 12c**. Representative Vevo F2X ultrasound images acquired at weeks 1 and 4 corroborated these longitudinal measurements. Vehicle-treated tumors expanded substantially over the course of the study, whereas tumors in the YXL-182 and gemcitabine groups remained smaller; the combination group showed the smallest tumor area at week 4 (**Figure 12d**).

To determine whether tumor control was accompanied by in vivo evidence of the proposed mechanism, tumor sections were examined by immunohistochemistry. Ki-67 staining was decreased in tumors treated with YXL-182 or gemcitabine and was lowest in the combination group, consistent with reduced tumor-cell proliferation. In parallel, p-STAT3(Y705) staining was reduced in YXL-182-treated tumors, supporting STAT3 target engagement in vivo. Cleaved cas-3 staining increased following YXL-182 treatment and was most apparent in the combination group, consistent with enhanced apoptotic cell death

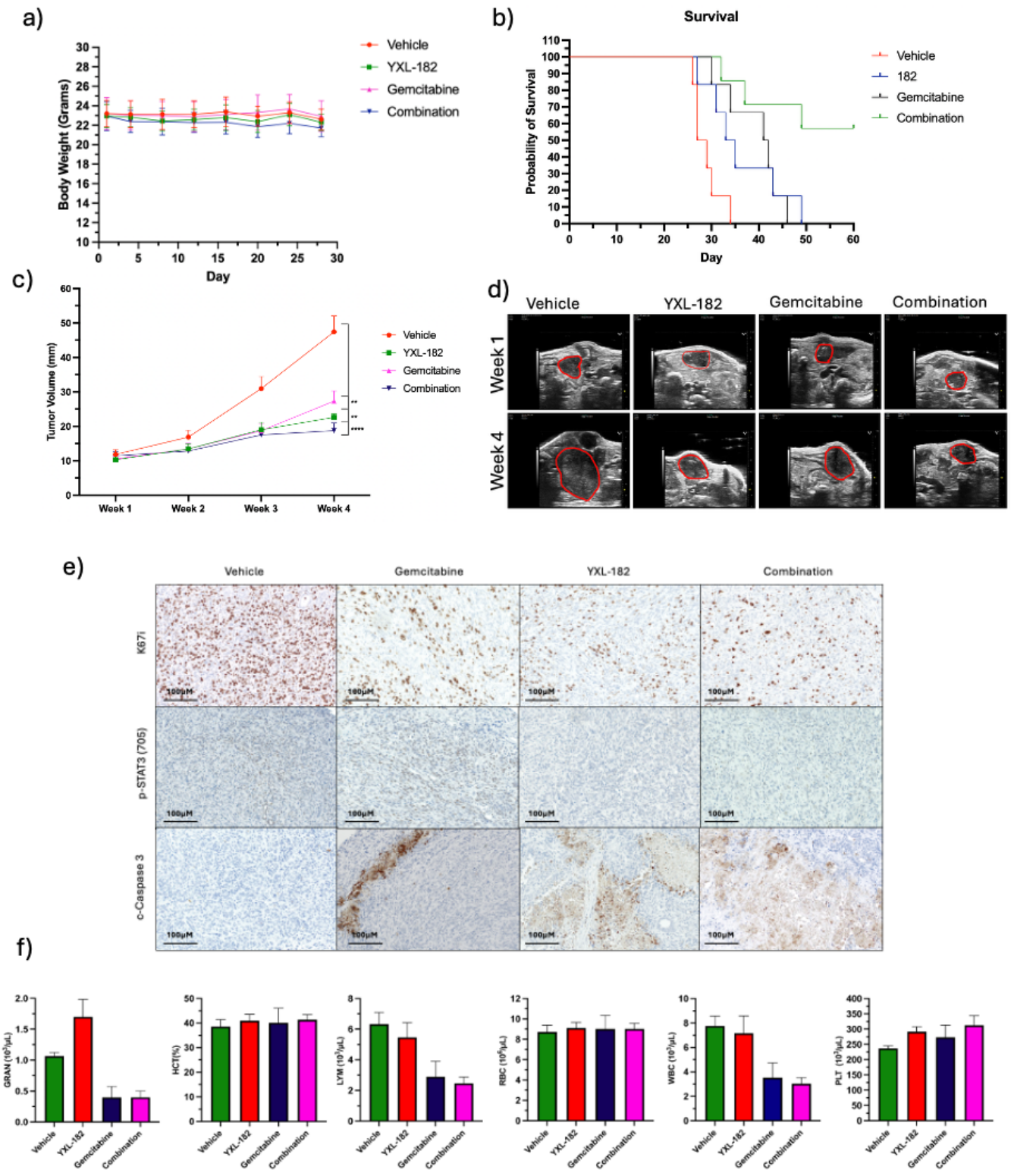

Figure 12. YXL-182 enhances gemcitabine activity in an orthotopic KPC PDAC model.
(A) Body weights of C57BL/6 mice treated with vehicle, YXL-182, gemcitabine, or the combination remained stable throughout the study. (B) Kaplan–Meier survival analysis showed that the combination treatment produced the greatest survival benefit, with approximately 57% of animals surviving to day 60 (n=8 per group). (C) Ultrasound-based tumor-volume measurements showed that combination treatment produced the greatest tumor-growth inhibition at week 4 (n=6per group). Statistical comparisons are indicated. D) Representative Vevo F2X ultrasound images at weeks 1 and 4; tumor boundaries are outlined in red. (E) Representative tumor immunohistochemistry for Ki-67, p-STAT3(Y705), and cleaved caspase-3. Combination treatment reduced proliferation and p-STAT3 while increasing apoptosis. Scale bars, 100 μm. (F) Hematologic analysis at endpoint. YXL-182 alone caused minimal changes; WBC and lymphocyte reductions were most apparent in gemcitabine-containing groups. Data are presented as mean of (n = 4).

(**Figure 12e**). These results link the improved tumor control observed with the combination to reduced proliferation, suppression of STAT3 signaling, and increased apoptosis within the tumor tissue.

Finally, hematologic analysis showed no evidence of major treatment-associated blood toxicity. YXL-182 alone produced minimal changes in hematologic parameters relative to vehicle-treated mice. Reductions in total white blood cell and lymphocyte counts were most apparent in the gemcitabine and combination groups, a pattern consistent with gemcitabine-associated myelosuppression. Importantly, the combination did not produce evidence of severe additional hematologic toxicity beyond that observed with gemcitabine-containing treatment (**Figure 12f**). Collectively, these data show that YXL-182 enhances gemcitabine activity in an orthotopic KPC model, producing superior tumor control and prolonged survival while maintaining an acceptable tolerability profile. Figure 6e. Representative immunohistochemical staining of tumor sections from vehicle-, gemcitabine-, YXL-182, and combination-treated mice. Ki-67 staining was reduced in tumors from YXL-182 and gemcitabine-treated groups and was lowest in the combination group, indicating decreased tumor-cell proliferation. Phosphorylated STAT3 at Tyr705 staining was also reduced following YXL-182 treatment, consistent with in vivo STAT3 target engagement. In contrast, cleaved caspase-3 staining increased in YXL-182-treated tumors and was most evident in the combination group, indicating enhanced apoptotic cell death. Scale bars, 100 μm.

3.4 Conclusion

In conclusion, this chapter identifies YXL-182 as a dual-function, mitochondria-accumulating STAT3 inhibitor with potent activity in PDAC models. YXL-182 directly binds and inhibits STAT3, suppresses canonical and mitochondrial STAT3 signaling, disrupts OXPHOS and mitochondrial homeostasis, and induces intrinsic apoptosis. Importantly, YXL-182 showed in vivo tolerability, prolonged survival in tumor-bearing mice, and enhanced the antitumor activity of gemcitabine in both in vitro and orthotopic KPC PDAC models. Together, these findings support further preclinical development of YXL-182 as a

mechanism based therapeutic strategy to overcome STAT3-driven survival signaling and metabolic adaptation in PDAC.

References

1. Wang XR, Jiang ZB, Xu C, Meng WY, Liu P, Zhang YZ, et al. Andrographolide suppresses non-small-cell lung cancer progression through induction of autophagy and antitumor immune response. Pharmacol Res. 2022 May 1;179:106198. doi:10.1016/j.phrs.2022.106198
2. Conroy T, Bachet JB, Ayav A, Huguet F, Lambert A, Caramella C, et al. Current standards and new innovative approaches for treatment of pancreatic cancer. Eur J Cancer. 2016 Apr 1;57:10–22. doi:10.1016/j.ejca.2015.12.026 PubMed PMID: 26851397.
3. Sansone P, Bromberg J. Targeting the Interleukin-6/Jak/Stat Pathway in Human Malignancies. J Clin Oncol. 2012 Mar 20;30(9):1005–14. doi:10.1200/JCO.2010.31.8907
4. Yang X, Lin Y, Shi Y, Li B, Liu W, Yin W, et al. FAP Promotes Immunosuppression by Cancer-Associated Fibroblasts in the Tumor Microenvironment via STAT3–CCL2 Signaling. Cancer Res. 2016 Jul 14;76(14):4124–35. doi:10.1158/0008-5472.CAN-15-2973
5. Sgrignani J, Garofalo M, Matkovic M, Merulla J, Catapano CV, Cavalli A. Structural Biology of STAT3 and Its Implications for Anticancer Therapies Development. Int J Mol Sci. 2018 Jun;19(6):1591. doi:10.3390/ijms19061591
6. Huang Q, Zhong Y, Dong H, Zheng Q, Shi S, Zhu K, et al. Revisiting signal transducer and activator of transcription 3 (STAT3) as an anticancer target and its inhibitor discovery: Where are we and where should we go? Eur J Med Chem. 2020 Feb 1;187:111922. doi:10.1016/j.ejmech.2019.111922
7. Chen H, Bian A, Yang L fang, Yin X, Wang J, Ti C, et al. Targeting STAT3 by a small molecule suppresses pancreatic cancer progression. Oncogene. 2021 Feb;40(8):1440–57. doi:10.1038/s41388-020-01626-z
8. Chen H, Bian A, Zhou W, Miao Y, Ye J, Li J, et al. Discovery of the Highly Selective and Potent STAT3 Inhibitor for Pancreatic Cancer Treatment. ACS Cent Sci. 2024 Feb 10;10(3):579–94. doi:10.1021/acscentsci.3c01440
9. Meier JA, Hyun M, Cantwell M, Raza A, Mertens C, Raje V, et al. Stress-induced dynamic regulation of mitochondrial STAT3 and its association with cyclophilin D reduce mitochondrial ROS production. Sci Signal. 2017 Mar 28;10(472):eaag2588. doi:10.1126/scisignal.aag2588
10. Genini D, Brambilla L, Laurini E, Merulla J, Civenni G, Pandit S, et al. Mitochondrial dysfunction induced by a SH2 domain-targeting STAT3 inhibitor leads to metabolic synthetic lethality in cancer cells. Proc Natl Acad Sci. 2017 Jun 20;114(25):E4924–33. doi:10.1073/pnas.1615730114

Chapter 4 :

Conclusion and Future Strategies for STAT3-Targeted YXL-182 Delivery

4.1 Overview of Integrated Therapeutic Strategy in PDAC

Pancreatic ductal adenocarcinoma remains difficult to treat due to the therapeutic resistance driven several factors discussed in Chapter 1. Current conventional chemotherapy, such as gemcitabine-based regimens have shown the ability to reduce tumor burden but are limited by insufficient intratumoral drug exposure and the ability of tumor cells to activate survival and metabolic pathways in response to treatment induced stress.

STAT3 is a central therapeutic target in PDAC because it regulates several key processes involved in tumor progression. Canonical STAT3 signaling promotes transcriptional programs involved in proliferation, survival, invasion, and chemoresistance, whereas mitochondrial STAT3 contributes to oxidative phosphorylation , redox homeostasis, and metabolic adaptation. (1) These functions are relevant in PDAC, where aggressive and therapy-resistant tumor cells depend on mitochondrial respiration and metabolic flexibility to survive chemotherapy.

YXL-182 was developed as a mitochondria-accumulating STAT3 inhibitor to disrupt both canonical and mitochondrial STAT3 functions. As shown in Chapter 3, YXL-182 directly interacts with STAT3, suppresses p-STAT3 signaling and downstream pathways such as, cyclin D1 and MMP-9. This compound accumulates in mitochondria, disrupts oxidative phosphorylation associated processes causing an increase in mitochondrial stress, inducing intrinsic apoptosis. YXL-182 was also well tolerated in vivo and enhanced gemcitabine toxicity in PDAC models. Taken together, these results suggest that blocking

STAT3 can make PDAC cells more responsive to chemotherapy and interfere with the metabolic processes that help the cells resist treatment.

4.2 Rationale for Nano-encapsulation of YXL-182

YXL-182 has demonstrated promising outcomes in preclinical studies. However, clinical efficacy will depend on many factors, including its mechanism of action and the ability to achieve effective intratumoral penetration. Because PDAC tumors contain a dense extracellular matrix, poor perfusion, intratumoral drug penetration is restricted. (2) As a result, even strong agents might not work well if they cannot reach high enough levels throughout the dense PDAC tumor microenvironment.

Encapsulation of YXL-182 could address several limitations of conventional small-molecule delivery. Lipid nanoparticles have shown to improve stability, circulation time, and tumor accumulation of small mole inhibitors payloads, all while reducing exposure to healthy tissues and minimizing off target toxicity. (1) Encapsulation can protect YXL-182 from degradation or systemic clearance and enable a sustained and controlled release once the nanoparticle reaches the tumor.

As highlighted in chapter 2, nanoplatforms can further be designed to respond to features withing the tumor microenvironment, such as its acidic pH, hypoxia, or specific enzyme presence . Stimuli-responsive delivery may enhance the localized release of YXL-182 within PDAC tissue while restricting systemic drug distribution. Along with the ability to co-deliver YXL-182 with gemcitabine or other therapies, creating a coordinated strategy to inhibit STAT3 dependent pathways while increasing chemotherapy induced tumor cell death the multiple mechanisms that maintain PDAC progression and therapeutic resistance.

4.3 Overall Conclusions

This dissertation supports a mechanism based therapeutic strategy that addresses one critical driver of PDAC resistance by simultaneously targeting STAT3-dependent signaling, mitochondrial metabolism, chemotherapy tolerance, and tumor-microenvironment barriers. YXL-182 is a promising candidate therapeutic because it directly targets STAT3, inhibits canonical signaling, accumulates in the mitochondria, disrupts

OXPHOS-associated functions and enhances gemcitabine activity in preclinical PDAC models (Chapter 3, Figures 7–12).

However, molecular potency alone is unlikely to overcome the complex barriers that limit treatment in PDAC. Encapsulation of YXL-182 would be a logical next step to improve pharmacokinetics, tumor delivery, and combination-treatment potential An immunomodulatory nanoplatform that has been carefully designed could combine the effect of YXL-182 on inhibiting STAT3 with gemcitabine and with therapies which target the tumor microenvironment. This method might weaken the survival signals of tumor cells, disrupt mitochondrial adaptation, increase drug exposure within tumors, and enhance the immune response against cancer. By targeting both tumor-intrinsic mechanisms, stromal and immune barriers surrounding PDAC, a YXL-182 based nanoplatform may provide a better scaffold for more effective and durable therapeutic approach.

References

1. Rébé C, Ghiringhelli F. STAT3, a Master Regulator of Anti-Tumor Immune Response. Cancers. 2019 Sep;11(9):1280. doi:10.3390/cancers11091280
2. Perez VM, Kearney JF, Yeh JJ. The PDAC Extracellular Matrix: A Review of the ECM Protein Composition, Tumor Cell Interaction, and Therapeutic Strategies. Front Oncol. 2021 Oct 6;11. doi:10.3389/fonc.2021.751311